VPI-SU-5648-1

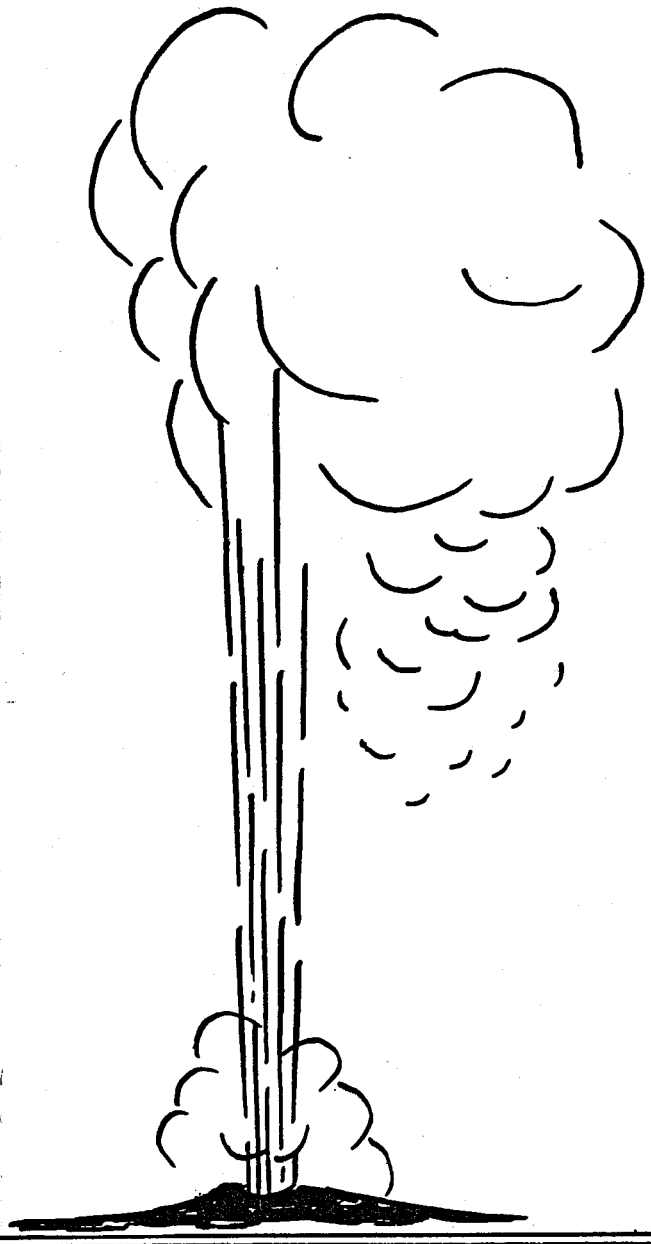

EVALUATION AND TARGETING OF GEOTHERMAL ENERGY RESOURCES IN THE SOUTHEASTERN UNITED STATES

Progress Report, October 1—December 31, 1977

By
John K. Costain
Lynn Glover, III
A. Krishna Sinha

Work Performed Under Contract No. ET-78-C-05-5648

Department of Geological Sciences
Virginia Polytechnic Institute and State University
Blacksburg, Virginia

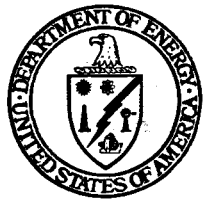

U. S. DEPARTMENT OF ENERGY

Geothermal Energy

NOTICE

VPI-SU-5648-1
Distribution Category UC-66a

EVALUATION AND TARGETING OF GEOTHERMAL ENERGY RESOURCES IN THE SOUTHEASTERN UNITED STATES

Progress Report

John K. Costain, Lynn Glover III, and A. Krishna Sinha
Principal Investigators
Department of Geological Sciences
Virginia Polytechnic Institute and State University
Blacksburg, VA 24061

October 1, 1977 - December 31, 1977

PREPARED FOR THE U. S. DEPARTMENT OF ENERGY UNDER
CONTRACT NO. ET-78-C-05-5648

TABLE OF CONTENTS

TABLE OF CONTENTS (CONTINUED)

ABSTRACT

The objective of this program is to develop and apply targeting procedures for the evaluation of low-temperature geothermal resources in the eastern United States utilizing geological, geochemical, and geophysical data. Primary programmatic emphasis is now being placed on the confirmation of radiogenic resources beneath sediments of the Atlantic Coastal Plain. Geothermal gradients known to date in the Atlantic Coastal Plain are consistent with those to be expected from concealed radiogenic sources. Collation of existing gravity and magnetic data available for the Atlantic Coastal Plain has been completed and modeling of selected negative gravity anomalies of the Cuffytown Creek (Edgefield) pluton, S.C., the Rolesville batholith, N.C., and the Petersburg granite, Va. are in progress. The study of the Cuffytown Creek granite is almost complete. Maps showing the distribution of gravity stations for the states of Georgia, South Carolina, and North Carolina have been prepared. A reconnaissance geologic map is being prepared of the Raleigh belt and Carolina slate belt rocks bounded by the Durham-Wadesboro Triassic basin on the west, Atlantic Coastal Plain sediments on the east, latitude 35°15', and the North Carolina-Virginia border. The purpose of this study is to determine the relationship of the Rolesville batholith to the surrounding country rocks, and to provide a geologic base for the geophysical interpretation of Piedmont

stratigraphy underlying Atlantic Coastal Plain sediments to the east. Whole rock chemistry shows that the gabbroic plutons of the southeastern U.S. are alkaline gabbro-diroite-syenite complexes and subalkaline gabbro/gabbro-norite complexes. Heat generation values of 1.2-1.8 HGU measured for the Concord syenite and Mt. Carmel syenite (part of an older magma series approximately 400 m.y.o.) indicate that differentiation alone is insufficient to explain high heat generation. The composition of the parent magma is a critical factor. The Siloam pluton, Greene Co., Ga., is a coarse-grained, late Paleozoic pluton selected for study because of high heat-generation values obtained in reconnaissance sampling. Field work demonstrates that the Siloam is similar to the other post-metamorphic plutons of the southeast; however, the heat generation is approximately twice the value for other coarse-grained granites in the southeast. Chemical analyses of the Petersburg batholith, Va., indicate that the major-element chemistry resembles most closely the Liberty Hill, S.C., fine-grained and Rolesville, N.C., surface samples; however, the average U content of the Petersburg surface samples is considerably higher than that from the surface of any other pluton.

INTRODUCTION AND OVERVIEW

Although the relatively stable tectonic setting of the eastern United States seems to rule out the possible occurrence of conventional, high-temperature hydrothermal resources, the region does contain geothermal resources which are being developed now, or which may be exploited in the future. The geothermal resources anticipated will be low- to moderate-temperature fluids that are best suited for direct heat applications.

The near-term resource assessment in the eastern United States places primary programmatic emphasis on the confirmation of radiogenic resources in the Atlantic Coastal Plain. This emphasis is based on the partial confirmation of the radiogenic model as described in DOE Reports VPI&SU-5103-4 and -5. Concurrent studies at VPI&SU, because of their geographic proximity to the Atlantic Coastal Plain, also bear directly on the assessment of other geothermal resource types (see VPI&SU-5103-5). The utilization of certain types of geothermal resources in the east, specifically the hot-dry-rock and normal gradient resources, may be dependent on technological advances before they can be economically developed, but an assessment of the geothermal potential of these resources cannot be made without a reliable data base.

Because it is not economically feasible to select drilling sites on the Atlantic Coastal Plain without

geophysical and geological models, it is advisable to base the development of these models on a substantial and accurate data base which can be partially derived from the exposed rocks of the Piedmont and enhanced by basement studies beneath the Atlantic Coastal Plain.

We emphasize the importance of understanding the geologic framework since it is this framework that controls the occurrence and distribution of geothermal resources.

Site-specific gravity surveys of the Atlantic Coastal Plain are now in progress by VPI&SU. Results of detailed gravity surveys in the Piedmont and the modeling of potential field data are given in this report. Preliminary studies indicate that the density contrast for plutonic rocks in the Piedmont is in the range of -0.15 to -0.25 gm/cc. These studies will help to define the shape and geologic framework of radiogenic sources concealed beneath the sediments of the Atlantic Coastal Plain. Maps showing the distribution of gravity stations in the states of Georgia, South Carolina, North Carolina, Virginia, Delaware, Maryland, and New Jersey are being prepared. Station distribution maps for Georgia, South Carolina, and North Carolina are given in this report and will be updated in subsequent reports as additional and new data become available. Included in this report are tabulated values of new gravity data obtained by VPI&SU.

A reconnaissance geologic map of portions of the Raleigh belt and Carolina slate belt, and structural mapping

of the Rolesville batholith will provide a geologic base for the geophysical interpretation of basement rocks beneath the sediments of the Atlantic Coastal Plain. Additional studies in the Piedmont continue to contribute to our understanding of the structural and petrologic setting of the late Paleozoic plutons.

Basement core was obtained from a hole in the Coastal Plain of Georgia in Wayne County. Total depth of the hole was 1332 m. The least-squares geothermal gradient over the interval 47-1328 m was 29.3 ± 0.14°C/km. Thermal conductivity and heat generation determinations, petrography, and geochronology of the basement core are in progress.

RESEARCH OBJECTIVES

The objective of this research is to develop and apply targeting procedures for the evaluation of low-temperature radiogenically-derived geothermal resources in the eastern United States utilizing geological, geochemical, and geophysical data.

The cptimum sites for geothermal development in the tectcnically-stable Eastern United States will probably be associated with areas of relatively high heat flow derived from crustal igneous rocks containing relatively high concentrations of radiogenic heat-producing elements. The storage of ccmmercially-exploitable geothermal heat at accessible depths (1-3 km) will also require favorable reservoir conditions in rocks overlying a radiogenic heat source. In order to systematically locate these sites, a methodclogy employing geological, geochemical, and geophysical propspecting techniques is being developed and applied. The distribution cf radiogenic sources within the igneous rccks of various ages and magma types will be determined by a correlation between radioelement composition and the bulk chemistry of the rock. Surface sampling and measurement of the radiogenic heat-producing elements are known to be unreliable as they are preferentially removed by ground-water circiulation and weathering. The correlation between the bulk chemistry of the rock (which can be measured reliably from surface samples) and radiogenic heat

generation is being calibrated by detailed studies at a number of locations in the eastern United States.

Initial studies are developing a methodology for the location of radiogenic heat sources buried beneath the insulating sedimentary rocks of the Atlantic Coastal Plain. Choice of a drill site in the Atlantic Coastal Plain with a high geothermal resource potential depends on favorable:

(1) concentration of radiogenic elements in granitic rocks beneath a sedimentary insulator;

(2) thermal conductivity of the sedimentary insulator;

(3) thickness of the sedimentary insulator; and

(4) reservoir conditions in the permeable sedimentary rocks overlying the radiogenic heat source.

Because it is not economically feasible to select drilling sites on the Atlantic Coastal Plain without geophysical and geological models, it is advisable to base the development of these models on a substantial and accurate data base which can be partially derived from the exposed rocks of the Piedmont and enhanced by basement studies beneath the Atlantic Coastal Plain.

PERSONNEL OF PROGRAM

(October 1, 1977 - December 31, 1977)

GEOLOGY AND PETROLOGY, Lynn Glover III, Principal Investigator

J. A. Speer, Research Associate
S. S. Farrar, Research Associate
S. W. Becker, Research Associate
A. Baldasari, Laboratory Aide

GEOCHEMISTRY, A. Krishna Sinha, Principal Investigator

B. A. Merz, Research Associate
S. Dickerson, Laboratory Aide

GEOPHYSICS, John K. Costain, Principal Investigator

A. H. Cogbill, Research Associate
L. D. Perry, Research Associate
J. A. Dunbar, Research Specialist
T. A. Arnold, part-time Laboratory Aide
R. Oslin, part-time Laboratory Aide

ADMINISTRATIVE ASSISTANT
Patricia C. Sullivan

SECRETARIES
Geraldine Barber
Margie Strickler

DRAFTSMAN-PHOTOGRAPHER
David Brown

DRILLERS
W. G. Coulson, Core Driller
R. G. Gravley, Driller Helper

TALKS PRESENTED TO DATE

1. Low-temperature resources of the eastern United States, Second NATO-CCMS Meeting on Dry Hot Rock Geothermal Energy, Los Alamos Scientific Laboratory, Los Alamos, New Mexico, June 28, 1977 (Speaker: J. K. Costain).

2. Low-temperature geothermal resources of the eastern United States, Geological Society of Washington, Washington, D. C., October 12, 1977 (Speaker: J. K. Costain).

3. Low-temperature geothermal resources in the eastern United States, 1977 Annual Meeting of the Geological Society of America, November 8, 1977 (Speaker: J. K. Costain).

4. Evaluation of the geothermal potential of hot springs in Northwestern Virginia, American Nuclear Society, Denver, Colorado, April 13, 1977 (Speaker: P. A. Geiser, University of Connecticut).

5. Low-temperature geothermal resources in the eastern United States, Potomac Geophysical Society, November 17, 1977 (Speaker: J. K. Costain).

6. Structural controls of thermal springs in the Warm Springs anticline, by P. A. Geiser and J. K. Costain, Southeastern Geological Society of America meeting, Winston-Salem, North Carolina, 1977 (Speaker: P. A. Geiser).

ABSTRACTS PUBLISHED TO DATE

1. Evaluation of the geothermal potential of the hot springs of northwestern Virginia, by P. A. Geiser and J. K. Costain, Abstracts of ANS Topical Meeting on Energy and Mineral Resource Recovery, Golden, Colorado, April 12-14, 1977, p. 33.

2. Structural controls of thermal springs in the Warm Springs anticline, Virginia, by P. A. Geiser and J. K. Costain, Abstracts, Geol. Soc. America SE Section, Winston-Salem, North Carolina, 1977.

3. Low-temperature geothermal resources in the eastern United States, by J. K. Costain, L. Glover III, and A. K. Sinha, Program with Abstracts, Annual Meeting of Geological Society of America, Seattle, Washington, 1977.

PAPERS SUBMITTED FOR PUBLICATION

1. Molybdenum mineralization in the Liberty Hill and Winnsboro Plutons, South Carolina, by J. Alexander Speer, Economic Geology, 1978 (in press).

PROGRESS

A. GEOLOGY

Lynn Glover III, Principal Investigator

J. A. Speer, Research Associate

S. S. Farrar, Research Associate

S. W. Becker, Research Associate

A. Baldasari, Laboratory Aid

OPERATIONS

During the last three months, from 10/1/77 to 12/31/77, 16 man-weeks were spent on fieldwork. The following is a listing of man-days of fieldwork in each area, and the number of samples collected.

Area of Pluton	Man-Days	Samples for Chemistry and Heat Production	Total Samples
Rolesville-Raleigh belt-slate belt, N.C.	25	-	73
Lilesville, N.C.	10	-	15
Winnsboro, S.C.	3	-	7
Cuffytown Creek (Edgefield), S.C.	7	-	53
Dutchmans Creek, S.C.	2	-	19
Palmetto, Ga.	14	11	39
Siloam, Ga.	18	18	41
Danburg, Ga.	1	1	5

Drill hole sites were located in the Siloam (2) and Palmetto (1) plutons. Drilling of the Pageland hole was completed at about 690 feet, and the Cuffytown Creek drill hole was begun and since completed at 964 feet.

RECONNAISSANCE LITHOLOGY AND STRUCTURE OF THE SOUTHERN RALEIGH BELT AND ADJACENT CAROLINA SLATE BELT, NORTH CAROLINA

Stewart S. Farrar

A reconnaissance map is being produced of the Raleigh belt and Carolina slate belt rocks bounded by the Durham-Wadesboro Triassic basin on the west, Atlantic Coastal Plain sediments on the east, latitude 35°15', and the North Carolina-Virginia border. This progress report covers the part of this area between latitudes 35°15' and 36° (Figure A1).

The purposes of this study are to determine the relationship of the Rolesville batholith tc the surrounding country rock and to provide a geologic base for the geophysical interpretation of Piedmont stratigraphy underlying Atlantic Coastal Plain sediments to the east.

Previous Work

Parker (1968) gave a brief summary of the structure and stratigraphy of this area. In addition, a number of theses at North Carolina State University, Raleigh, and the University of North Carolina, Chapel Hill, cover parts of this area (Carpenter, 1970; Cook, 1972; Dickey, , Farquhar, 1952; Fortson, 1958; Glover, 1963; Juli. 1972).

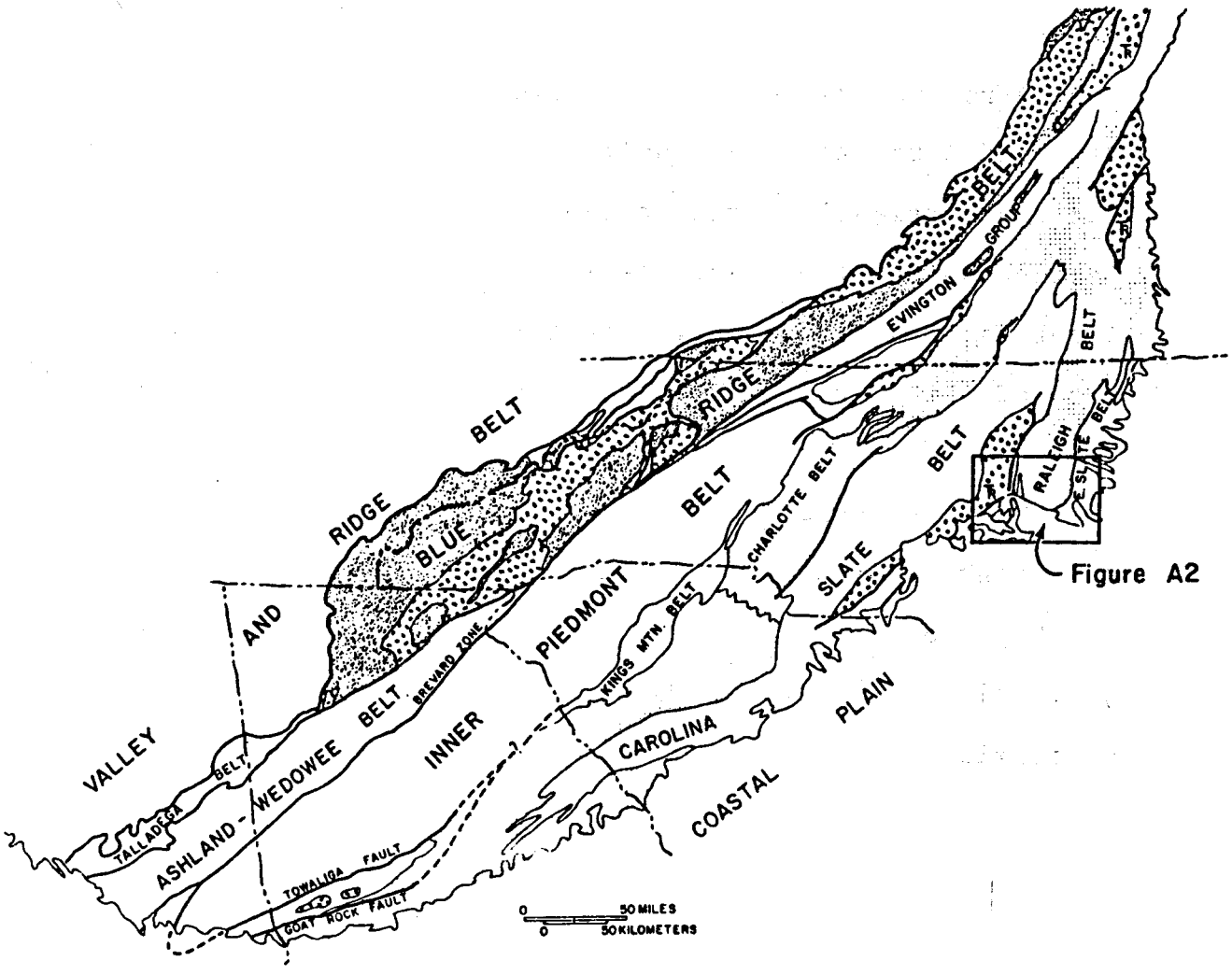

Figure A1. Generalized geology of the southern Appalachians modified by L. Glover III from Fisher and others (1970).

Petrography, chemistry and geophysical investigations of the Rolesville batholith rocks, and a brief discussion of the surrounding country rocks have been previously presented in progress reports (VPI&SU-5103-3, 5103-4, 5103-5).

Lithologies

Abbreviations given in parentheses refer to map units in Figure A2.

Rolesville Batholith

The Rolesville batholith, including its various phases--Rolesville main phase (Rmp), Archers Lodge porphyritic phase (App), Louisburg pluton, and Castalia pluton (Cp)--were described in Progress Report VPI&SU-5103-3. Descriptions of these bodies are not elaborated on here except to differentiate a border phase along part of the western contact of the Rolesville main phase. The Rolesville main phase (Rmp) consists of medium- to coarse-grained biotite granite, with a weak to moderate biotite foliation parallel to very weak alignment of K-feldspar crystals. The Rolesville border phase (Rbp) consists of typical Rolesville main phase biotite granite, but contains major infolded layers and xenoliths of the strongly layered biotite-hornblende gneiss which is in contact with the Rolesville batholith in this area.

Explanation

$\overline{TR}$	Triassic rocks of the Durham-Deep River-Wadesboro basin
Sgr	Sims pluton. Medium-grained, post-tectonic biotite granite
Cp	Castalia pluton. Medium-grained, post-tectonic biotite granite
Rmp Rbp App	Rolesville batholith. Rolesville main phase (Rmp) - medium-grained, syntectonic, biotite granite; Rolesville border phase (Rbp) - Rolesville main phase with very plentiful xenoliths of adjacent country rock; Archers Lodge porphyritic phase (App) - very coarse-grained, K-feldspar porphyritic biotite granite
gr	Unnamed, small plutons of medium-grained biotite granite-granitic gneiss
mv	Metavolcanics undivided. Greenschist facies metamorphosed mafic and felsic flows, pyroclastics, and minor associated metasiltstone and phyllite
mfv	Felsic metavolcanics. Greenschist and lower amphibolite grade metamorphosed crystal and lithic tuffs, minor devitrified obsidian, and near surface porphyritic felsic intrusives. Unit includes minor mafic metavolcanics and phyllites
mmv	Mafic metavolcanics. Greenschist grade metamorphosed basaltic flows, now greenstone, some with quartz-epidote amygdules; includes some interlayered felsic metavolcanics and phyllite
ph	Chlorite-muscovite-quartz phyllite
ph-mst	Interlayered chlorite-muscovite-quartz phyllite and muscovite-chlorite-albite-quartz metasiltstone
am	Quartz-epidote-chlorite-plagioclase-hornblende metagabbro (am_1); quartz-epidote-chlorite-plagioclase-hornblende amphibolite, probably metavolcanic (am_2)
gms	Biotite-garnet-quartz-muscovite schist
qt-gms	Biotite-garnet-quartz-muscovite schist ± staurolite, kyanite; garnet-staurolite-graphite-quartz-muscovite schist; biotite-muscovite quartzite; and muscovite-plagioclase-quartz gneiss
kq	Muscovite-kyanite quartzite
ms	Quartz-muscovite schist, and muscovite-quartz-plagioclase microgneiss; includes some felsic metavolcanics
gd	Biotite-hornblende-microcline-quartz-plagioclase metagranodiorite
lgn	Fine-grained biotite-opaque-plagioclase-quartz-microcline leucogneiss; includes 10-15 percent hornblende-plagioclase amphibolite
bhg	Biotite-hornblende-microcline-quartz plagioclase gneiss, layered; includes numerous, small quartz-plagioclase-microcline pegmatites, and minor lenses of Rolesville biotite granite
———	Triassic fault
– – – – – –	Approximate contact from field data
—·—·—·—	Approximate contact from aeromagnetic data
—?—?—	Contact querried where very speculative

Figure A2--(facing page). Lithologic map of the southern Raleigh belt and adjacent Carolina slate belt, North Carolina.

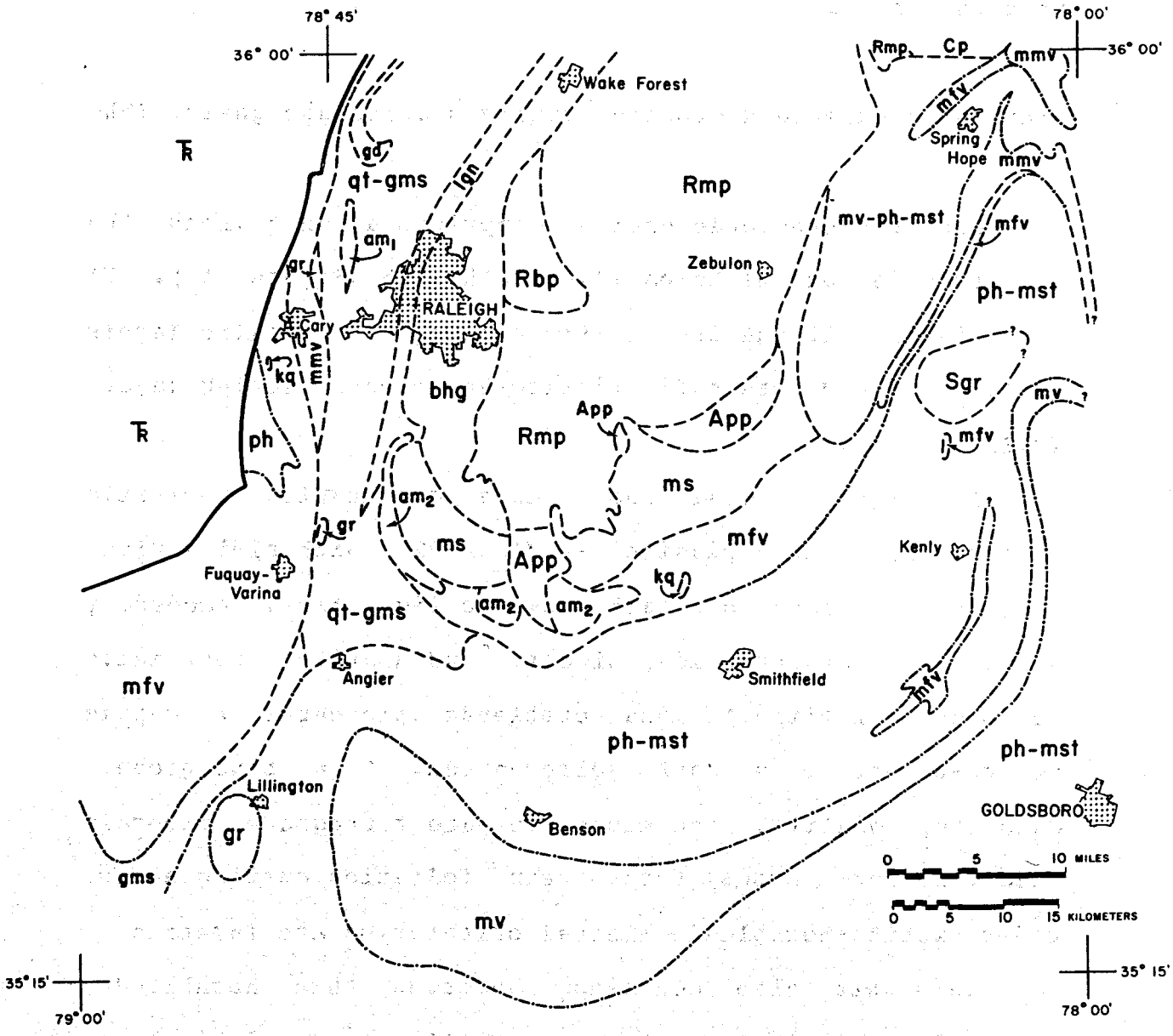
78° 45'
36° 00'
78° 00'
36° 00'
35° 15'
79° 00'
35° 15'
78° 00'
Wake Forest
Zebulon
Spring Hope
RALEIGH
Cary
Fuquay-Varina
Angier
Lillington
Benson
Smithfield
Kenly
GOLDSBORO
qt-gms
Rmp
Rbp
bhg
App
ms
mfv
ph
ph-mst
mv-ph-mst
Sgr
mmv
Cp
gms
gr
mv
0 5 10 MILES
0 5 10 15 KILOMETERS

A revised interpretation of the structure of the Rolesville batholith can be found in the structure section of this report.

Biotite-hornblende-microcline-quartz plagioclase gneiss (bhg)

Biotite-hornblende gneiss comprises a unit along the western side of the Rolesville batholith (Figure A2). It consists of alternating biotite bearing leucocratic layers (C.I. 2-5) and more mafic biotite-hornblende bearing layers (C.I. 10-15).

The major mineral constituents are quartz, perthitic microcline, unzoned plagioclase (An18-22) with albite rims, and biotite (pleochroic dark brown to light tan). Accessory minerals are opaque oxide, zircon, and apatite. More mafic bands contain titanite and hornblende (pleochroic X = pale yellow-brown, Y = dark yellow-green, Z = blue-green). Chlorite, hematite, and muscovite are retrograde minerals which, in some cases, form a weak foliation cutting across older biotite-hornblende mineral orientation and layering.

This unit also contains numerous thin hornblende-plagioclase amphibolite layers. Small quartz-plagioclase-microcline pegmatites are also common in this unit. The contact with the Rolesville granite is complex, with lenses of granite in the gneiss, and xenoliths of gneiss in the granite. This complexity resulted in the mapping of the Rolesville border phase (Rbp) described above. At least

part of the complexity of this contact results from post-intrusive folding of the contact.

(Biotite)-opaque oxide-plagioclase-quartz-microcline leucogneiss (lgn)

This is a fine-grained, light tan to white leucogneiss (C.I. 1-3). It forms a near-vertical, 1.0-1.5 km thick unit which is continuous along strike for at least 40 km (Figure A2). Very weak layering, formed by concentrations of quartz and very minor biotite, shows tight to isoclinal minor folds. The axes of these folds, and the parallel concentration of oxides cause a very strong lineation which is characteristic of this unit. Several saprolite outcrops of hornblende-plagioclase amphibolite occur in this area, suggesting that as much as 10-15 percent of this unit may be amphibolite.

This rock unit is associated with a distinct magnetic high on the aeromagnetic map of this region (Raleigh Sheet, U. S. Geological Survey, 1976). This magnetic lineament was useful in joining exposures into a continuous map unit.

Metapelite, feldspathic metaquartzite, quartzose gneiss (qt-gms)

This unit consists of (1) kyanite-staurolite-garnet-muscovite-biotite-quartz schist; (2) garnet-staurolite-graphite-quartz-muscovite schist; (3) (biotite)-muscovite quartzite; and (4) (biotite)-muscovite-plagioclase-quartz gneiss. These rock types are interlayered and complexly folded in a unit exposed for a width of up to 10 km and a length of at least 50 km. There are good exposures of these rock types along Crabtree Creek and U.S. 70 west of Raleigh. This area was described in some detail by Fortson (1958), and Broadhurst and Parker (1959).

The assemblage kyanite-staurolite-garnet-muscovite-biotite-quartz has been found only in the eastern edge of this unit, on the northwest outskirts of Raleigh. However, the assemblage without kyanite occurs in a schistose layer 5 km farther west. The assemblage kyanite-garnet-biotite-muscovite-plagioclase-quartz occurs within this map unit and the gms map unit at least as far south as 7 km north of Lillington. It may extend farther, but fresh samples for petrography have not been obtained farther south.

The assemblage garnet-staurolite-graphite-quartz-muscovite occurs in a sequence of graphitic layers which are found in a band approximately 1.5 km west of the lgn map unit. The individual graphitic layers are usually on the

order of 1-5 m thick and the group can be traced along strike about 25 km. Another graphitic layer 4 km farther west has been traced southeast into the phyllite-metasiltstone unit (ph-mst, Figure A2) (mapping by Parker, in Wilson and Carpenter, 1975). As mapped by Parker, this indicates that at least part of map unit qt-gms is the higher metamorphic grade equivalent of unit ph-mst.

A subordinate, but common, rock type is chlorite-biotite-muscovite quartzite which is, at least in part, the retrograde equivalent of the higher grade assemblages above, but for the most part is much richer in quartz.

The fourth important rock type is (biotite)-muscovite-plagioclase-quartz gneiss. Where least deformed, this rock type has relict plagioclase phenocrysts(?) which suggest that it is a highly recrystallized felsic volcanic unit. This could be equivalent of the felsic volcanic units to the south and southeast which have better preserved textures at lower metamorphic grade.

Quartz-muscovite schist and felsic microgneiss (ms)

This is a very poorly exposed unit which is usually found as muscovite schist saprolite. Rare fresh samples of the schist have the assemblage garnet-magnetite-quartz-muscovite, with or without minor chlorite and biotite. The unit also includes at least 20 percent muscovite-quartz-

plagioclase microgneiss, and minor epidote-quartz-(actinolite)-hornblende-plagioclase amphibolite. Lesser deformed portions of the microgneiss have well-preserved plagioclase phenocrysts in a fine-grained muscovite-quartz-plagioclase groundmass--suggesting that the microgneiss as a whole may be recrystallized felsic volcanics.

Amphibolite (am)

There are two textural varieties of amphibolite in this area. Am1, west of Raleigh (Figure A2), is a chlorite-epidote-quartz plagioclase-hornblende amphibolite. Chlorite-epidote-quartz is concentrated along a late, poorly-developed foliation. Undeformed volumes of plagioclase-hornblende have a relict texture shown by concentrations of fine, dusty, opaque inclusions. The inclusions are believed to have formed in clinopyroxene which has since reacted with much of the plagioclase to form hornblende. The relict subophitic texture shown by the dusty inclusion distribution indicates that this was a gabbroic intrusion.

Am2 has essentially the same mineralogy as am1--chlorite-epidote-quartz-plagioclase-hornblende (actinolite). However, it has no relict igneous texture, and the minor opaque oxide occurs as larger grains than the dusty inclusions of am1. This amphibolite is found

interlayered with felsic volcanic rocks, presenting the strong possibility that it is a metabasalt.

Metavolcanics (mfv, mmv, mv)

The southern and eastern portions of the mapped area consist dominantly of greenschist facies metavolcanics and metasediments. Areas of dominantly metavolcanic rocks are shown as felsic metavolcanics (mfv), mafic metavolcanics (mmv), and undivided metavolcanics (mv) (Figure A2). Particularly in the extreme south and east, exposures are very sparse, occurring only where major streams cut through overlying Coastal Plain deposits. These few outcrops are joined into major map units through the use of aeromagnetic anomalies (Raleigh Sheet, U. S. Geological Survey, 1976). Both felsic and mafic metavolcanics are associated with magnetic highs relative to surrounding metasediments, the mafic generally having higher anomalies than the felsic rocks.

The mafic metavolcanics are particularly well exposed along minor tributaries of the Tar River 5 km south of Spring Hope (Figure A2). It is a fine-grained, green-grey to green greenstone with elliptical quartz blobs (amygdules?) in some layers. Mineralogically, it is a monotonous assemblage of opaque-quartz-albite-epidote. Texturally, thin sections are uninformative, since the

dominant mineral--epidote--retains relict textures very poorly.

Felsic metavolcanics are the most resistant and best exposed of the greenschist facies rock types. Pyroclastic deposits are exposed adjacent to the greenstones along the Tar River south of Spring Hope. Crystal and lithic fragments up to 4-5 cm in diameter are common in the tuffaceous rock. A 1 m thick volcanic conglomerate with rounded felsic cobbles 8-10 cm in diameter is exposed in this sequence. At the Princeton I and Princeton II Nello Teer quarries 16 km east of Smithfield, a major porphyritic felsic metavolcanic unit is exposed. Most of the Princeton II quarry consists of probable crystal tuffs. The rock consists of plagioclase phenocrysts in a fine-grained epidote-muscovite-quartz-albite groundmass. The Princeton I quarry has several textural varieties, including (1) lithic, crystal tuffs with scattered lapilli 2-4 cm in diameter; (2) crystal tuff similar to Princeton II rocks; (3) probable devitrified glass--extremely fine grained, thin layered, epidote-muscovite-quartz-albite rock--with probable flow layering preserved in complex folds; (4) another probable flow, with epidote-muscovite-quartz-albite groundmass and epidote-quartz amygdules up to 2.5 cm in diameter.

West of Fuquay-Varina, an area shown as granite on the Geologic Map of North Carolina (Stuckey, 1958) is actually a rock with plagioclase phenocrysts in a graphic groundmass of

microcline and quartz. This plagioclase-rich rock is associated with a typical plagioclase crystal tuff. Both rocks have suffered greenschist facies metamorphism, and the intrusive quite possibly is the shallowly-emplaced equivalent of the felsic extrusives. A similar body 6 km north of Fuquay-Varina has been found at only one outcrop, and may be a dike or larger body. The largest expanse of felsic metavolcanics extends southwest from Fuquay-Varina in an area which appears as mica gneiss on the Geologic Map of North Carolina (Stuckey, 1958). This unit is dominantly a crystal metatuff, with thin quartz-muscovite and quartz-biotite schist layers.

Phyllite-metasiltstone (ph-mst)

The phyllite-metasiltstone unit is a major but very poorly-exposed sequence. The sparcity of outcrop can be surmised from the thin distribution of structural data (Figure A3). The map unit consists of fine-grained chlorite-quartz-muscovite phyllite and metasiltstone. Both rocks contain minor biotite, which increases in abundance toward higher grade rocks to the north and northwest. Very fine-grained muscovite-sericite is most abundant in the phyllite which has a very prominent muscovite foliation. Chlorite and quartz and, in some cases, epidote and albite are dominant in the metasiltstone. The metasiltstone

Explanation

Map units and contacts defined as in Figure A2.

Strike and Dip of


S_0+S_1


S_2


S_3


Vertical S_1+S_0, S_2, S_3


Horizontal S_3


Fold axis or mineral lineation

Figure A3. Geologic map of the southern Raleigh belt and adjacent Carolina strike belt, North Carolina.

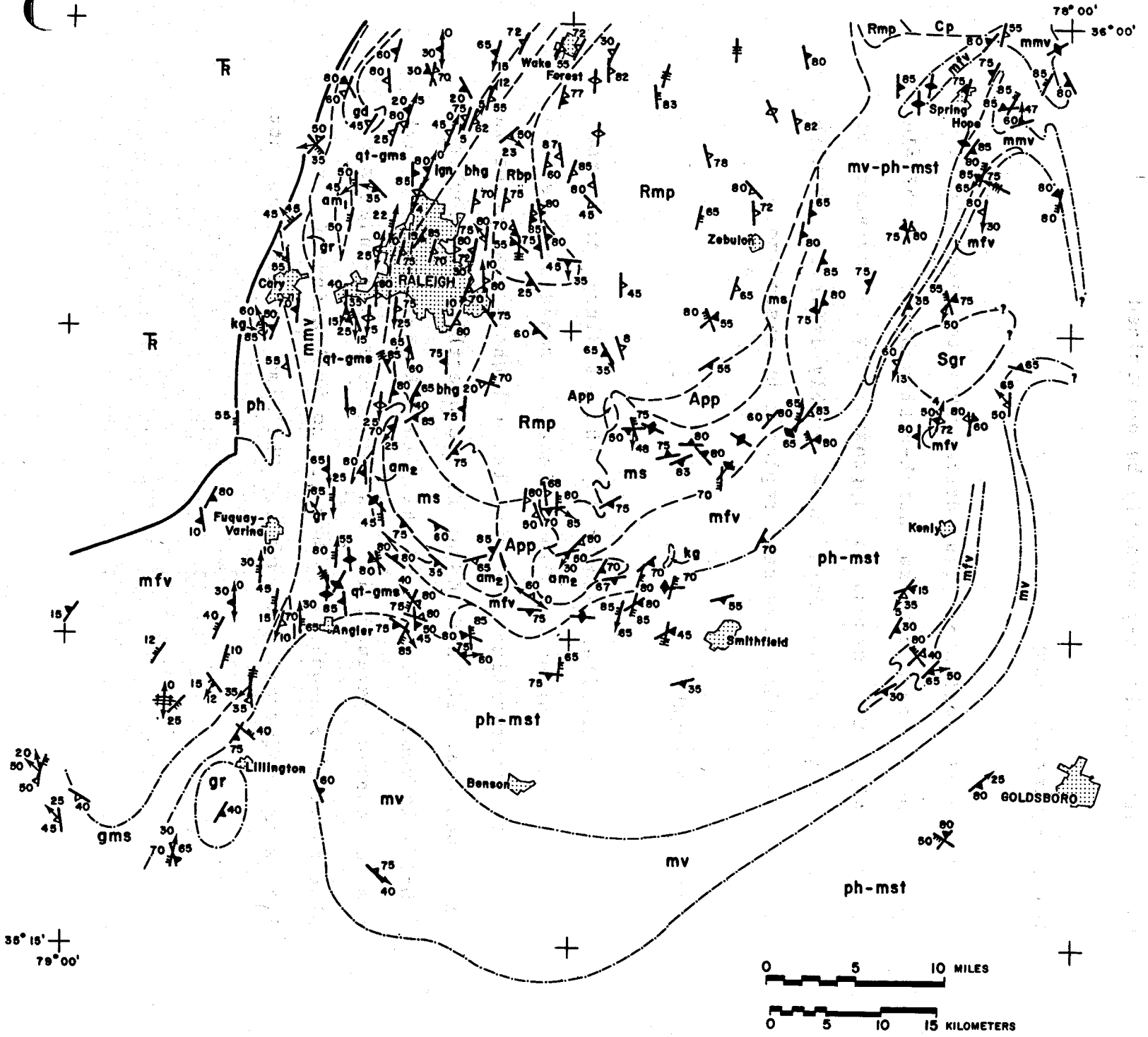
78° 00'
36° 00'
35° 15'
79° 00'
Rmp
Cp
mmv
mfv
Spring Hope
mv-ph-mst
Wake Forest
Zebulon
RALEIGH
Cary
Rmp
App
ms
mfv
Sgr
Fuquay-Varina
Kenly
ph-mst
Angier
Smithfield
Lillington
Benson
GOLDSBORO
mv
gms
gr
ph
qt-gms
bhg
Rbp
lgn
gd
kg
0 5 10 MILES
0 5 10 15 KILOMETERS

commcnly has graded bedding, and where least deformed, top-bottcm relationships may possibly be determined.

Kyanite-quartzite (kq)

Twc small bodies of (muscovite)-kyanite quartzite have been mapped. One is 8 km north-northwest of Smithfield (Figure A2). The second is approximately 10 km west of Raleigh (Figure A2). Both have highly deformed kyanite laths, scme of which have been replaced by muscovite.

Sims granite (Sgr)

The Sims granite (Figure A2) is a medium- to coarse-grained bictite granite. Plagioclase is zoned and has been extremely saussuritized, giving it a light-green color in hand specimen. The K-feldspar is macroperthitic microcline. Biotite is mostly altered to chlorite. A phyllitic xenolith has the contact metamorphic assemblage chlorite-andalusite-biotite-musccvite-quartz. There is no indication of a post-intrusive deformational event. The Sims granite has not been dated.

Unnamed small granites (gr)

Three small granite bodies have been mapped west and southwest of Raleigh. All three are medium-grained biotite granites. The northern two have strong, late muscovite-chlorite foliations. The more southern of these two is a protomylonite. The southernmost of the three--southwest of Lillington--nas a weak biotite foliation. It has macroperthitic microcline and slightly saussuritized plagioclase. It is very similar to the Rolesville main phase.

Granodiorite (gd)

Northwest of Raleigh there is a medium-grained biotite-hcrnblende-quartz-plagicclase granodiorite intrusive (Figure A2). Plagioclase has been highly saussuritized, but has not been recrystallized. Biotite and hornblende form a moderate to strong foliation. Accessory minerals include titanite, opaque, and apatite. This intrusive has apparently been subjected to the same metamorphic event as the surrounding country rock.

Ultramafics

Numerous small chlorite-talc-serpentine-amphibole ultramafic bodies have been mapped in the qt-mgs unit, starting about 10 km north of Raleigh and continuing north of this map area (Wilson and Carpenter, 1975; Dickey, 1963). They are not shown in Figure A2, since their contacts were not mapped in this study.

Diabase

Numerous diabase dikes transect the map area. Most of them have a northwest to north-northwest strike, and approximately vertical dip. Those observed have a gabbroic composition, but they were not examined in this study. In order to avoid clutter, they are not shown in Figure A2.

Structure

The Raleigh belt and Carolina slate belt rocks east of the Durham Triassic basin (Figure A3) have been subjected to a minimum of three deformational events. The following structural interpretation expands, and it is hoped, corrects the structural interpretation of the more limited Rolesville area presented by Becker and Farrar in Progress Report VPI&SU-5103-3.

S-surfaces

Bedding, Sb, can be observed in metasediments and metatuffs of the least deformed greenschist facies Carolina slate belt rocks. Sb is also observed as probable flow layering in both mafic and felsic flows in the Carolina slate belt rocks. Attitudes of Sb are not shown in Figure A3, because they have been observed only on the limbs of small-scale folds.

S0 is defined as compositional layering, the earliest observed surface in the more highly recrystallized rocks of the Carolina slate belt and Raleigh belt. S0 may, in some cases, be Sb, but in most instances it is probably a metamorphically-formed layering.

S1 is a strongly-developed penetrative foliation of planar and elongate minerals formed during the D1 deformational event. It is generally axial planar to isoclinal folds in Sb and S0. In many outcrops, S1 parallel to S0, or S1 parallel to Sb is the only measurable surface. F1 hinge surfaces (parallel to S1) folded into F2 folds give proof of the existence of separable D1 and D2 events. F1 folds have only been defined on outcrop scale; none were large enough to show on Figure A3.

S2 is a strong- to moderately-developed locally penetrative foliation. In some felsic rock types it is poorly defined, and exists only as the hinge surfaces of

tight to isoclinal F2 folds. In micaceous rocks, S2 is a biotite or muscovite foliation or, in some cases, a crenulation cleavage. F2 folds are generally close to tight, and have been found both as refolded F1 folds, and refolded by F3 folds. F2 folds ranging in scale from microscopic to regional have been found.

S3 is highly variable in its development. In the greenschist facies rocks south of the Raleigh belt, S3 commonly occurs as a fine penetrative crenulation cleavage, which is axial planar to small, 20 cm to 1 m wavelenth, open F3 folds and approximately axial planar to regional F3 folds. In the Spring Hope area, the few measurements of S3 are on crenulation cleavage, which is very difficult to distinguish from S2. West and southwest of Raleigh, S3 is a strongly-developed retrograde muscovite-chlorite foliation or fracture cleavage in the pelitic and quartzo-feldspathic rocks which form the western border of the Raleigh belt and adjacent Carolina slate belt rocks.

Structural Interpretation

The structure of this area is discussed in terms of subareas for convenience of presentation (Figure A4a). Area I is dominated by moderately to gently westward-dipping S3. Area II occupies the core of the Wake-Warren anticlinorium of Parker (1968). This is a major F3 structure. Area III

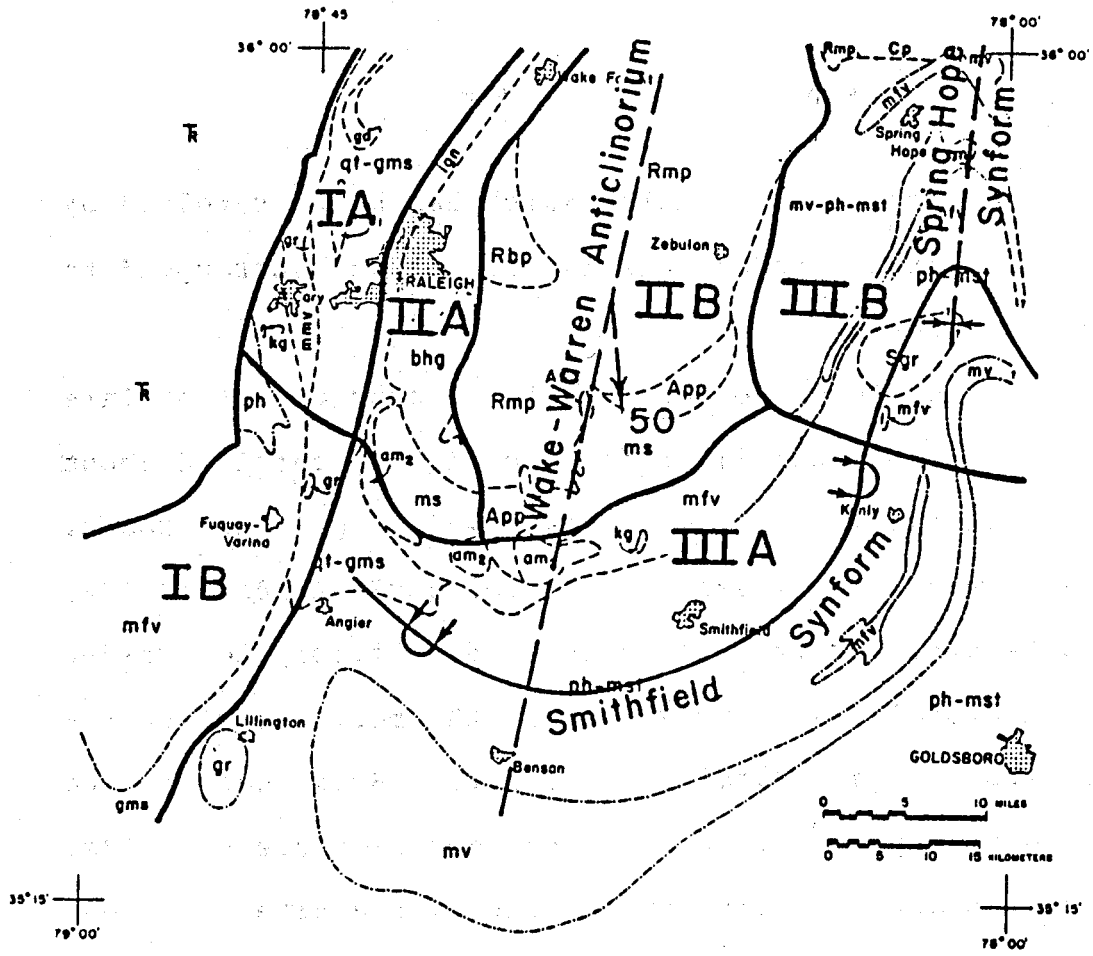

Figure A4a. Major structures of the southern Raleigh belt and adjacent slate belt. Numbered subdivisions are those for stereographic projections in Figure A5.

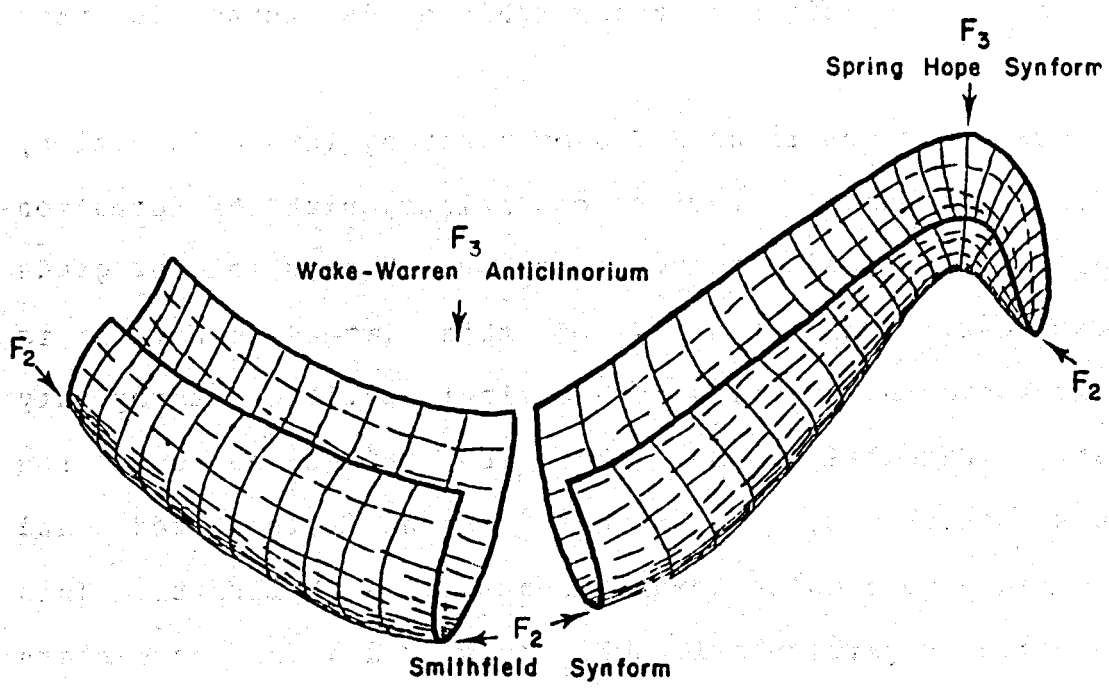

Figure A4b. Cartoon of the Smithfield F2 synform, refolded by F3 folds. Numbered subdivisions are those for stereographic projections in Figure A5. Surface shown is the major metavolcanic unit. F2 and F3 are not coaxial.

encompasses a regional F2 fold which has been refolded by F3. Stereographic projections in Figure A5 correspond to subareas in Figure A4.

Area I is, for the most part, a zone of major late deformation. Isoclinal F1 folds are tightly refolded about F2 axes. Textural study, particularly of pelitic rocks, indicates that the D2 event, producing F2 folds and S2, occurred before, or at the height of, metamorphic grade. Tight F2 microfolds are preserved in the form of graphite-rich layers in a graphitic schist. Both garnet and staurolite porphyroblasts have grown across these F2 folds. The porphyroblasts in this particular sample have not been rotated or deformed in any way. This texture indicates that there was post-D2 crystallization under amphibolite facies conditions--the highest metamorphic grade found in this area.

Most outcrops in area I show a strong late deformation, D3, under greenschist facies conditions, with the formation of a muscovite-chlorite foliation which cuts higher grade assemblages. The intensity of this late deformation is highly variable. Samples from a single pelitic outcrop vary greatly. Parallel to S3, there are thin zones of a few meters thickness, which have been mylonitized and retrograded to a chlorite-quartz-muscovite phyllonite. This assemblage is particularly well developed along the eastern border of subarea IB, north of Angier. Some outcrops

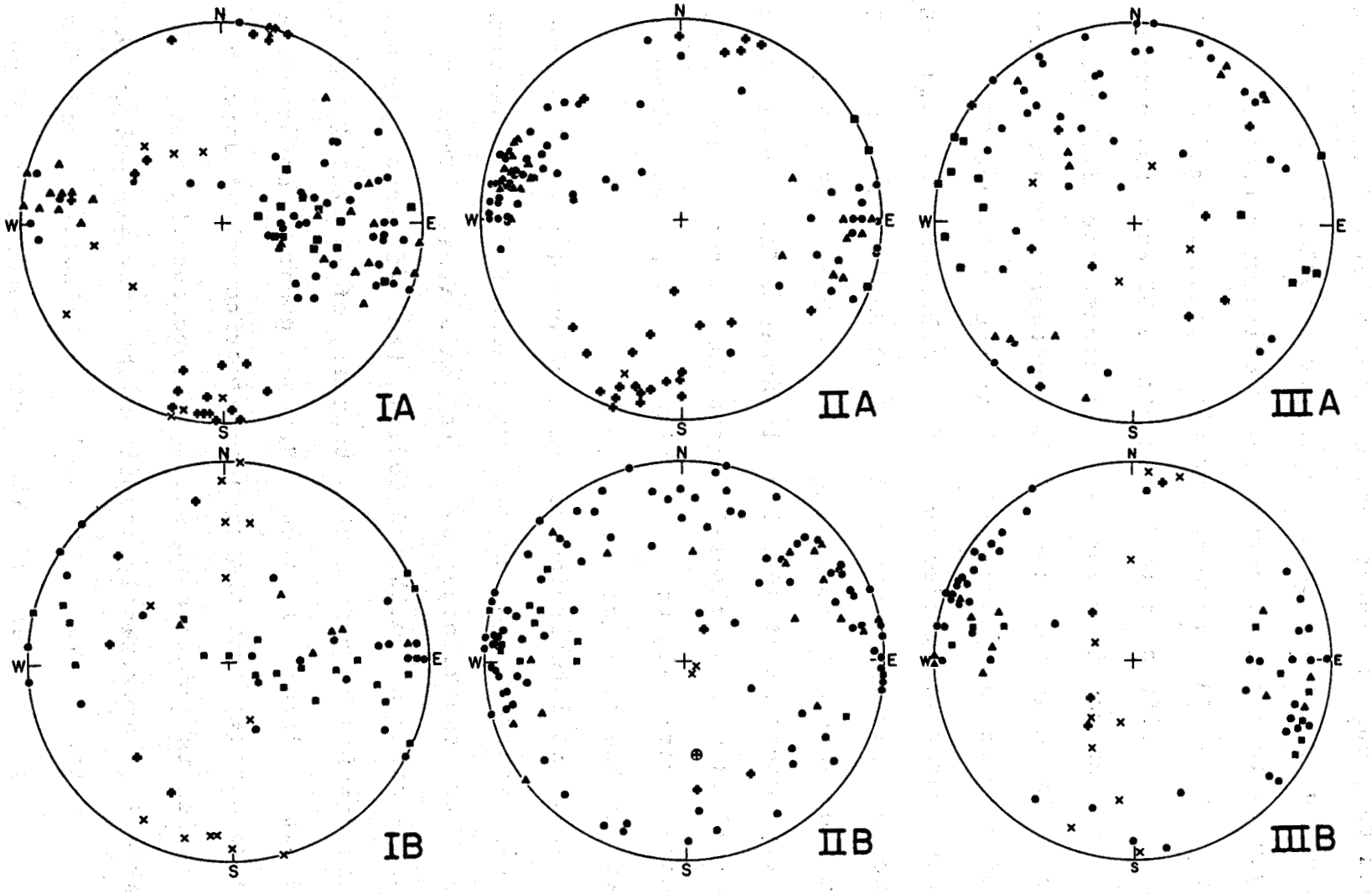

Figure A5. Stereographic projections of data from areas outlined in Figure A4a. Symbols are: poles to S_0+S_1 (●), poles to S_2 (▲), poles to S_3 (■), F_1 and F_2 fold axes and lineations (✚), and F_3 fold axes (×).(⊕) in IIB is the approximate F_3 fold axis (50, S05E).

contain only chlorite-quartz-muscovite, while others contain rotated and partially retrograded porphyroblasts of garnet and kyanite in a chlorite-quartz-muscovite groundmass.

In subarea IB, where metamorphic grade was not as high as IA, it is difficult to differentiate S2 and S3, both of which are muscovite-chlorite foliations, cutting mostly felsic volcanic assemblages. This probably results in some confusion in the assignment of foliations to S2 and S3.

Stereographic projections for subareas IA and IB (Figure A5) illustrate the dominance of S3 in this area. S3 varies from vertical to horizontal in subarea IB, while it is nearly constant at N0E, 35W in subarea IA. Both areas have fold axes and mineral lineations concentrated near horizontal parallel to the strike of S3, and plunging westward in the plane of S3.

Area I is interpreted to be a major deformation zone which dips moderately westward. This zone forms the western boundary of the Raleigh belt in this area. This zone apparently narrows northward toward the Virginia border, where it continues to form the boundary of the Raleigh belt (Casadevall, 1977). In area IB, the greatest deformation may be concentrated in the garnet-muscovite schist unit, but S3 foliation is moderate to strong throughout the area.

Area II approximately comprises the southern end of the Raleigh belt. The Rolesville batholith occupies approximately 70 percent of this area. Subarea IIA (Figure

A4) is dominated structurally by tightly compressed F2 folds with axial surfaces N10E, vertical, and approximately horizontal hinge lines and mineral lineations. S3 is almost absent in this area. F1 folds are found as small, isoclinal folds which have been refolded by F2 folds. Subarea IIB includes the Rolesville batholith and country rocks which occur both as xenoliths and folds projecting into the batholith. The Rolesville batholith is a pre- or syn-F2 intrusion. It has a weak to moderate S2 biotite foliation. S1 plus S0 can be measured in many gneissic xenoliths and areas of country rock folded into the granite (Figure A3).

The S2 foliation of subarea IIB has been folded to form the Wake-Warren anticlinorium (Parker, 1968). This major F3 structure plunges 50, S05E (based on folded S2), and weak S3 measurements give the axial surface N20E, 70E (Figure A5). The refolding of previously folded S1, about F3 axes, produces the complex pattern of stereoplot IIB (Figure A5). Fold axes defined by folded layering tend to be steep to moderately southward plunging.

Area III is dominated by a regional scale F2 isoclinal fold which is outlined by the pattern of major metavolcanic layers in a phyllite-metasiltstone sequence. Individual outcrops of the volcanic rocks in this area have been joined into map units through the slight topographic expression and relatively strong magnetic anomalies of the volcanic units. This regional F2 fold has been refolded in the F3 Wake-

Warren anticlinorium and the parallel F3 Spring Hope synform (Figure A4). Stereoplot IIIA (Figure A5) illustrates the complexity of folding of S1 which results from folding the Smithfield F2 fold by the Wake-Warren F3 fold. The Smithfield F2 fold is overturned for most of its length, and both limbs dip moderately to steeply south (Figure A4).

Good exposures of interfering F1, F2 and F3 folds can be found in the closed Princeton I Nello Teer quarry, which is in a felsic volcanic sequence 16 km east of Smithfield. At this quarry, major, tight F2 folds refold smaller scale F1 folds, and are weakly refolded by D3, producing a weakly-developed crenulation cleavage in thin phyllite layers.

In area IIIB, the Spring Hope F3 fold is the dominant regional structure. It has tightly refolded the F2 Smithfield structure. This area presents the best case for the Smithfield F2 fold being synformal. Minor fold axes plunge toward the trough of the structure from both north and south. Figure A4b is a cartoon of the unerded portion of the Smithfield F2 synform, showing the non-coaxial nature of the F2 and F3 folds.

Conclusions

The southern Raleigh belt, and adjacent Carolina slate belt, have suffered a minimum of three deformational events (prior to late brittle faulting, which does not appear to have involved major movements within the mapped area). D1

and D2 were accompanied by a metamorphic event which reached amphibolite facies in the Raleigh belt, but only greenschist facies in the slate belt. The Carolina slate belt-Raleigh belt contact appears to be a metamorphic grade change along the eastern and southern margins of the Raleigh belt. The contact could reasonably be placed approximately along the contact between muscovite schist (ms, Figure A2) and the metavolcanics and amphibolite (mfv and am2, Figure A2). No attempt was made in this reconnaissance to tie down the location of isograds. The western boundary of the Raleigh belt may also have been a metamorphic grade change, but it is now a major deformation zone. This westward-dipping deformation zone is part of the Eastern Piedmont fault system of Hatcher et al. (1977).

From examination of this area, it appears that the major northeast-trending structures of the Piedmont in this region are D3 folds which have refolded F2 structures which had generally east-west trends. It is therefore to be expected that there are culminations and troughs in the F3 regional fold axes as they cross the pre-existing F2 folds. In some areas attenuation parallel to S3 has been great enough to produce mylonites, or at least protomylonites along the limbs of the S3 structure--this appears to be the case along the western border of the Raleigh belt in this area.

It seems reasonable to expect similar structures in covered slate belt rocks to the east--major north-northeast trending F3 folds refolding the more nearly east-west trending F2 structures.

COMPOSITIONAL VARIATIONS OF SOUTHEASTERN GABBROS

S. W. Becker

The gabbroic plutons of the southeastern U. S. are closely related in time, space, and origin to the 300 m.y. granitic plutons (Figure A6; see previous report, VPI&SU-5103-5). Chemical variations in these gabbroic bodies should outline differences between the mafic plutons, and may aid in determining the relationship between the origins of the granitic and gabbroic plutons.

Divisions based on fundamental differences between the mafic plutons were first made by Medlin et al. (1972), who recognized two types of intrusions: those composed of gabbro-diorite-syenite, and those of gabbro/gabbro-norite. The Mt. Carmel and Concord complexes comprise the first group; all other mafic plutons that have been studied fall in the second category.

As a basis of further comparison, the gabbroic plutons can be classified according to their whole rock compositions. The classification scheme used in this report is that proposed by Irvine and Baragar (1971), which is derived primarily from divisions for basic volcanic rocks proposed by Kennedy (1933) and Tilley (1950). In this scheme, all igneous rocks fall into one of two categories: alkaline or subalkaline; subalkaline rocks are further subdivided into tholeiitic and calc-alkaline series.

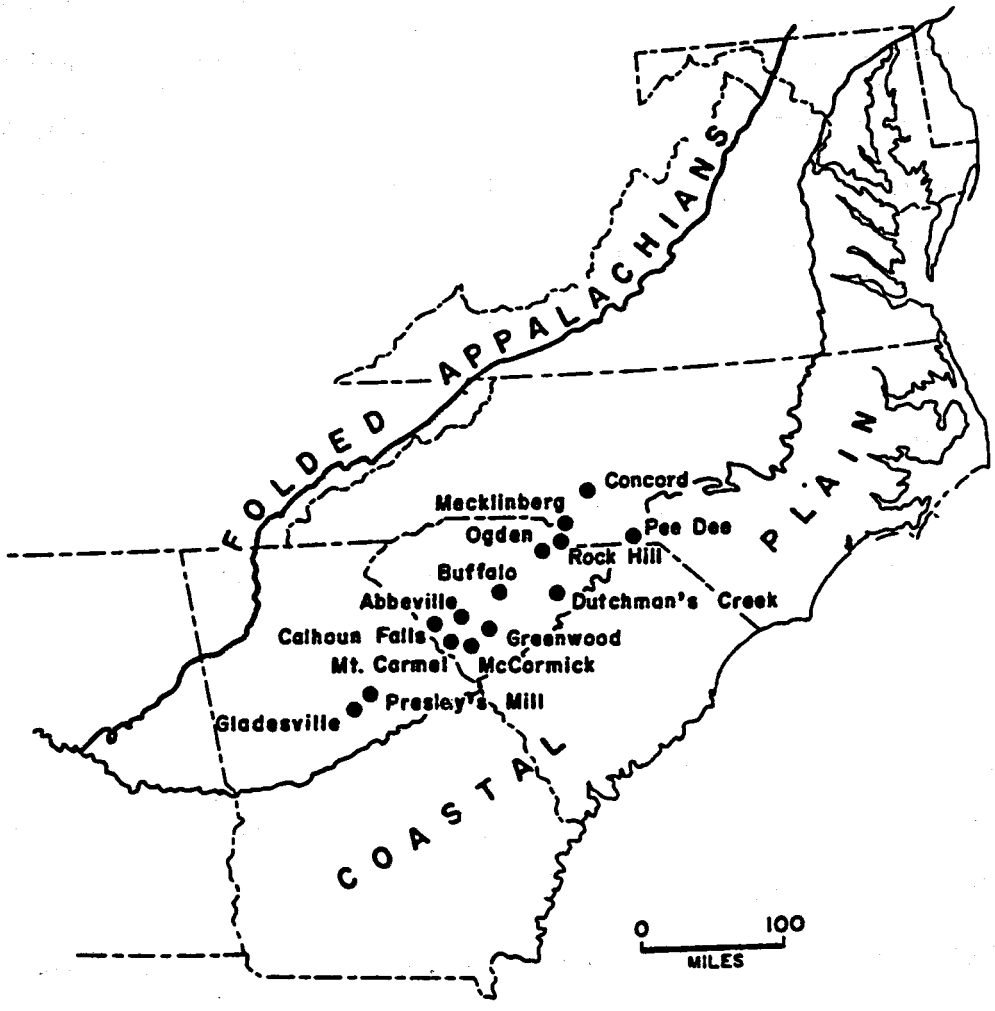

Figure A6. Locations of gabbroic plutons of the southeastern U.S.

Chemical distinctions between these series are not always clear-cut, and commonly analyses of rocks with a wide range of SiO2 values are needed to determine whether an igneous province is more nearly "tholeiitic" or "calc-alkaline."

Whole rock compositions were found in the literature for the following gabbroic plutons: Concord (gabbro, Cabaup, 1969; average for syenite, Butler and Ragland, 1969); Mecklenberg (Hermes, 1967); Ogden (average, Butler, and Ragland, 1969); Presley's Mill (Libby, 1971); Buffalo and Mt. Carmel (Medlin, 1968). (Compositions of the Cleveland gabbro reported by Constantino-Herrera (1971) were not used because of the low totals.) In many of the analyses, ferrous/ferric iron ratios are lacking. The relation proposed by Irvine and Baragar (1971, p. 526) for assigning an artificial Fe^{2+}/Fe^{3+} (%Fe2O3 = %TiO2 + 1.5) is inappropriate because of the high titanium content of some samples (>5% for some Mt. Carmel rocks). For uniform comparison, therefore, all iron has been converted to Fe^{2+}. This assignation has several effects on the normative calculations. Magnetite and hematite cannot be formed. Moreover, because of the increased amounts of Fe^{2+} available to combine with SiO2 where Fe^{3+} forms hematite and magnetite in the norm), the rock appears to be more undersaturated; the amount of normative hypersthene decreases and olivine and nepheline increase. Classification diagrams involving normative olivine, orthopyroxene, nepheline, albite, or quartz, therefore, cannot be used with any accuracy, and

classification of the gabbros is based instead on diagrams showing variations in percent oxides.

Classification Diagrams

Given the above limitations, the division between alkaline and subalkaline rocks can best be seen on a plot of Na2O + K2O versus SiO2 (Figure A7). On this diagram, rocks of all compositions from the Mt. Carmel plutonic complex and the syenite from the Concord ring dike fall in the alkaline field; all other compositions fall in the subalkaline field, although many are near the dividing line. Rocks from the Buffalo, Mecklenberg, and Presley's Mill gabbros show a fairly wide scatter; compositions of gabbro from the Concord ring dike form a tight cluster close to the alkalic field.

The plutonic complexes containing diorite and syenite thus appear to have strong alkaline affinities: rocks of all compositions from the Mt. Carmel complex are alkalic, as are the Concord syenites, and Concord gabbros have relatively high alkali contents as well. Medlin (1968) similarly concludes that the Mt. Carmel complex is alkalic, and that the Concord complex probably has alkalic tendencies. Cabaup (1969), however, did not mention that clinopyroxene in the Concord gabbro was titanaugite (a characteristic mineral of alkaline rocks), and proposed that the Concord gabbro is most like continental margin tholeiites. The comparison was based on the sum of the

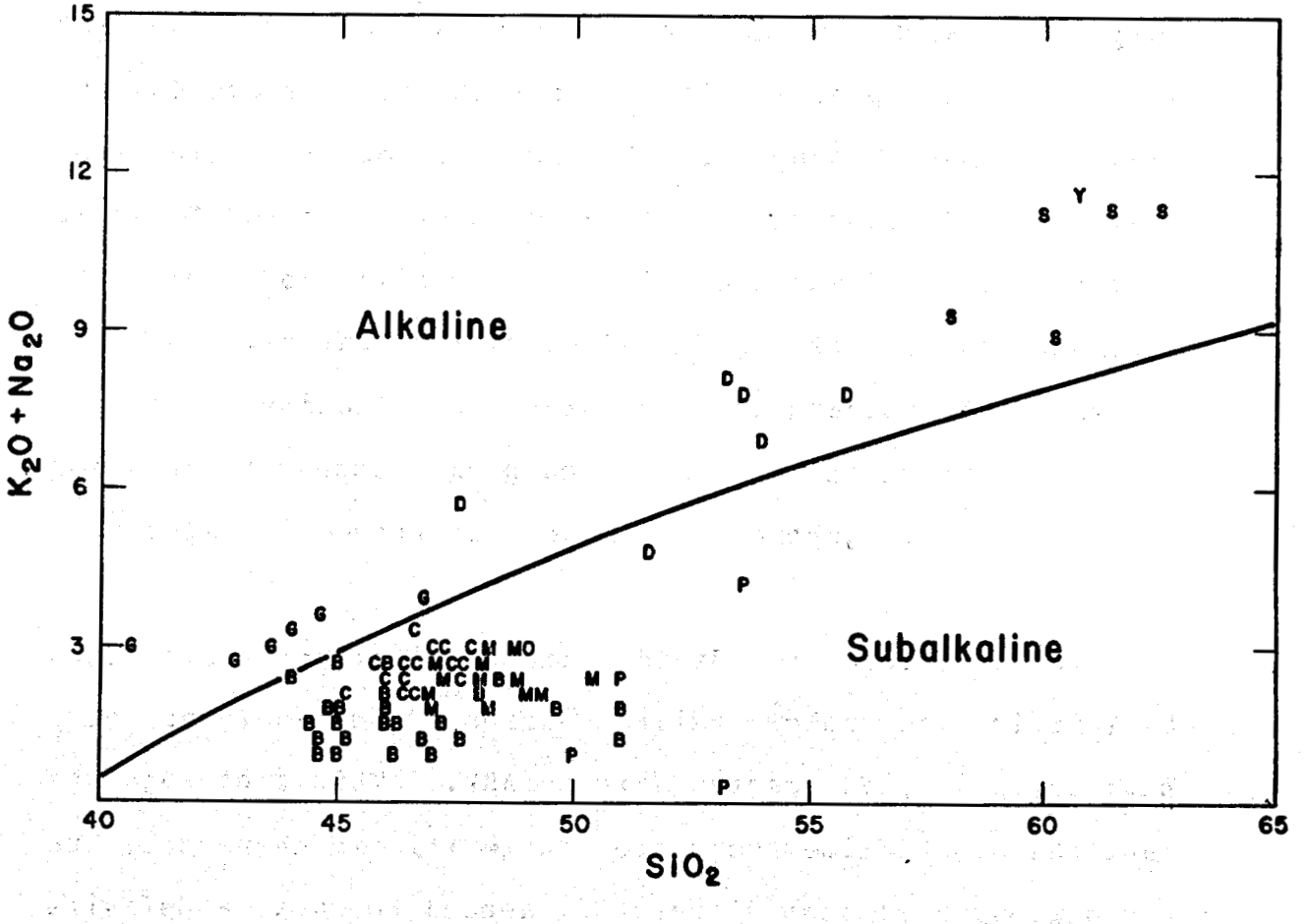

Figure A7. Alkalies-silica plot showing alkaline and subalkaline compositions. Dividing line from Irvine and Baragar (1971). Symbols: B--Buffalo; C,Y--Concord gabbro and syenite; G,D,S--Mt. Carmel gabbro, diorite, and syenite; M--Mecklenberg; O--Ogden; P--Presley's Mill. Sources of data listed in text.

differences in percent oxides of the average Concord gabbro and other types of mafic rocks; the sum was smallest for continental margin tholeiites. By this method of comparison, 1% difference in K2O is equivalent to 1% difference in SiO2 or Al2O3, and relations between elements during magmatic evolution are not taken into account. Comparison with average rock compositions (Irvine and Baragar, 1971, Appendix II) shows that the average Concord gabbro (Cabaup, 1969, p. 26) is too low in potassium, aluminum, and titanium to be called even a "K-poor" alkali olivine basalt. The rock is most similar to the high-aluminum basalt of the calc-alkaline series, but the presence of titanaugite indicates an alkaline tendency. Both the Concord and Mt. Carmel complexes appear to be older than the other gabbros; the age difference is discussed below.

In an effort to divide the subalkaline rocks into tholeiitic and calc-alkaline series, the analyses were plotted on an AFM diagram (Figure A8). This plot suggests that the subalkaline rocks are tholeiitic in character, but a wider span of compositions is needed to show a definite trend. Medlin et al. (1972) note that the Buffalo gabbro shows both calc-alkaline and tholeiitic affinities. Butler and Ragland (1969) conclude that the gabbros form an alkali-calcic magma series, although in an earlier study (1966) they proposed that the gabbros are derived from a tholeiitic magma.

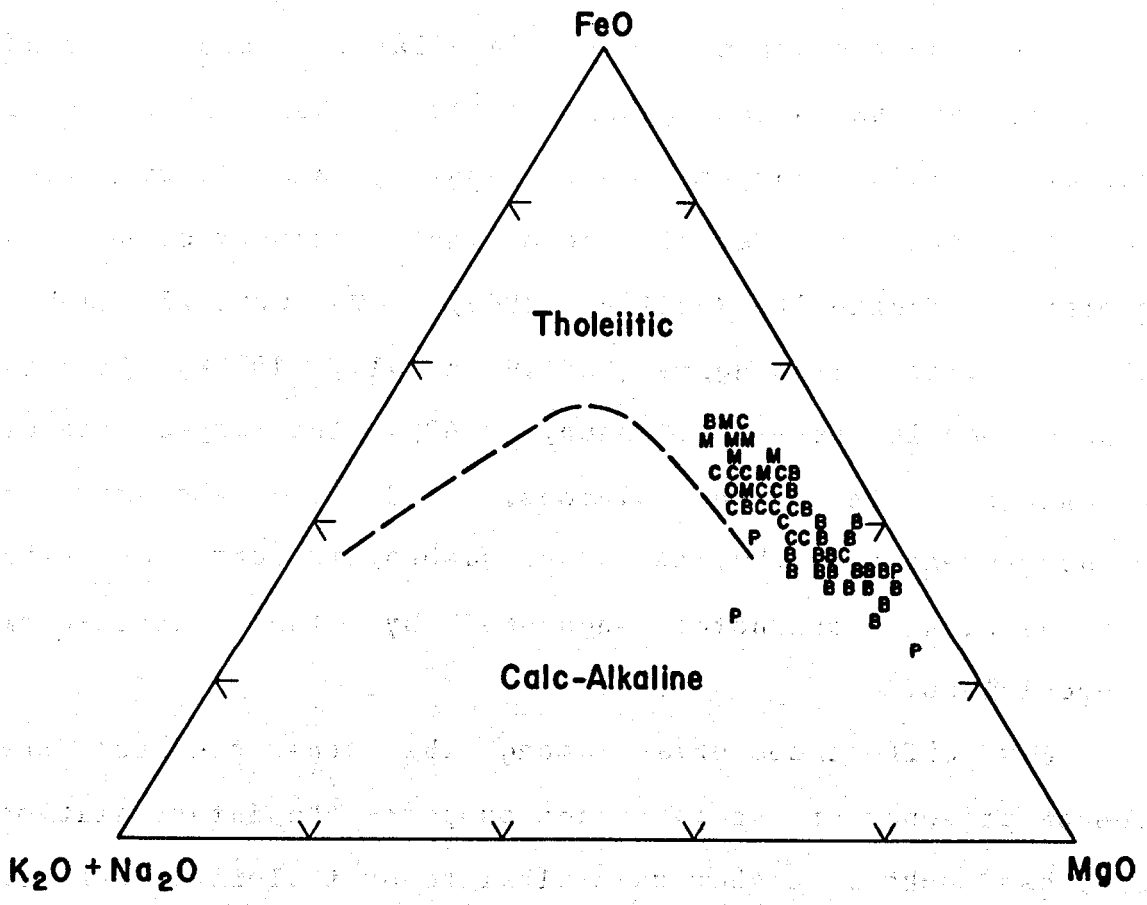

Figure A8. Ternary plot of total alkalies, iron as FeO, and MgO divided into calc-alkaline and tholeiitic fields, after Irvine and Baragar (1971). Symbols as in Figure A7.

Mineralogy

Alkali basalts can be characterized by the usual absence of orthopyroxene and by the high titanium content of a calcium-rich augite. Tholeiitic and calc-alkaline rocks, in contrast, generally contain both orthopyroxene and a low-calcium clinopyroxene (Irvine and Baragar, 1971).

The petrographic data available show strong similarities among the gabbro plutons (Table A1). Most contain olivine, hypersthene, augite, and labradorite. Notably, the Mt. Carmel gabbro lacks orthopyroxene and contains titanaugite (Medlin, 1968). The Concord gabbro also contains titanaugite (Medlin et al., 1972), although hypersthene is present (Cabaup, 1969). The appearance of titanaugite in these plutons, and the absence of orthopyroxene from the Mt. Carmel gabbro, is consistent with the alkaline character suggested by their whole-rock compositions.

Few differences exist among the other plutons; the common presence of two pyroxenes supports the interpretation of these rocks as either calc-alkaline or tholeiitic series. Texturally, where such data have been reported, most of the subalkaline plutons are similar as well. Olivine crystals in the Buffalo, Gladesville, Mecklenberg, and Rock Hill gabbros are all mantled by complex reaction rims of pyroxene or amphibole. McSween and Nystrom (in press) note that such rims are lacking in the Dutchman's Creek gabbro.

TABLE A1.

MINERALOGY OF SOUTHEASTERN U. S. GABBROS

Pluton	Olivine	Orthopyroxene	Clinopyroxene	Plagicclase	Reference
Buffalo	Fo68-79	En75-78	Wo41.5En44.5 -Wo44En41	An53-79	Medlin, 1968
Cleveland	yes	hyp + en	augite-diopside	An42-74	Constantino-Herrera, 1971
Concord	Fo67-84	hyp	titanaugite	An61	Cabaup, 1961; Medlin et al., 1972
Dutchman's Creek	Fo66-88	En64-78	augite	An41-76	McSween and Nystrom (in press)
Gladesville	Fo79-86	En82-83	augite	An65-69	Matthews, 1967
Mecklenberg	Fo61-72	En59-71	augite	An51-67	Hermes, 1967
Mt. Carmel	Fo57	no	titanaugite Wo47En40	An52-62	Medlin, 1968
Ogden	yes	hyp	augite	yes	Chalcraft, 1977
Pee Dee	yes	yes	augite	An38-45	this report
Presley's Mill	no	En63-74	augite	An44-67	Libby, 1971; Myers, 1968
Rock Hill	yes	hyp	augite	An32-72	Chalcraft, 1968

Plagioclase crystals are generally only slightly zoned; such lack cf strong zoning is characteristic of adcumulate growth, and suggests that the gabbros crystallized as adcumulates.

Relatien cf Heat Production to Whole Rock Chemistry

Syenite in the Mt. Carmel complex is thought to represent the late-stage differentiate cf a gabbroic magma (Medlin, 1968); the Concord syenite, toc, is probably a product cf prclonged fractionation. In spite cf the high degree of differentiation needed to form these syenites, they have very low heat productions: values of 1.2 and 1.8 X 10^{-13} cal/cm^3-sec have been measured for Concord syenite, and Mt. Carmel syenite produces 1.6 x 10^{-13} cal/cm^3-sec (Report VPI&SU-5103-5). These values are much lower than average heat production of southeastern granites with similar K2O and SiO2 contents. High degree of magma differentiation alone is clearly not sufficient for high heat prcduction; the composition of the parent magma is a critical factor. Basaltic magmas contain very low amounts of U and Th, and even prolonged fractionation cannot concentrate these elements enough to cause high heat production in the late-stage differentiates.

Conclusions

Whole rock chemistry shows that the gabbroic plutons of the southeastern U.S. fall into two categories. Gabbro-diorite-syenite complexes are alkaline; gabbro/gabbro-norite complexes are subalkaline, and cannot with any certainty be called calc-alkaline or tholeiitic. The alkaline gabbros appear to be somewhat older than the other mafic plutons. Concord syenite has been dated at 413 m.y. (Rb-Sr, 1 = ±21 m.y., Fullagar, 1971) and 425 ± 110 m.y. (Overstreet and Bell, Table 7, p. 93, 1965). Biotite from Mt. Carmel diorite has been dated at 380, 386, and 387 m.y. (K-Ar, Medlin, 1968). None of the subalkaline plutons has been dated directly. The Pee Dee gabbro intrudes, and is probably contemporaneous with, the Lilesville granite, which has been dated at 322 ± 14 m.y. (Rb-Sr, Fullagar, reported by Bell et al., 1974). The Buffalo gabbro is interpreted to be younger than the Mt. Carmel complex (Medlin, 1968). Data are not available for other gabbroic plutons, but their lack of metamorphic textures suggests that they are younger than 350 m.y.

The relation between the chemical affinities of the gabbros and granites is not clear. As a bimodal suite, the plutons should all generally be either tholeiitic or calc-alkaline, or of a common middle ground. Fullagar and Butler (1977) postulate that the granites are calc-alkaline.

Bimodal suites, however, are relatively rare in calc-alkaline series, and further work may show that the mafic and felsic plutons together follow trends more characteristic of tholeiitic suites.

DESCRIPTION OF THE SILOAM PLUTON

J. Alexander Speer

The Siloam pluton, Greene Co., Georgia, is the first ccarse-grained, Late Paleozoic pluton studied for the new ccntract period. This report is based largely on field work supplemented by some thin-section petrography. Of the other coarse-grained, Late Paleozoic plutons in the southeast (Figure A9), the Winnsboro, Liberty Hill, Pageland, and Lilesville have been studied in some detail, whereas the Churchland, Bald Knob, South Carolina U1, Rabon Creek, Danberg, and Appling have been locked at only on a reconnaissance basis. The Palmetto granite will be described in the next quarterly report.

The Siloam was studied because of the high heat generation values (average 10.3 HGVU, VPI&SU-5103-5) obtained in the reconnaissance sampling. This value is approximately twice the value for other coarse-grained granites in the southeast. Field work demonstrates that the Siloam is similar to the other post-metamorphic plutons of the southeast, a multiple-intrusive granitic complex with the ccncentric distribution of rock units indicative of a centered complex. The rock units are largely textural varieties. A distinct feature of the Silcam described below in more detail is a pervasive deformation, evident for the most part only in thin-section.

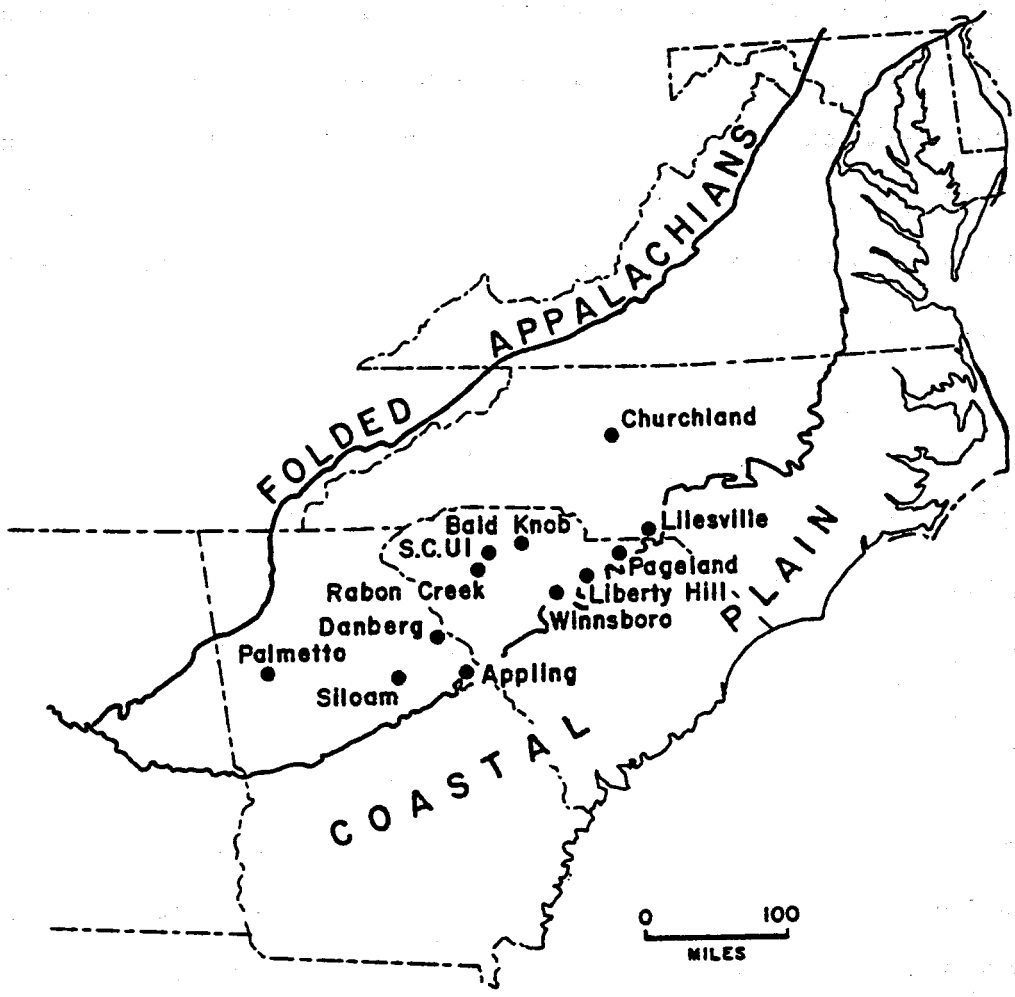

Figure A9. Location map of the coarse-grained, post-metamorphic, Late Paleozoic plutons of the southeastern United States.

Previous Work

The first descriptions of rocks from the Siloam pluton were by Watson (1902), who described three of the four facies of the Siloam recognized in this report. The Siloam pluton was first mapped and systematically described in a study of the geology of Greene and Hancock counties by Humphrey (1970). This subsequently provided data for an open-file report and map on these counties (Humphrey and Radcliffe, 1971), and abstracts on the petrology of the Siloam (Humphrey and Radcliffe, 1970) and its chemistry (Radcliffe and Humphrey, 1971). The Siloam pluton has been dated by Rb-Sr methods at 269 ± 3 m.y. with an initial $^{87}Sr/^{86}Sr$ ratio of 0.7052(1) by Jones and Walker (1973) who also give a petrographic description. A K-Ar biotite date of 261 m.y. for the Siloam had been previously reported by Smith et al. (1969). Wenner et al. (1977) reported on the oxygen isotopes of the Siloam ($\delta\ ^{18}O$ values relative to SMOW are 6.2 to 7.9) as well as other southeastern granites to elucidate the origin of the magmas.

The crystallization temperatures for coexisting plagicclase and alkali feldspar pairs of the Siloam have been calculated by Whitney and Stormer (1977a) using the equation of Whitney and Stormer (1977b). The zoning of the Siloam plagioclases require initial conditicns of 10 kb and temperatures in excess of 750°C which drop to 2 kb and 650°C with emplacement of the Siloam magma at its final location.

The Siloam pluton has been postulated to cut the projection of the Goat Rock fault by Hatcher et al. (1977). This would date the latest movement along this segment of their Eastern Piedmont fault system, although there is no direct evidence of faulting in the country rock adjacent to the Silcam.

Petrography

General Relations

The Siloam pluton has an elliptical outcrop, elongated north-south, of 99 km² which crosscuts the northeasterly structural trend of the country rock. Five distinct facies of the Siloam granite, based on differing textures or mineralogies, are recognized and form mappable units:

	% of area
porphyritic, coarse-grained granite (psg)	53%
medium-grained granite (msg)	22%
coarse-grained granite (csg)	12%
garnet-bearing granite (gsg)	9%
fine-grained granite (fsg)	4%

The map distribution of the differing facies is illustrated in Figure A10. There are varieties of the above rock types

which do not form mappable units but are described below. Classification of the Silcam granite samples collected for chemistry and heat production according to rock type is listed in Table A2 and located in Figure A11.

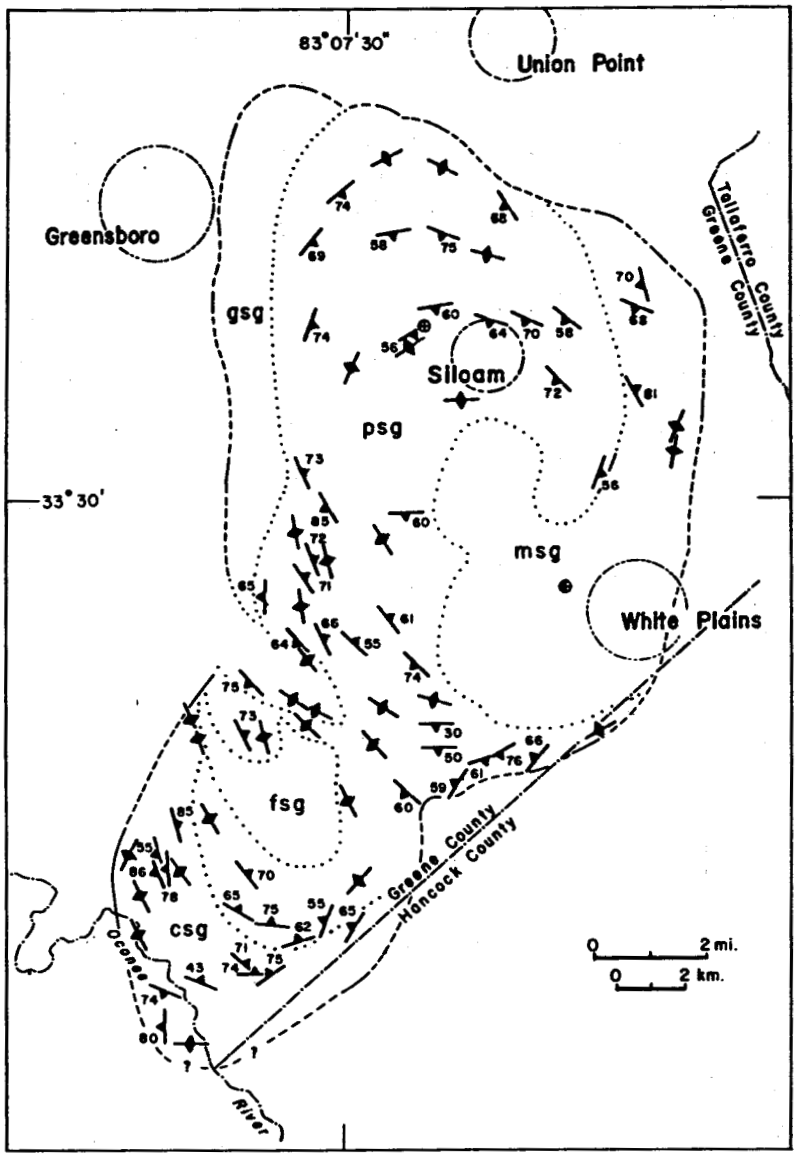

Figure A10. Geologic map of the Siloam pluton with the differing facies (psg) porphyritic Siloam granite, (msg) medium-grained Siloam granite, (csg) coarse-grained Siloam granite, (gsg) garnet-bearing Siloam granite, and (fsg) fine-grained Siloam granite. Strike and dip symbols indicate attitudes of alkali feldspar flow foliation and tabular xenoliths. Porposed heat flow sites are indicated by the drill hole symbols.

TABLE A2.

LISTING OF SILOAM CHEMISTRY AND HEAT PRODUCTION SAMPLES BY ROCK TYPE.

Porphyritic Siloam granite (psg)

CB7-7 AS7-108 -114 -136 -155

CB7-8 -111 -125 -139

Mafic porphyritic Siloam granite (contaminated?)

AS7-116 -117 -179 CB7-7B

Medium-grained Siloam granite (msg)

AS7-112 -149 -150

Fine-grained Siloam granite (fsg)

AS7-158

Garnet-bearing Siloam granite (gsg)

AS7-102 -99

Aplite dike cutting the Siloam granite

AS7-157

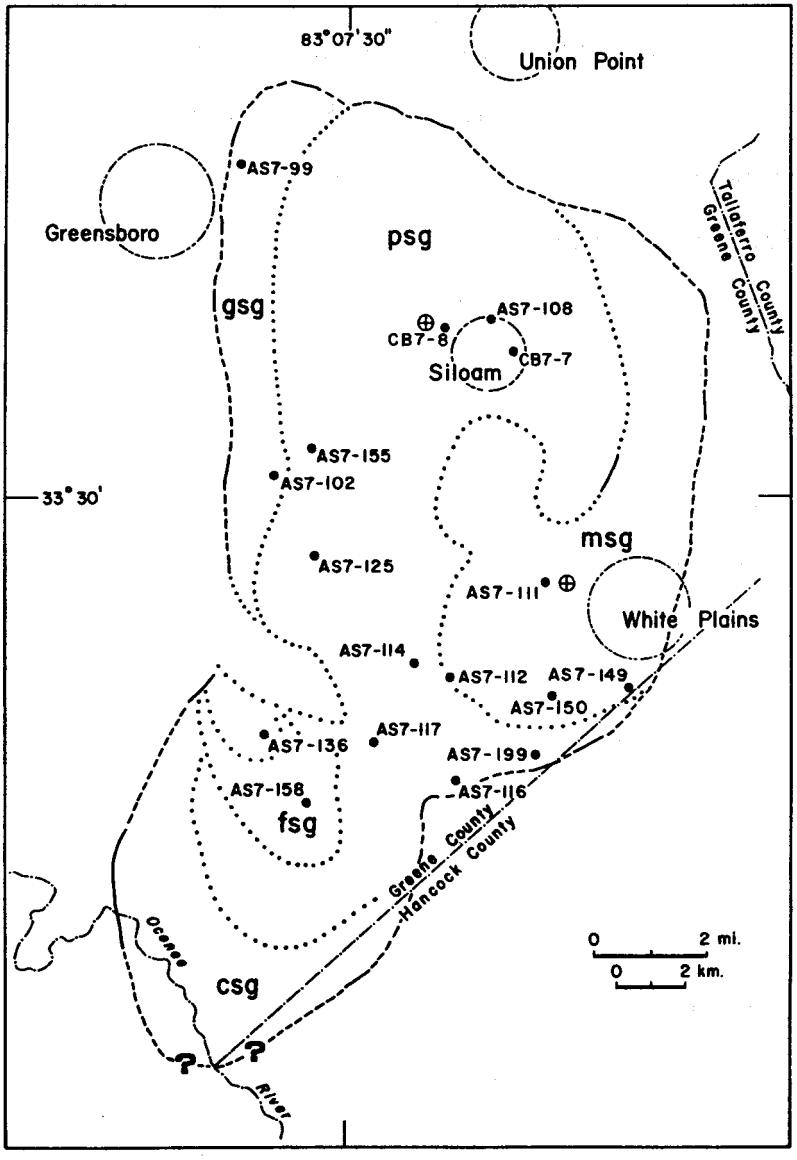

Figure A11. Geologic map of the Siloam pluton showing locations of the chemistry and heat production samples. Symbols are the same as Figure A10.

Porphyritic Siloam Granite

The porphyritic Siloam granite is a coarse-grained, hypidiomorphic, biotite-feldspar-quartz rock containing 4-7 cm megacrysts of alkali feldspar. The amount of feldspar megacrysts varies, but remains generally over 20%. Although granite of this type is of very coarse-grained appearance, the average grain size of matrix minerals is 3 mm or less. However, the rock is too coarse to have a uniform color, the colors of the individual minerals being evident.

The porphyritic facies accounts for about 53% of the outcrop of the Siloam. It concentrically crops out, enclosing the medium-grained Siloam granite in its core (Figure A10). On the west it is separated from the country rocks by the coarse-grained and garnet-bearing facies of the Silcam. The porphyritic facies may be intruded by lenses of the fine-grained facies. A strong igneous flow foliation, defined by the alignment of the tabular alkali feldspar megacrysts, confirms the concentric nature of this facies. The extremely high angle of the dip of the foliation hinders prediction of the change in shape of the pluton with depth.

A modal analysis of the porphyritic facies by Vistelius and Hurst (1964) show it to be a monzogranite. Humphrey

(1970) and Radcliffe and Humphrey (1971) report only average modes. As they did not distinguish among the textural varieties of the Siloam, the meaning of the modes is uncertain. In addition, the modes were performed on single thin sections, an inappropriate sample size for such coarse-grained rocks.

Tabular, subhedral to euhedral, pink alkali feldspar is the most conspicuous mineral because of its large size (1-7 cm). The feldspar is microcline micro- and macroperthite exhibiting both primary growth twins, largely Carlsbad twins, and albite and pericline inversion twins. Commonly, the alkali feldspar is poikilitic with oriented inclusions of plagioclase, quartz, and biotite, which are particularly abundant in some zones. A wiborgite texture is occasionally noted. Whitney and Stormer (1977a) have found the exsolved phases of the alkali feldspar to be nearly pure albite (An2) and K-feldspar (Or94) with a bulk composition of between Or65 and Or77 with less than 3% An. The sub- to anhedral plagioclase grains are smaller (less than 10 mm) than the alkali feldspars and are white with a locally greenish tint as a result of saussuritization. Optical compositional determinations by the a -normal method (Smith, 1974) show that the plagioclase is oligoclase having normal oscillatory zoning, with cores of An30-28 and rims of An10-12. Most grains have a discontinuous rim of albite, usually associated with myremekite. Biotite, in most cases the only

mafic mineral, is 3 mm or less in size. It is pleochroic dark brown to tan. Locally, amphibole occurs as subhedral prismatic crystals up to 2 mm long. They have the pleochroic formula X = yellow brown green, Y = brown green, Z = blue green.

Primary accessory minerals include allanite, titanite, apatite, zircon, magnetite, ilmenite with exsolved hematite, pyrite, pyrrhotite, and fluorite. Phyrrhotite occurs only as inclusions in what is interpreted as early crystallized phases. The large, zoned allanites, up to 2 mm long, and the abundant titanite are characteristic accessories similar to those in other late Paleozoic plutons in the southeast. Secondary minerals include white mica, epidote, carbonate, chlorite and hematite.

A more mafic variety of the porphyritic Siloam granite contains greater modal amounts of amphibole, biotite, and epidote, as well as a more calcic plagioclase (An38). This variety occurs throughout the pluton, but its abundance at the southeast contact of the porphyritic facies with the country rock suggests that it results from contamination with the country rocks, although its origin as an early segregation cannot be ruled out.

The hypidiomorphic-inequigranular texture of the porphyritic Siloam granite is modified by a deformational fabric plainly evident in thin section and rarely seen in outcrop. The quartz has undulose extinction and sutured

grain boundaries. The larger quartz grains are criss-crossed by planes of fluid inclusions. The alkali feldspar megacrysts not aligned in the plane of foliation have granulated edges. Zones of granulated quartz and feldspar are also evident in thin section. The deformation has little effect on the other minerals.

This deformation is evident throughout the Siloam, and varies unsystematically in intensity. As this feature was not noticed in the field, its orientation is not known. Examination of the hand specimens suggests that the deformational foliation parallels the igneous foliation. No retrograde metamorphism is associated with the deformation.

Medium-grained Siloam Granite

Nestled in the core of the concentric porphyritic Siloam granite and along the eastern margin of the pluton is a medium-grained granite (Figure A10). It is mineralogically identical to the porphyritic facies and differs only in the size of the mineral grains. The alkali feldspar is less than 10 mm in size, plagioclase and quartz less than 4 mm, and biotite less than 1 mm. The finer grain size gives the rocks a more uniform pink to white color. Robust muscovite in some specimens suggests that muscovite was an important late magmatic mineral. This granite facies is not the groundmass of the porphyritic facies, which has

little alkali feldspar and much plagioclase. This medium-grained Siloam granite is affected by the deformation described previously.

Toward the eastern outside margin of the medium-grained facies, the granite becomes finer-grained, less than 2 mm, and contains sparse to abundant, subhedral phenocrysts of quartz (up to 5 mm) and alkali feldspar (up to 7 mm). It also devlops a planar flow foliation which parallels tabular xenoliths and xenolith trains. This is in contrast to the normally massive, equigranular, medium-grained granite.

The medium-grained Siloam granite, near its border with the porphyritic facies, contains isolated megacrysts of alkali feldspar similar to those of the porphyritic facies. The proportion of feldspar megacrysts increases in the medium-grained granite towards the porphyritic facies. The increase in the proportion of megacrysts is not uniform and the boundary between the two facies is both gradational and irregular.

Fine-grained Siloam Granite

In the southwest part of the Siloam, at Liberty, is a lens of fine-grained, biotite granite. It is more even grained than the medium-grained granite, as well as smaller in grain size with an average of 1-2 mm. It has a mineralogy identical to that of the medium-grained granite

and resembles the finer-grained border varieties of that facies, excepting the presence of phenocrysts and foliation.

Garnet-bearing Siloam Granite

Along the northwest margin of the Siloam pluton is a unit of medium-grained, equigranular, pink to grey granite. The quartz and feldspar measure 4-6 mm. The granite is more felsic than any other Siloam granite with a color index of 2 or less. The mineralogy is quartz, microcline, unzoned plagicclase (An23), biotite, muscovite, and garnets (up to 4 mm in size). Accessory minerals are zircon, apatite, and opaques. Secondary minerals include chlorite and rutile. A deformational texture is evident in thin section, although none is evident in outcrop.

Coarse-grained Siloam Granite

The southwest lobe of the Siloam pluton consists of a coarse-grained biotite granite with an average grain size of 5 mm and alkali feldspars up to 10 mm. It is distinguished from the porphyritic facies by its higher color index, C.I. = 5-10, smaller alkali feldspars, and anhedral to subhedral alkali feldspar phenocrysts rather than the nearly euhedral alkali feldspars of the porphyritic facies. The mineralogy is quartz, microcline microperthite, plagioclase, and biotite. The plagioclase has weak oscillatory zoning with overall composition of An20. Accessory minerals include titanite, allanite, fluorite, apatite, zircon, and opaques.

The coarse-grained Siloam granite has a well-developed foliaticn defined by the roughly tabular alkali feldspars, biotite, and xenoliths or mafic clots. The foliation parallels the contact with the country rock as well as the flow fcliation of the porphyritic phase (Figure A10). The foliation of the coarse-grained facies is in large part the cataclastic texture, evident throughout the Siloam. It is the best developed in these rocks and appears to increase to the south.

Aplite and Pegmatite Dikes

The Silcam pluton is cut by a small number of pegmatite and aplite dikes. The aplite mineralogy is quartz, microcline, and plagioclase (An15-10) with minor or accessory biotite, muscovite, garnet, opaques, epidote, and apatite. The pegmatites consist of microcline and quartz, commonly graphically intergrown in sub- to euhedral crystals up tc 5 cm, albite (2 cm), and muscovite plates (2 cm). The pegmatites locally contain pyrite cubes up to 2 cm on a side and small amounts of biotite (3 mm).

Relaticnship Among the Various Rock Types of the Silcam

The garnet-bearing Siloam granite is different enough from the remaining granite facies to suggest it is a country

rock granite. In outcrop, it is similar to outcrops of granitic gneiss mapped by Humphrey (1970) and Humphrey and Radcliffe (1971) to the west of the Siloam.

Specimens from each of the four remaining granite facies appear to have been used by Jones and Walker (1973) to date the Siloam by Rb-Sr methods. That they define an isochron suggests they are contemporaneous. Experience with the Liberty Hill and Winnsboro plutons indicates the fine-grained facies was emplaced later than the coarse-grained facies. The isolated megacrysts in the border of the medium-grained granite with the porphyritic facies is reminiscent of the xenocrysts of coarse-grained Liberty Hill in the fine-grained facies. But northeast of the town of Siloam, a boulder of medium-grained granite is cut by an irregular mass of porphyritic granite, suggesting that the coarse-grained is later. The transition from the porphyritic to the coarse-grained Siloam facies in the southwest part of the pluton appears gradual as the exterior borders of the Siloam granite are reached. Perhaps the coarse-grained granite is only a border effect on the melt, in contrast with the contamination effects of the southeast contact. In addition, the coarse-grained facies shows effects of a stronger deformation than the other parts of the Siloam. The lack of evidence concerning the age relations of the Siloam granite facies suggests they are contemporaneous in a relative as well as absolute sense.

Composition of the Siloam Granites

Among the many chemical analyses of the Siloam granite are three individual analyses of the porphyritic granite (#1-3, Table A3) and an average of 40 grid samples (#4, Table A3). As Radcliffe and Humphrey (1971) did not recognize differing facies of the granite, their average composition is difficult to interpret. The presence of the differing facies of the Siloam granite may also explain in large part their observed chemical trends--increasing $Fe_2O_3/Fe_2O_3 + MgO$ to the west and increasing $K_2O/K_2O + Na_2O + CaO$ concentrically from margin to core. These trends are possible if the porphyritic facies is more iron rich and less potassic than the medium-grained granite.

TABLE A3.

CHEMICAL ANALYSES OF THE SILOAM GRANITE.

	1	2	3	4
SiO2	70.95	73.68	69.13	71.1
Al2O3	15.59	13.80	17.14	14.20
CaO	1.44	1.74	1.85	1.30
MgO	0.71	0.87	0.79	?
K2O	5.26	3.95	5.49	4.7
FeO	2.19	2.39	-	-
Fe2O3	-	-	1.52	3.10
Na2O	3.66	3.52	4.06	2.8
MnO	0.05	0.06	-	0.05
TiO2	0.35	0.40	-	0.5
P2O5	0.18	0.19	-	-
Ign.	-	-	0.52	-
TOTAL	100.38	100.60	100.50	

1. . .porphyritic granite, CB7-7

2. . .porphyritic granite, CB7-8

3. . .porphyritic granite (Watson, 1902)

4. . .average of 40 samples (Radcliffe and Humphrey, 1971)

Preliminary Statement on Depth of Emplacement of the Siloam

Pelitic xenoliths of the Siloam pluton contain the assemblage garnet-sillimanite-biotite-K feldspar-plagioclase-quartz. If these pelitic rocks have a composition corresponding to that of the pelitic rocks enclosing the Winnsboro, Liberty Hill, Pageland, and Lilesville, the assemblage indicates a greater depth of emplacement. The reaction:

cordierite garnet + sillimanite + quartz

divides the low pressure assemblages containing cordierite from the high-pressure garnet + sillimanite assemblages, the reaction curve having a small negative slope in P-T space (Holdaway and Lee, 1977). In addition, the reaction is largely free of the effects of partial water pressure.

This depth of emplacement of probably more than 4 kb contrasts with the 2 kb estimate of Whitney and Stormer (1977a) based on coexisting feldspar pairs.

Heat Generation

The Siloam was originally chosen for more detailed study this contract period because of the high heat

production of its porphyritic facies as well as its location as one of the southernmost post-metamorphic plutons. Results of the gamma-ray spectrometer for the Siloam samples collected during the reconnaissance survey are (Report VPI&SU-5103-5):

	U, ppm	Th, ppm	K2O, wt%	HGVU
CB7-7 (psg)	7.7	37.3	4.9	12.0
CB7-7B xenolith	7.2	20.9	4.1	8.8
CB7-8 (psg)	5.7	35.4	3.7	10.2

Preliminary results on samples collected for this study are:

AS7-125 (psg)	3.8	23.4	4.8	7.0
AS7-149 (msg)	4.9	33.3	4.7	9.2

CB7-7 contains veins of fluorite and sulfides which may account for the high uranium contents of the samples at that locality. The remaining samples, lower in uranium, are too few to characterize the pluton in terms of heat production, but they are generally higher than coarse-grained granites of other post-metamorphic granites.

REFERENCES

Bell, H., J. R. Butler, D. E. Howell, and W. H. Wheeler, 1974, Geology of the Piedmont and Coastal Plain near Pageland, South Carclina and Wadesboro, North Carolina. Carclina Geol. Soc. Fieldtrip Guidebook, S.C. State Devel. Board, Div. of Geol.

Broadhurst, S. D. and J. M. Parker, III, 1959, Guidebook for Piedmcnt field trip, featuring metamorphic facies in the Raleigh area, North Carolina: North Carolina Div. of Mineral Resources, 24 p.

Butler, J. R. and P. R. Ragland, 1966, Petrography and geochemistry of differentiated plutons in the Carolina Piedmcnt (abs.): Southeastern Section, Geol. Soc. America, Abs. with Prog. for 1966, 12.

_____, _____, 1969, A petrochemical survey of plutonic intrusions in the Piedmont, southeastern Appalachians, U.S.A.: Contrib. Mineral. Petrol. 24, 164-190.

Cabaup, J. J., 1969, origin and differentiation of the gabbro in the Concord Ring Dike, North Carolina Piedmcnt: M.S. thesis, Univ. North Carolina, Chapel Hill, 42 p.

Carpenter, P. A., 1970, Geology of the Wilton area, Granville Co., N. C.: M.S. thesis, North Carolina State Univ., Raleigh.

Casadevall, T., 1977, The Nutbush Creek dislocation, Vance County, North Carolina, and Mecklenburg County, Virginia--a probable fault of regional significance: Geol. Soc. America, Abs. with Prog. 9, 127-128.

Chalcraft, R. G., 1968, Petrography and geophysics of the Rock Hill gabbro pluton, York County, South Carolina: M.S. thesis, Univ. North Carolina, Chapel Hill, 40 p.

_____, 1977, A petrographic study of the Ogden pluton, York and Chester Counties, South Carolina (abs.): Geol. Soc. America, Abs. with Prog. 9, 128.

Constantino-Herrera, S. E., 1971, Geology of the Cleveland gabbro, Rowan County, North Carolina: M.S. thesis, Univ. North Carolina, Chapel Hill, 35 p.

Cook, R. B., Jr., 1972, Exploration for disseminated molybdenum-copper mineralization in the Conner stock, Wilson and Nash Co., North Carolina (abs.): Econ. Geol. 67, 1003-1004.

Dickey, J. B., 1963, The geology of the Barton Creek area, northern Wake County, North Carolina: M.S. thesis, North Carolina State Univ., Raleigh, 55 p.

Farquhar, C. R., 1952, Crystalline rocks of north central Wake County, North Carolina: M.S. thesis, North Carolina State Univ., Raleigh, 33 p.

Fisher, G. W., F. J. Pettijohn, J. C. Reed, Jr., and K. N. Weaver, 1970, Studies of Appalachian Geology: Central and Southern: John Wiley & Sons, 460 p.

Fortson, C. W., Jr., 1958, Geology of the Crabtree Creek area northwest of Raleigh, N. C.: M.S. thesis, North Carolina State Univ., Raleigh, 101 p.

Fullagar, P. D., 1971, Age and origin of plutonic intrusions in the Piedmont of the southeastern Appalachians: Geol. Soc. america Bull. 82, 2845-2862.

_____, and J. R. Butler, 1977, 300 m.y.old post-tectonic granitic plutons of the southeastern Appalachians (abs.): Transactions, Am. Geophys. Union 58, 531.

Glover, D. P., 1963, A gravity study of the northeastern Piedmont batholith of North Carolina: M.S. thesis, Univ. of North Carolina, Chapel Hill, 41 p.

Hatcher, R. D., Jr., D. E. Howell, and P. Talwani, 1977, Eastern Piedmont fault system: speculations on its extent: Geology 5, 636-640.

Hermes, O. D., 1967, Geology and petrology of the Mecklenburg gabbro-metagabbro complex, North Carolina: Ph.D. dissertation, Univ. North Carolina, Chapel Hill, 112 p.

Holdaway, M. J. and S. M. Lee, 1977, Fe-Mg cordierite stability in high-grade pelitic rocks based on experimental, theoretical and natural observations: Contrib. Mineral. Petrol. 63, 175-198.

Humphrey, R. C., 1970, The geology of the crystalline rocks of Greene and Hancock counties, Georgia: M.S. thesis, Univ. Georgia, 57 p.

_____, and D. Radcliffe, 1970, The petrology of the Siloam granite, Greene County, Georgia (abs.): Geol. Soc. America Abs. Prog., S.E. Section 2, 220.

_____, and D. Radcliffe, 1971, Geology, petrology and mineral resources of the crystalline rocks of Greene and Hancock counties: Georgia Dept. Mines, Mining, and Geology Open-file Rep., 55 p.

Irvine, T. N. and W. R. A. Baragar, 1971, A guide to the chemical classification of the common volcanic rocks: Can. J. Earth Sci. 8, 523-548.

Jones, L. M. and R. L. Walker, 1973, Rb-Sr whole-rock age of the Siloam granite, Georgia: a Permian intrusive in the southern Appalachians: Geol. Soc. America Bull. 84, 3653-3658.

Julian, E. L., 1972, The Castalia adamellite in Franklin and Nash counties, North Carolina, and the petrogenesis of some associated aplites and pegmatites: M.S. thesis, North Carolina State Univ., Raleigh, 61 p.

Kennedy, W. Q., 1933, Trends of differentiation in basaltic magmas: Am. Jour. Sci., Ser. 5, 25, 239-256.

Libby, S. C., 1971, Petrology of the igneous rocks of Putnam County, Georgia: M.S. thesis, Univ. Georgia, Athens, 99 p.

Matthews, V., III, 1967, Geology and petrology of the pegmatite district in southwestern Jasper County, Georgia: M.S. thesis, Univ. Georgia, Athens, 68 p.

McSween, H. Y., Jr., and P. G. Nystrom, Jr., Differentiation of the Dutchmans Creek gabbrcic intrusion, South Carclina (in press).

Medlin, J. H., 1968, Comparative petrology of two igneous ccmplexes in the South Carolina Piedmont: Ph.D. dissertation, The Pennsylvania State Univ., University Park, 358 p.

_____, C. P. Thornton, and D. P. Gold, 1972, Petrology of the mafic igneous complexes in the scutheastern U. S. Piedmont. II. The Buffalo mafic igneous complex, Unicn County, South Carolina: Southeastern Geology 14, 73-106.

Myers, C. W., II, 1968, Geology of the Presley's Mill area, northwest Putnam County, Georgia: M.S. thesis, Univ. Georgia, Athens, 67 p.

Overstreet, W. C. and H. Bell, III, 1965, The crystalline rocks of South Carolina: U. S. Geol. Surv. Bull. 1183, 126 p.

Parker, J. M., III, 1968, Structure of the easternmost North Carolina Piedmont: Southeastern Geol. 9, 117-131.

Radcliffe, D. and R. Humphrey, 1971, Chemistry of the Siloam granite, Greene County, Georgia (abs.): Geol. Soc. America Abstr. Prog., S.E. Section 3, 342.

Smith, J. V., 1974, Feldspar Minerals, Vol. I, Springer-Verlag, 627 p.

Smith, J. W., J. M. Wampler, and M. A. Green, 1969, Isotopic dating and metamorphic isograds of the crystalline rocks of Georgia: Georgia Dept. Mines, Mining and Geology Bull. 80, 121-139.

Stuckey, J. L., 1958, Geologic map of North Carolina: North Carolina Div. Mineral Resources.

Tilley, C. E., 1950, Some aspects of magmatic evolution: Quart. Jour. Geol. Soc. London 106, 37-61.

U. S. Geological Survey, 1976, Aeromagnetic maps of parts of Georgia, South Carolina, and North Carolina: Open-file maps 76-181, 13 pls.

Vistelius, A. B. and V. J. Hurst, 1964, Phosphorus in granitic rocks of North America: Geol. Soc. America Bull. 75, 1055-1092.

Watson, T. L., 1902, The granites and gneisses of Georgia: Georgia Geol. Survey Bull. 9-A, 637 p.

Wenner, D. B., J. A. Whitney, and J. C. Stormer, Jr., 1977, Oxygen isotopic evidence for the genesis of two distinctive suites of 300 m.y. granitic plutons from the southern Appalachian Province: Geol. Soc. America, Abstr. Prog. 9, 1221.

Whitney, J. A. and J. C. Stormer, Jr., 1977a, Two-feldspar geothermometry, geobarometry in mesozonal granitic intrusions: three examples from the Piedmont of Georgia: Contrib. Mineral. Petrol. 63, 51-64.

_____, _____, 1977b, The distribution of NaAlSi3O8 between coexisting microcline and plagioclase and its effect on geothermometric calculations: Am. Mineral. 62, 687-691.

Wilson, W. F. and P. S. Carpenter, 1975, Region J Geology: a guide for North Carolina mineral resource development and land use planning: North Carolina Dept. of Natural and Economic Resources, 76 p.

B. GEOCHEMISTRY

A. K. Sinha, Principal Investigator

B. A. Merz, Research Associate

Petersburg Batholith

Thirty-nine surface samples and 11 samples from the 250 m deep PET1 borehole have been analyzed for major element chemistry. The average surface and core compositions, together with U and Th values obtained by gamma-ray spectrometry, are given in Table B1. Two samples described as gneissic and one pegmatite were omitted from the surface average. In comparison with the data given in Table B1 of our previous report (VPI & SU-5103-5), it can be seen that in major element chemistry, the Petersburg surface average resembles most closely the Liberty Hill fine grained and Rolesville surface samples. However, the average U content of the Petersburg surface samples is considerably higher than that from the surface of any other pluton. In terms of Th content, the Petersburg surface samples show normal apparent values and the average is comparable with that from Rolesville.

The PET 1 core has an average major element composition which is significantly more mafic, having lower SiO2 and higher CaO, MgO and TiO2, than the surface samples. This is reflected in its lower U and Th abundances.

According to Streikessen's (1976) classification scheme, which uses a normative An-Ab-Or plot to define rock types, the Petersburg surface samples with >17% normative Qz are monzogranites, syenogranites and alkali feldspar

TABLE B1
AVERAGE COMPOSITIONS FROM PETERSBURG BATHOLITH

NO. SAMPLES	SURFACE (36)	PET1 CORE (11)	
U ppm	7.6	4.8	Note U and Th of core
(st dev)	(4.1)	(0.6)	are averages of only 5 samples.
Th ppm	18.7	14.9	
(st dev)	(7.2)	(2.6)	
SiO2	71.44	67.06	
(st dev)	(3.83)	(1.47)	
Al2O3	15.40	16.46	
(st dev)	(0.71)	(0.68)	
CaO	1.64	2.24	
(st dev)	(0.77)	(0.17)	
MgO	0.81	1.47	
(st dev)	(0.61)	(0.13)	
K2O	5.05	5.38	
(st dev)	(0.83)	(1.08)	
FeO	2.03	2.78	
(st dev)	(1.10)	(0.21)	
Na2O	3.85	4.16	
(st dev)	(0.35)	(0.25)	
MnO	0.05	0.07	
(st dev)	(0.02)	(0.01)	
TiO2	0.34	0.53	
(st dev)	(0.20)	(0.06)	
P2O5	0.12	0.21	
(st dev)	(0.07)	(0.02)	

granites. Four surface samples have <17% normative Qz and are classified as calc-alkaline monzonites. The core samples all have <17% normative Qz and fall in the calc-alkali syenite field of the appropriate diagram. The trend from most to least felsic, i.e., from alkali-feldspar granite to monzonite, is paralleled by a trend of decreasing average U and Th contents:

alkali feldspar granite (4 samples) U = 10 ppm, Th = 19 ppm
syenogranite (17 samples) U = 8 ppm, Th = 20 ppm
monzogranite (8 samples U = 6 ppm, Th = 17 ppm
monzonite (3 samples) U = 5 ppm, Th = 13 ppm

On a K-Na-Ca diagram, the points cluster about the average calc-alkaline trend of Nockolds and Allen (1953).

Figure B1 is a Q-Ab-Or phase diagram for PH2O = P total. The Petersburg surface samples plot in a rather large field, the position of which indicates a pressure at the time of crystallization of about 2 kb PH2O. However, the Petersburg is a large and probably complex batholith made up of several different lithologies (see Geology section of report VPI & SU-5103-4). The dominant lithology is medium to coarse grained, weakly or non-foliated massive granite. The five samples shown on Figure A7 of the above report as belonging to this lithology have Q-Ab-Or data which fall in the smaller surface sample field of Figure B1.

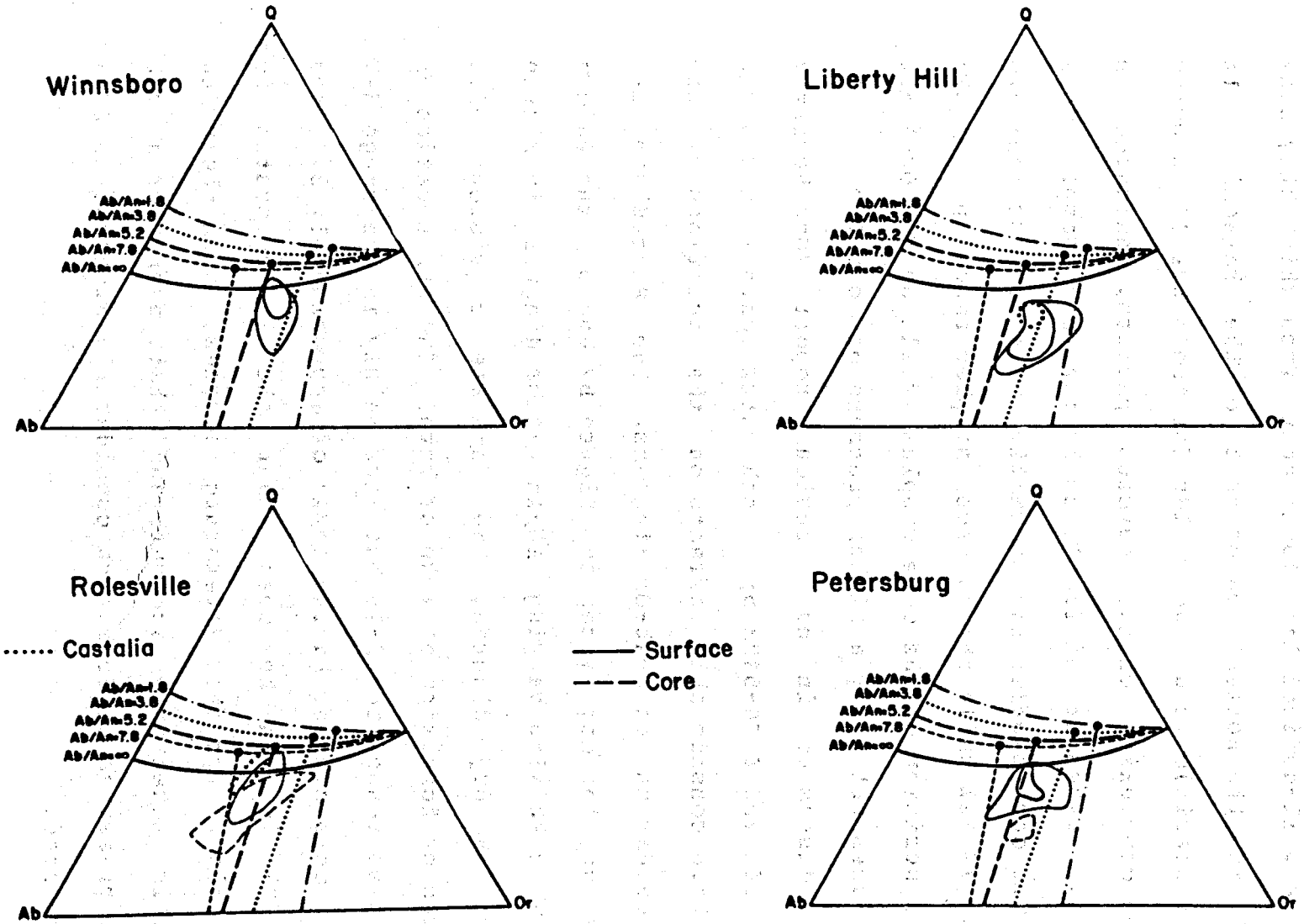

Figure B1. Normative Q-Ab-Or diagram for the saturated system

This group of samples has an average U = 8.1 ppm, Th = 21.1 ppm. The well-defined lithologic unit from which they come probably is the hottest major unit of the batholith. It might be possible to define fields for the other lithologies but the complexity of the outcrop pattern, indicated in Figure A7, makes it difficult to assign each sample to a unit. The core samples have normative Qz + Ab + Or contents of only 79-82% while the surface samples range up to 95%; thus the position of the core samples' field on the Qz-Ab-Or diagram does not imply a higher pressure of formation.

As discussed in our previous report (Geochemistry section of VPI & SU-5103-5), both water content and Ab/An ratio have considerable effects on the positions of the phase boundaries on Q-Ab-Or diagrams. The Petersburg data is shown on the dry system in Figure B2 and on the PH2O = Ptotal = 2 kb with varying Ab/An ratios diagram in Figure B3. On the dry diagram, the data are consistent with pressures of formation of 4 kb or more. The Ab/An ratios of the samples range from 2-19 but are mainly in the range 3-7 with the core samples having Ab/An of approximately 3. From Figure B3 it can be seen that the 2 kb system is inappropriate for the Petersburg samples, when their An content is taken into account, and that, even for a wet system, pressures of formation considerably higher than 2 kb are suggested.

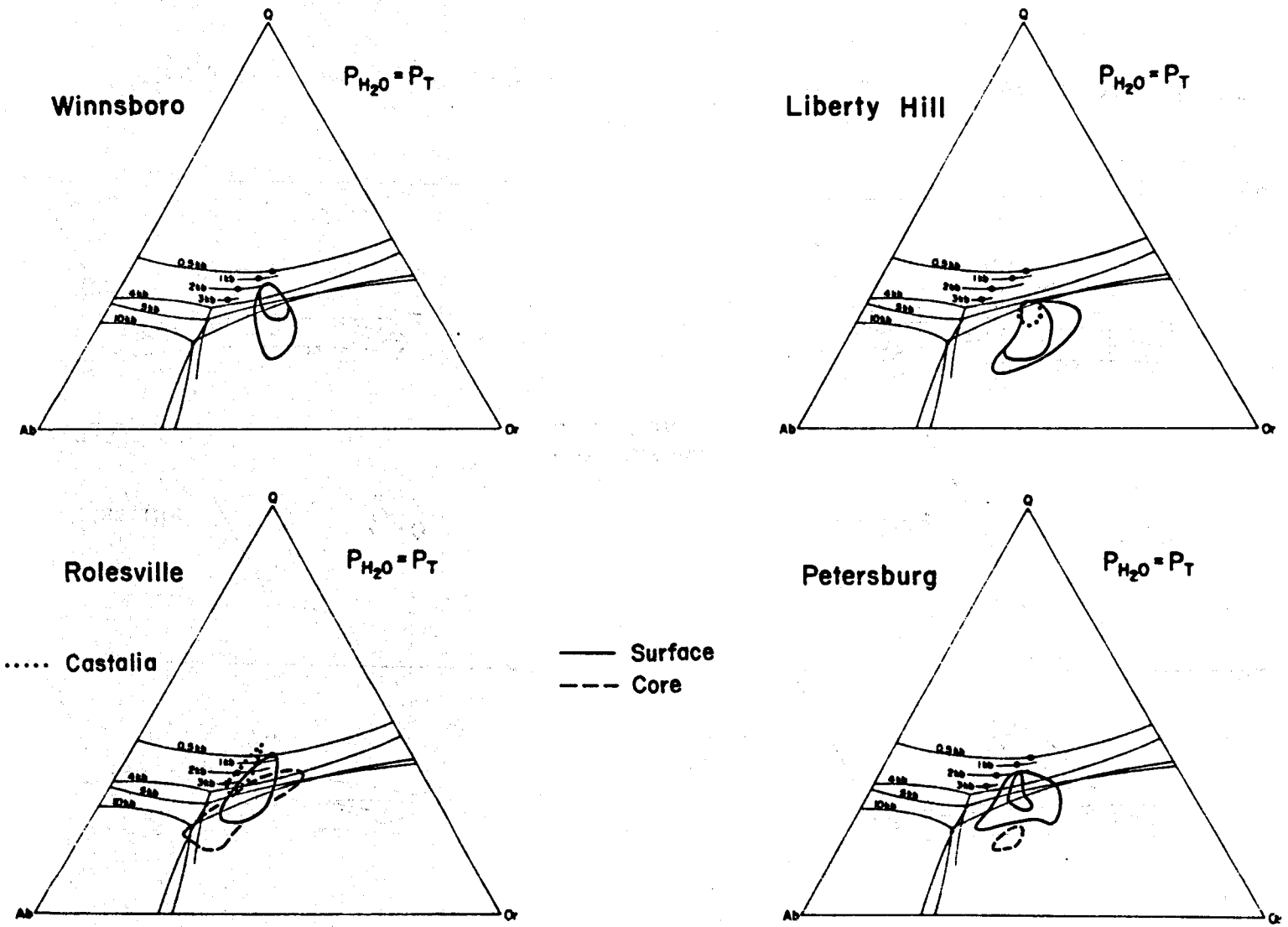

Figure B2. Normative Q-Ab-Or diagram for the dry system

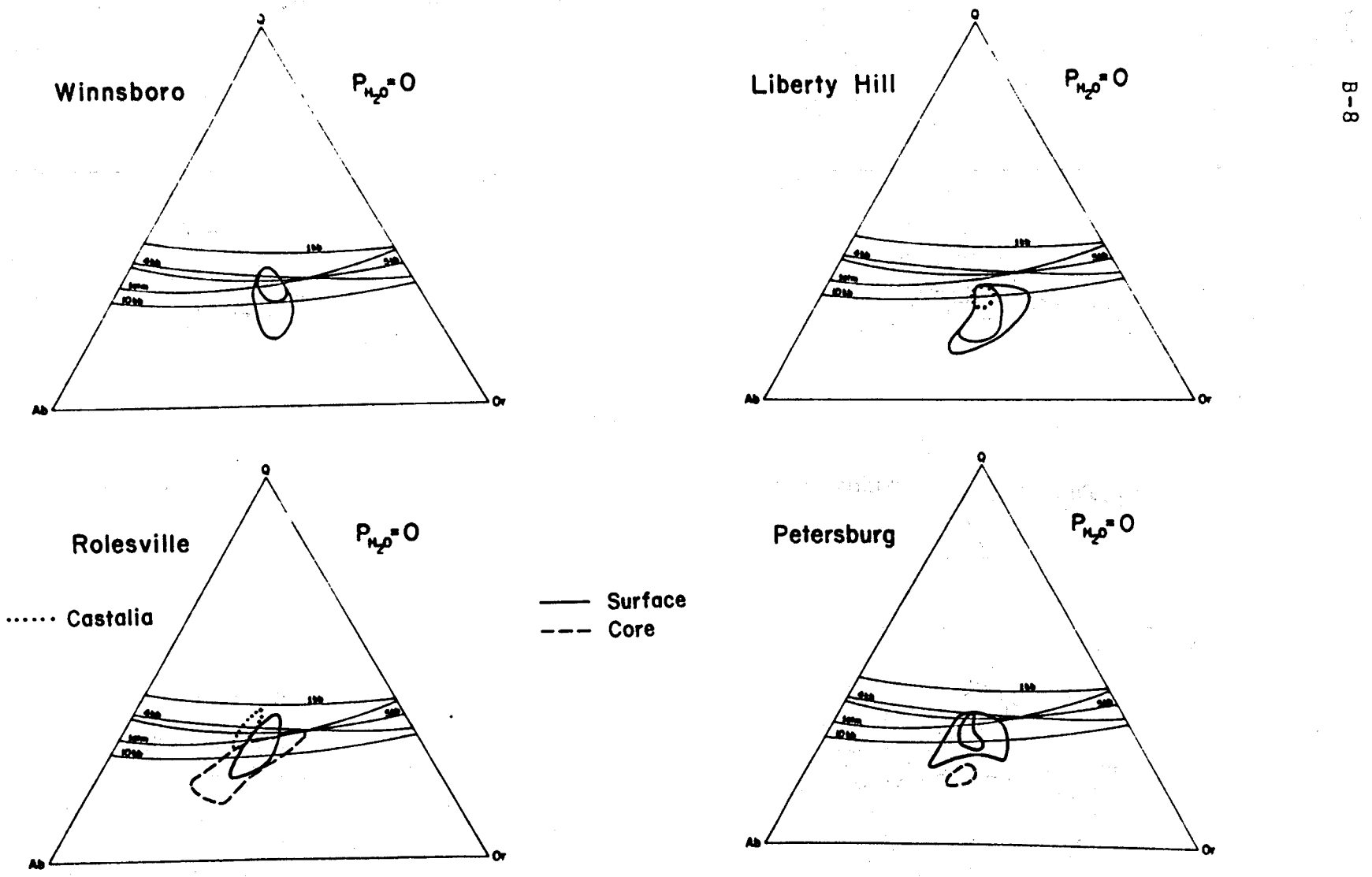

Figure B3. Normative Q-Ab-Or diagram for P_{H_2O}=2 kb showing the effect of an An component

Rolesville Cores

Samples from one borehole, RL1, within the Castalia pluton of the Rolesville complex and from three boreholes, RI2, RL4, and RL5 located in the main Rolesville pluton have been analyzed. The average major element and U and Th contents of each core are given in Table B2 along with the Rolesville surface data from our previous report (Geochemistry section of VPI & SU-5103-5). Samples described as being mixed granite and pegmatite were omitted from the averages.

In comparing the Castalia surface and RL1 data, it must be noted that only three surface samples from this more than 20 km long pluton were analyzed and so might not be representative of the pluton as a whole. Sixteen samples from the 210 m core were analyzed. The core composition is less felsic than the surface average, having lower SiO2 and higher CaO, MgO, FeO and TiO2, but the U and Th contents are quite similar, U being slightly higher and Th lower in the core than the surface samples. The core shows little chemical variation throughout its length, as indicated by the small standard deviation values, and there are no significant variations with depth either for major elements or U and Th. Three of the R1 core samples come from the parts of the core described as altered in the Geology section of Report VPI & SU-5103-5 but their chemistry is not

TABLE B2. AVERAGE COMPOSITIONS OF ROLESVILLE SAMPLES.

	Castalia surface	Rolesville surface	RL1 Castalia core	RL2	RL4 Rolesville cores	RL5
No. samples	(3)	(18)	(18)	(10)	(19)	(9)
U ppm	4.3	4.0	5.1	5.1	5.4	4.2
(st dev)	(1.7)	(1.6)	(0.5)	(1.1)	(1.8)	(1.7)
Th ppm	13.76	17.8	11.83	14.46	16.4	18.6
(st dev)	(3.57)	(4.5)	(0.46)	(2.23)	(2.7)	(3.0)
SiO2	75.26	71.18	71.34	69.85	70.95	70.81
(st dev)	(3.43)	(2.91)	(1.01)	(3.21)	(3.75)	(1.43)
Al2O3	14.12	15.59	15.41	16.71	16.26	16.56
(st dev)	(0.44)	(0.94)	(0.20)	(1.20)	(0.99)	(0.61)
CaO	1.59	1.82	2.28	2.12	1.83	1.81
(st dev)	(0.64)	(0.44)	(0.26)	(0.68)	(0.53)	(0.16)
MgO	0.54	0.70	0.92	0.73	0.76	0.64
(st dev)	(0.47)	(0.27)	(0.18)	(0.34)	(0.46)	(0.13)
K2O	4.22	4.52	4.02	4.36	4.91	4.78
(st dev)	(0.53)	(0.46)	(0.75)	(0.88)	(0.68)	(0.26)
FeO	1.26	1.77	2.01	1.66	1.60	1.32
(st dev)	(0.79)	(0.55)	(0.37)	(0.63)	(0.83)	(0.23)
Na2O	3.70	3.73	4.01	4.22	3.98	4.34
(st dev)	(0.34)	(0.30)	(0.32)	(0.47)	(0.45)	(0.36)
MnO	0.05	0.04	0.05	0.03	0.03	0.04
(st dev)	(0.01)	(0.01)	(0.00)	(0.01)	(0.01)	(0.01)
TiO2	0.17	0.30	0.26	0.28	0.28	0.21
(st dev)	(0.11)	(0.11)	(0.05)	(0.11)	(0.15)	(0.03)
P2O5	0.06	0.11	0.09	0.09	0.09	0.08
(st dev)	(0.03)	(0.04)	(0.01)	(0.04)	(0.07)	(0.02)

appreciably different from the rest of the samples either in major element or U and Th contents. The normative Qz-Ab-Or data from both surface and core fall in the small field shown on Figure B1. Although the Castalia field on this diagram appears to cross the 0.5 kb cotectic into the primary Qz field, when the effect of an An component is considered, as in Figure B3, it can be seen that the entire Castalia field falls below the 2 kb phase boundary for Ab/An = 3.8, which is the approximate ratio in the Castalia samples. The phase diagrams suggest a lower pressure of equilibration for the Castalia and Rolesville main plutons than for the other three plutons shown.

Thirteen samples from the 213 m RL2 core, 21 from the 200 m RL4 core and 13 from the 213 m RL5 core were analyzed. These three cores are less homogeneous than the RL1 core, as indicated by their larger standard deviation and also by the large field which they occupy on the Qz-Ab-Or diagram, Figure B1. Again there is no regular variation in major element or U and Th contents with depth. This is no significant difference between the surface average composition and the core compositions; in all cases the average element contents differ by amounts less than their standard deviations. The conclusions drawn from the Rolesville surface data (Report VPI & SU-5103-5) hold equally for the core samples.

REFERENCES

Nockolds, S. R. and Allen, R. 1953. The Geochemistry of some igneous rock series. Geochim. Cosmochim. Acta 4, 105-142.

Streckeisen, A. 1976. Classification of the common igneous rocks by means of their chemical composition. A provisional attempt. N. Jb. Mineral. Mh. H. 1, 1-15.

C. GEOPHYSICS

J. K. Costain, Principal Investigator

A. H. Cogbill, Research Associate

L. D. Perry, Research Associate

J. A. Dunbar, Research Specialist

POTENTIAL FIELD DATA

A.H. Cogbill

Gravity and Magnetic Data in the Southeast

Efforts utilizing gravity and magnetic measurements to constrain the locations and sizes of heat-producing granitic bodies that possibly lie beneath the Coastal Plain have now begun in a systematic manner. In these first phases of work, particular attention has been given to the gravity measurements available to us, with less attention focused upon the aeromagnetic data. This is chiefly due to logistical reasons, because the gravity measurements are, for the most part, readily available in a discrete form, whereas the magnetic data were available only on maps and thus more difficult to transfer readily into a computing machine; this problem should become less important in the near future with the acquisition of an x-y digitizer. Therefore the discussion to follow will be devoted to the analysis of the gravity measurements: emphasis will be placed on the gravity data available in the states of Georgia, South Carolina, and North Carolina, where most of our work has been concentrated thus far.

Sources of gravity data

We have used measurements provided by 1) NOAA, 2) Virginia Division of Mineral Resources, and 3) the National Geodetic Survey. Additionally, we have begun to acquire our own measurements in those localities where the density of data from the above three sources is particularly sparse. The acquisition of these new measurements has been made possible through the loan of two LaCoste-Romberg geodetic gravity meters by the National Geodetic Survey.

The gravity data provided by NOAA constitute the overwhelming portion of the data available to us, and thus it is helpful to examine the distribution of the data provided by NOAA. Toward this end we have prepared station maps for the states of Georgia, South Carolina, and North Carolina [Figures (C-1)-(C-3)]. Similar maps of the station distributions in Virginia, Maryland-Delaware, and New Jersey will be prepared within the coming weeks as attention broadens to include those areas. As may be seen in these figures, the station distributions in Georgia and North Carolina are relatively uniform, with some exceptions. Measurements in these states are sufficiently dense to provide adequate, but not outstanding, regional coverage. For local studies the data are really too sparse, and thus we intend to acquire more measurements for such studies.

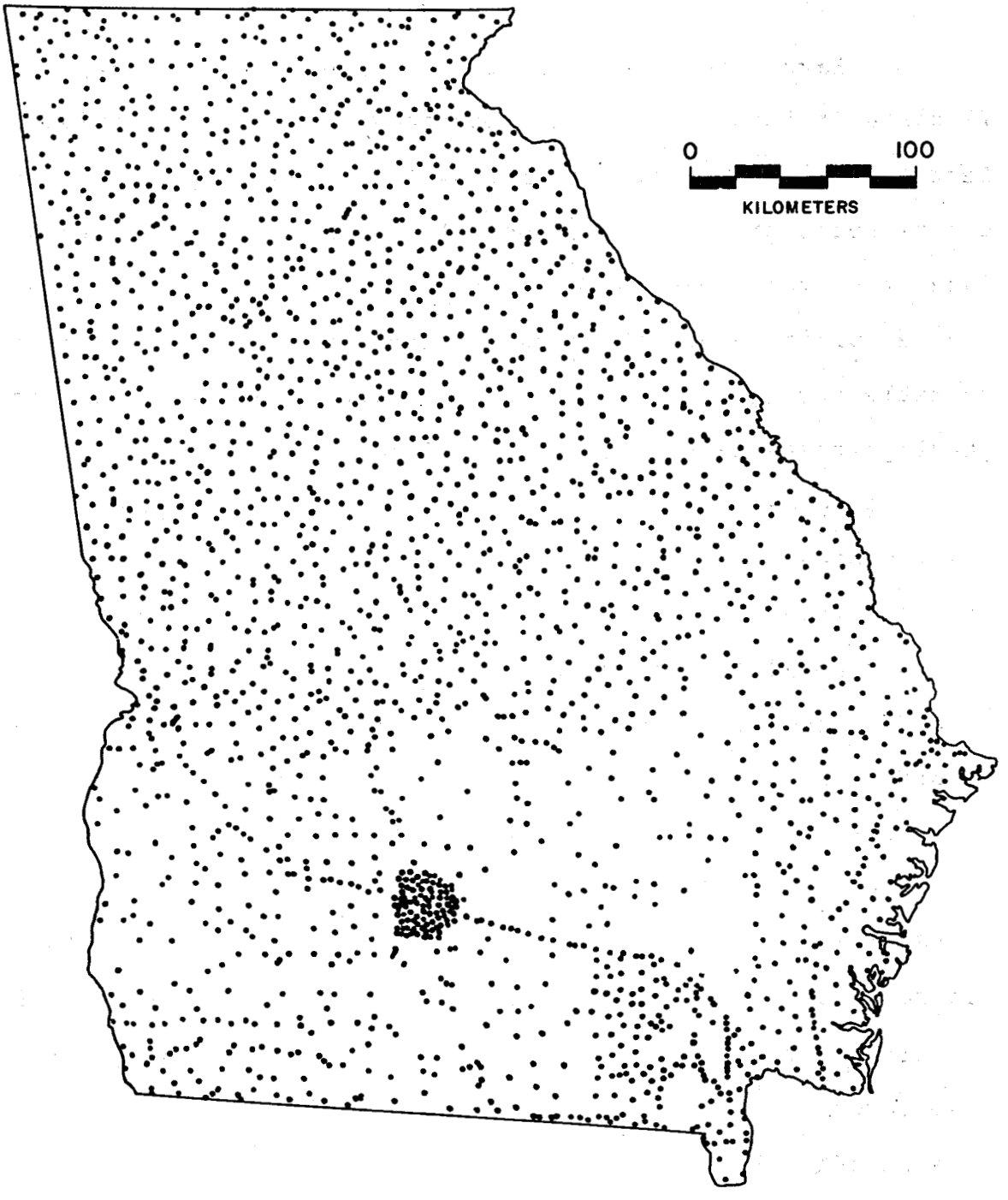

Figure C-1. Distribution of gravity stations in Georgia. Sources of data are NOAA and the National Geodetic Survey.

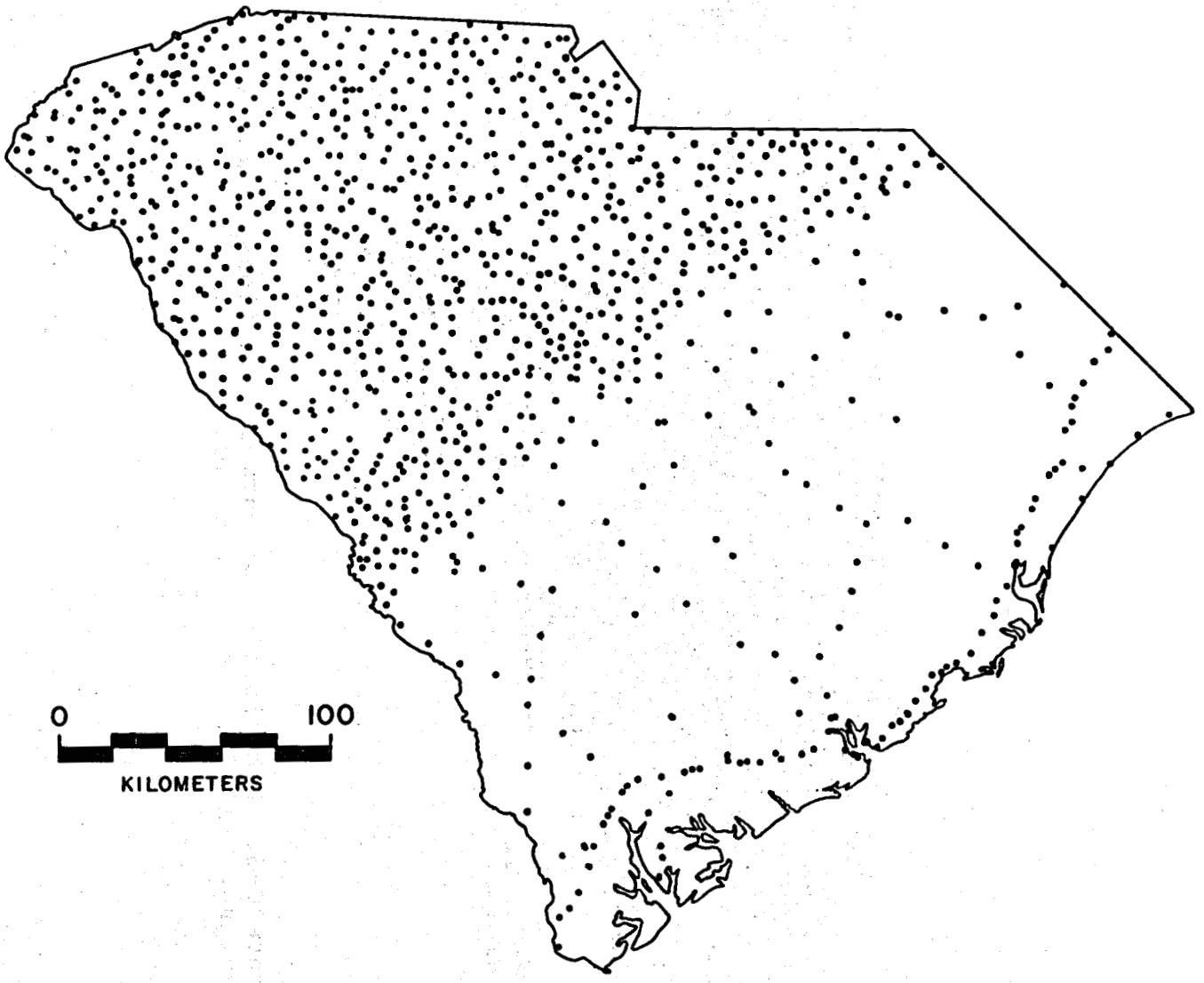

Figure C-2. Distribution of gravity stations in South Carolina. All data provided by NOAA.

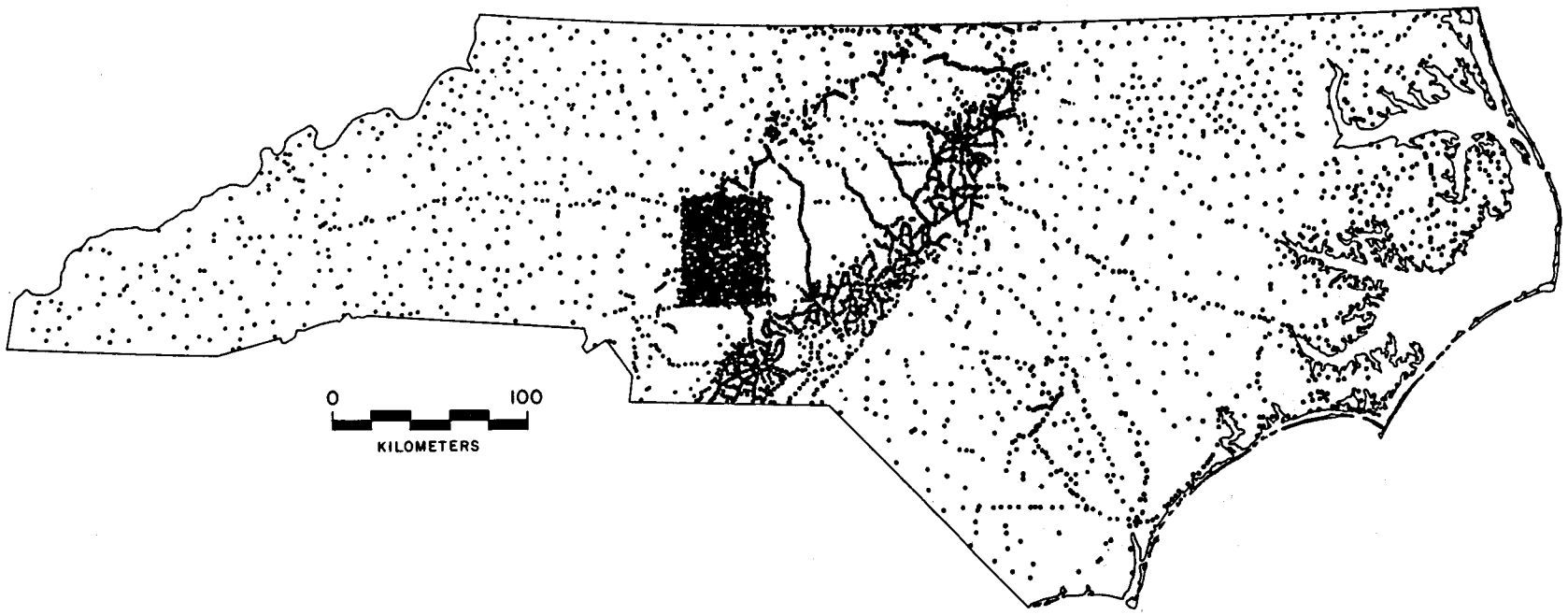

Figure C-3. Distribution of gravity stations in North Carolina. All data provided by NOAA.

The distribution of gravity measurements in South Carolina, however, is remarkably bimodal, a fact probably attributable to a lack of recent topographic maps in much of eastern South Carolina. The extreme paucity of data in eastern South Carolina presents many difficulties to the gravity field analysis, and to help remedy this unhappy situation we shall make major efforts in the next few months to augment the gravity data set in this region.

Local Studies

We have begun to interpret gravity measurements made in the vicinity of three granitic bodies - the Edgefield granite, the Rolesville batholith, and the Petersburg granite. Results for the Rolesville and the Petersburg areas are as yet incomplete, but the study of the Edgefield granite is very nearly finished, and many results from that study are presented in this report.

Edgefield granite (Cuffytown Creek pluton)

The Edgefield granite is a granitic body located in southwestern South Carolina (Figure C-4). Although its exposed area is fairly small, a rather large, negative Bouguer anomaly is coincident with it. A gravity study of the Edgefield was begun in January, 1978; the principal objectives of the study were: 1) to place bounds upon the total depth of the pluton, and 2) to estimate the shape of the body within the subsurface. Examination of the gravity data supplied us by NOAA revealed that there were only two measurements in their catalog which were located upon the exposed portion of the pluton. Therefore we acquired some 150 additional measurements in the vicinity of the pluton. These are all tabulated in Table C-1: the locations of most of these measurements are also shown in Figure C-4 (some stations lie outside the boundaries of Figure C-4). However, the NOAA-supplied measurements were used to estimate the low-frequency (regional) portion of the field. This part of the field was subtracted from the raw Bouguer field; the resulting field is termed the anomalous field. The term residual field or residual anomaly will be used only when comparing model fields to the anomalous field: in these cases a "residual" is defined as (anomaly - calculated value).

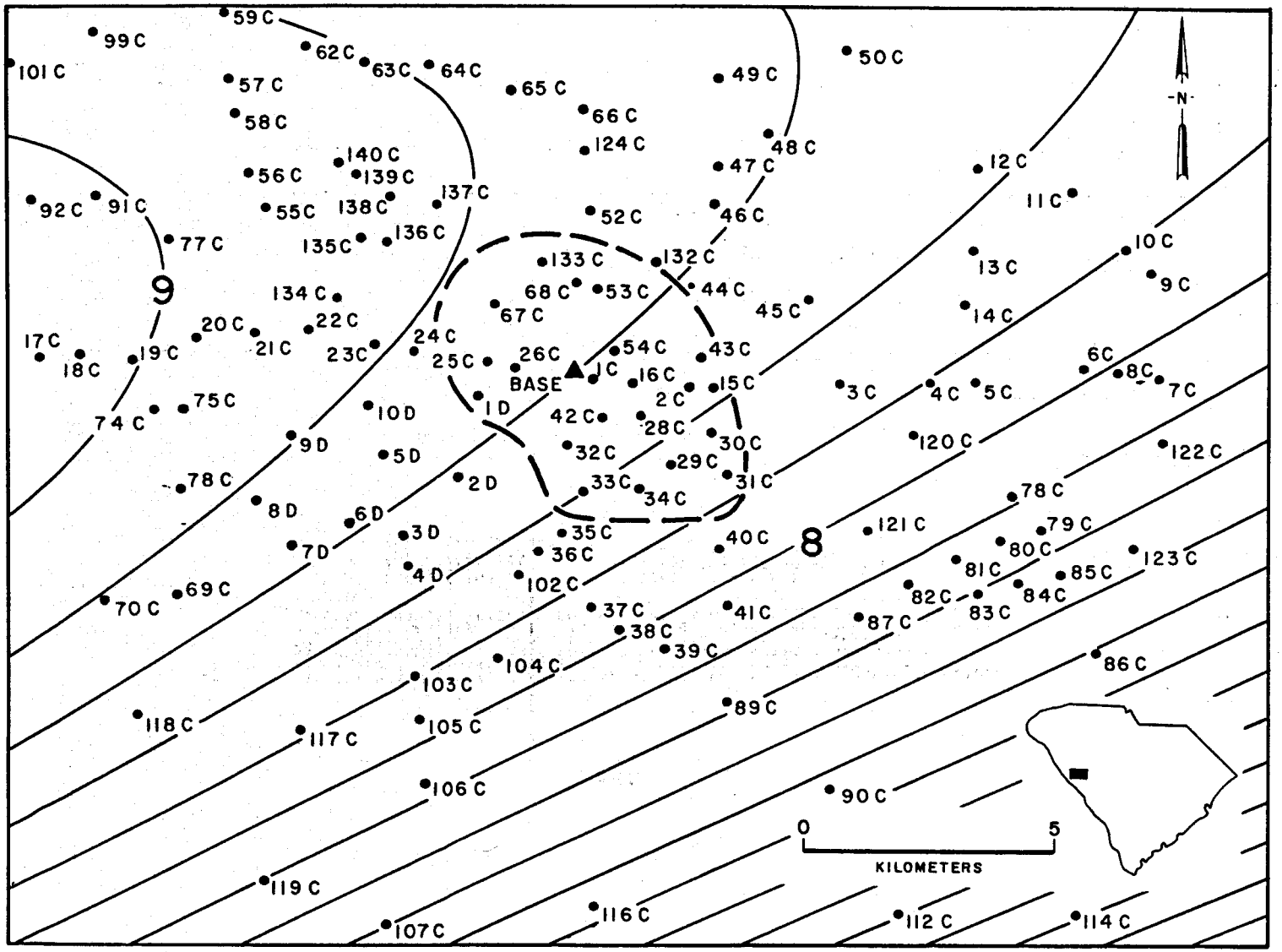

Figure C-4. Distribution of gravity measurements near the Edgefield, SC, granitic pluton, showing station codes of Table C-1. Bold outline is the exposed portion of pluton; lighter lines are contours of 2nd-degree trend surface used for regional Bouguer field.

TABLE C-1.

GRAVITY MEASUREMENTS TAKEN BY A. H. COGBILL AND J. A. DUNBAR OF V.P.I. THE MEASUREMENTS ARE LOCATED IN THE VICINITY OF MCCORMICK, SC. AND WERE ACQUIRED IN AN EFFORT TO STUDY A GRANITIC BODY KNOWN AS THE EDGEFIELD (OR MCCORMICK) GRANITE. THE PRINCIPAL REFERENCE BASE WAS A GRAVITY STATION IN BATESBURG, SC, ESTABLISHED BY AMS IN THE 1960'S. GRAVITY METERS USED WERE THE LACOSTE MODELS G-107 & G-58.

BECAUSE THE BASE AT BATESBURG, SC WAS NOT ON THE ISGN 1971, 13.71 MILLIGALS WAS SUBTRACTED FROM ALL THE OBSERVATIONS PRIOR TO REFERENCE TO THE INT. ELLIPSOID OF 1967.

TABLE C-1 (continued).

GRAVITY REDUCTIONS: GRAVITY MEASUREMENTS NEAR THE GRANITIC PLUTON LOCATED NEAR MCCORMICK, SC. DATE: 14/02/78

STATION	LATITUDE	LONGITUDE	ELEV	OBS GRAV	(USGS) FREE-AIR	(USGS) BOUGUER	CC	(NOAA) FREE-AIR	(NOAA) BOUGUER	REFERENCE STATION	STATION	COUNT
EDBASE	33 55.29	82 7.61	538.0	979591.85	0.51	-18.07	0.23	0.50	-17.85	BASE	EDBASE	1
ED1C	33 55.26	82 7.36	524.0	979592.53	-0.09	-18.18	0.22	-0.09	-17.96	EDBA	ED1C	2
ED2C	33 55.24	82 6.16	514.0	979593.05	-0.48	-18.23	0.22	-0.48	-18.01	EDBA	ED2C	3
ED3C	33 55.37	82 4.36	422.0	979605.74	3.37	-11.20	0.18	3.37	-11.02	EDBA	ED3C	4
ED4C	33 55.47	82 3.28	463.0	979606.87	8.22	-7.77	0.20	8.22	-7.57	EDBA	ED4C	5
ED5C	33 55.50	82 2.72	464.0	979609.24	10.64	-5.38	0.20	10.64	-5.19	EDBA	ED5C	6
ED6C	33 55.73	82 1.41	392.0	979618.92	13.21	-0.33	0.17	13.21	-0.16	EDBA	ED6C	7
ED7C	33 55.65	82 0.51	484.0	979617.26	20.34	3.62	0.21	20.33	3.82	EDBA	ED7C	8
ED8C	33 55.70	82 1.01	443.0	979618.15	17.30	2.00	0.19	17.30	2.19	EDBA	ED8C	9
ED9C	33 56.73	82 0.69	445.0	979618.85	16.75	1.38	0.19	16.75	1.57	EDBA	ED9C	10
ED10C	33 56.98	82 1.01	391.0	979620.46	12.93	-0.57	0.17	12.93	-0.41	EDBA	ED10C	11
ED11C	33 57.50	82 1.68	459.0	979615.13	13.27	-2.58	0.20	13.27	-2.39	EDBA	ED11C	12
ED12C	33 57.70	82 2.82	490.0	979612.14	12.92	-4.00	0.21	12.92	-3.80	EDBA	ED12C	13
ED13C	33 56.85	82 2.83	499.0	979608.20	11.01	-6.22	0.21	11.01	-6.01	EDBA	ED13C	14
ED14C	33 56.29	82 2.89	494.0	979607.09	10.21	-6.85	0.21	10.21	-6.64	EDBA	ED14C	15
ED15C	33 55.24	82 5.86	495.0	979594.39	-0.93	-18.02	0.21	-0.93	-17.81	EDBA	ED15C	16
ED16C	33 55.26	82 6.86	526.0	979592.22	-0.21	-18.38	0.23	-0.21	-18.15	EDBA	ED16C	17
ED17C	33 55.09	82 14.06	449.0	979623.97	24.53	9.03	0.19	24.53	9.22	EDBA	ED17C	18
ED18C	33 55.13	82 13.59	396.0	979626.84	22.36	8.69	0.17	22.36	8.85	EDBA	ED18C	19
ED19C	33 55.13	82 12.95	450.0	979621.46	22.06	6.52	0.19	22.06	6.71	EDBA	ED19C	20
ED20C	33 55.39	82 12.20	460.0	979618.85	20.03	4.14	0.20	20.03	4.34	EDBA	ED20C	21
ED21C	33 55.46	82 11.49	390.0	979620.61	15.11	1.64	0.17	15.11	1.80	EDBA	ED21C	22
ED22C	33 55.55	82 10.84	402.0	979616.92	12.42	-1.46	0.17	12.42	-1.29	EDBA	ED22C	23
ED23C	33 55.47	82 10.03	424.0	979611.31	8.99	-5.65	0.18	8.99	-5.47	EDBA	ED23C	24
ED24C	33 55.42	82 9.53	463.0	979604.14	5.56	-10.43	0.20	5.56	-10.23	EDBA	ED24C	25
ED25C	33 55.34	82 8.64	521.0	979594.89	1.88	-16.11	0.22	1.88	-15.89	EDBA	ED25C	26
ED26C	33 55.31	82 8.29	532.0	979593.25	1.32	-17.06	0.23	1.31	-16.83	EDBA	ED26C	27
ED27C	33 53.31	82 5.23	423.0	979601.66	2.26	-12.35	0.18	2.26	-12.17	EDBA	ED27C	28
ED28C	33 54.92	82 6.71	506.0	979592.54	-1.30	-18.77	0.22	-1.30	-18.56	EDBA	ED28C	29
ED29C	33 54.44	82 6.33	523.0	979591.25	-0.32	-18.38	0.22	-0.32	-18.16	EDBA	ED29C	30
ED30C	33 54.80	82 5.86	508.0	979592.18	-1.30	-18.85	0.22	-1.30	-18.63	EDBA	ED30C	31
ED31C	33 54.38	82 5.63	493.0	979593.61	-0.70	-17.72	0.21	-0.70	-17.51	EDBA	ED31C	32
ED32C	33 54.56	82 7.60	509.0	979592.67	-0.38	-17.96	0.22	-0.39	-17.75	EDBA	ED32C	33
ED33C	33 54.11	82 7.35	457.0	979595.99	-1.33	-17.11	0.20	-1.33	-16.92	EDBA	ED33C	34
ED34C	33 54.17	82 6.70	498.0	979592.16	-1.38	-18.58	0.21	-1.39	-18.37	EDBA	ED34C	35
ED35C	33 53.66	82 7.59	444.0	979599.76	1.85	-13.49	0.19	1.85	-13.30	EDBA	ED35C	36
ED36C	33 53.44	82 7.84	431.0	979601.66	2.83	-12.05	0.19	2.83	-11.87	EDBA	ED36C	37
ED37C	33 52.94	82 7.16	451.0	979600.45	4.20	-11.38	0.19	4.20	-11.18	EDBA	ED37C	38
ED38C	33 52.70	82 6.81	445.0	979601.30	4.82	-10.55	0.19	4.82	-10.36	EDBA	ED38C	39
ED39C	33 52.56	82 6.24	410.0	979604.22	4.64	-9.52	0.18	4.64	-9.34	EDBA	ED39C	40
ED40C	33 53.60	82 5.69	429.0	979599.15	-0.09	-14.91	0.19	-0.09	-14.72	EDBA	ED40C	41
ED41C	33 53.65	82 5.52	427.0	979601.42	2.76	-11.99	0.18	2.76	-11.81	EDBA	ED41C	42
ED42C	33 54.88	82 7.20	493.0	979593.29	-1.71	-18.74	0.21	-1.72	-18.53	EDBA	ED42C	43
ED43C	33 55.57	82 6.04	506.0	979594.56	-0.18	-17.66	0.22	-0.19	-17.44	EDBA	ED43C	44
ED44C	33 56.30	82 6.21	533.0	979595.62	2.40	-16.01	0.23	2.39	-15.78	EDBA	ED44C	45
ED45C	33 56.24	82 4.77	469.0	979604.39	5.23	-10.97	0.20	5.23	-10.77	EDBA	ED45C	46
ED46C	33 57.11	82 6.01	515.0	979604.54	8.49	-9.29	0.22	8.49	-9.07	EDBA	ED46C	47
ED47C	33 57.51	82 5.98	540.0	979606.59	12.34	-6.31	0.23	12.33	-6.08	EDBA	ED47C	48
ED48C	33 57.88	82 5.40	548.0	979609.24	15.22	-3.70	0.23	15.22	-3.47	EDBA	ED48C	49
ED49C	33 58.42	82 6.04	503.0	979614.64	15.64	-1.73	0.22	15.63	-1.52	EDBA	ED49C	50

TABLE C-1 (continued).

GRAVITY REDUCTIONS: GRAVITY MEASUREMENTS NEAR THE GRANITIC PLUTON LOCATED NEAR MCCORMICK, SC. DATE: 14/02/78

STATION	LATITUDE	LONGITUDE	ELEV	OBS GRAV	(USGS) FREE-AIR	(USGS) BOUGUER	CC	(NOAA) FREE-AIR	(NOAA) BOUGUER	REFERENCE STATION	STATION	COUNT
ED50C	33 58.79	82 4.53	549.0	979614.31	19.12	0.16	0.24	19.11	0.39	EDBA	ED50C	51
ED51C	33 59.54	82 3.76	520.0	979619.85	20.88	2.92	0.22	20.88	3.14	EDBA	ED51C	52
ED52C	33 56.98	82 7.49	493.0	979603.84	5.91	-11.12	0.21	5.90	-10.91	EDBA	ED52C	53
ED53C	33 56.19	82 7.35	537.0	979594.53	1.84	-16.71	0.23	1.83	-16.48	EDBA	ED53C	54
ED54C	33 55.56	82 7.11	553.0	979591.55	1.24	-17.86	0.24	1.24	-17.62	EDBA	ED54C	55
ED55C	33 56.77	82 11.44	490.0	979620.45	22.53	5.60	0.21	22.52	5.81	EDBA	ED55C	56
ED56C	33 57.09	82 11.68	500.0	979622.35	24.92	7.65	0.21	24.92	7.87	EDBA	ED56C	57
ED57C	33 58.06	82 11.98	509.0	979627.37	29.43	11.86	0.22	29.43	12.07	EDBA	ED57C	58
ED58C	33 57.69	82 11.89	511.0	979626.00	28.77	11.12	0.22	28.77	11.34	EDBA	ED58C	59
ED59C	33 58.76	82 12.10	455.0	979636.35	32.36	16.64	0.20	32.36	16.84	EDBA	ED59C	60
ED60C	33 59.49	82 11.26	512.0	979628.31	28.66	10.98	0.22	28.66	11.19	EDBA	ED60C	61
ED61C	33 59.47	82 10.41	538.0	979625.96	28.78	10.20	0.23	28.78	10.43	EDBA	ED61C	62
ED62C	33 58.45	82 11.08	538.0	979624.38	28.63	10.05	0.23	28.62	10.28	EDBA	ED62C	63
ED63C	33 58.32	82 10.35	466.0	979624.80	22.46	6.36	0.20	22.45	6.56	EDBA	ED63C	64
ED64C	33 58.34	82 9.57	488.0	979621.37	21.07	4.21	0.21	21.07	4.42	EDBA	ED64C	65
ED65C	33 58.14	82 8.55	442.0	979619.81	15.46	0.19	0.19	15.46	0.38	EDBA	ED65C	66
ED66C	33 57.99	82 7.66	414.0	979618.03	11.26	-3.04	0.18	11.25	-2.87	EDBA	ED66C	67
ED67C	33 55.96	82 8.57	498.0	979597.47	1.43	-15.77	0.21	1.43	-15.56	EDBA	ED67C	68
ED68C	33 56.24	82 7.62	544.0	979594.40	2.30	-16.49	0.23	2.29	-16.26	EDBA	ED68C	69
ED69C	33 52.74	82 12.20	474.0	979610.45	16.64	0.27	0.20	16.64	0.47	EDBA	ED69C	70
ED70C	33 52.64	82 13.09	437.0	979616.60	19.45	4.36	0.19	19.45	4.54	EDBA	ED70C	71
ED71C	33 52.64	82 14.28	374.0	979623.07	20.00	7.08	0.16	19.99	7.24	EDBA	ED71C	72
ED72C	33 52.83	82 14.94	396.0	979622.65	21.38	7.70	0.17	21.38	7.87	EDBA	ED72C	73
ED73C	33 54.35	82 14.49	470.0	979621.34	24.91	8.68	0.20	24.91	8.88	EDBA	ED73C	74
ED74C	33 54.62	82 12.66	398.0	979622.13	18.55	4.81	0.17	18.55	4.98	EDBA	ED74C	75
ED75C	33 54.65	82 12.28	385.0	979621.88	17.04	3.74	0.17	17.04	3.90	EDBA	ED75C	76
ED76C	33 53.83	82 12.26	446.0	979616.80	18.84	3.44	0.19	18.84	3.62	EDBA	ED76C	77
ED77C	33 56.39	82 12.60	488.0	979624.03	26.45	9.60	0.21	26.45	9.80	BATE	ED77C	78
ED78C	33 54.36	82 2.16	438.0	979611.68	12.23	-2.90	0.19	12.22	-2.71	ED16	ED78C	79
ED79C	33 54.02	82 1.82	401.0	979615.25	12.79	-1.06	0.17	12.79	-0.89	ED16	ED79C	80
ED80C	33 53.88	82 2.27	398.0	979614.01	11.46	-2.28	0.17	11.46	-2.11	ED16	ED80C	81
ED81C	33 53.66	82 2.80	380.0	979613.27	9.34	-3.79	0.16	9.34	-3.63	ED16	ED81C	82
ED82C	33 53.37	82 3.39	401.0	979610.90	9.35	-4.50	0.17	9.35	-4.33	ED16	ED82C	83
ED83C	33 53.32	82 2.52	387.0	979613.71	10.91	-2.46	0.17	10.91	-2.29	ED16	ED83C	84
ED84C	33 53.47	82 2.01	365.0	979616.42	11.34	-1.27	0.16	11.34	-1.11	ED16	ED84C	85
ED85C	33 53.59	82 1.52	377.0	979616.43	12.31	-0.71	0.16	12.31	-0.55	ED16	ED85C	86
ED86C	33 52.80	82 1.05	386.0	979616.46	14.29	0.96	0.17	14.29	1.12	ED16	ED86C	87
ED87C	33 53.01	82 3.94	410.0	979608.32	8.12	-6.04	0.18	8.11	-5.87	ED16	ED87C	88
ED89C	33 52.05	82 5.46	372.0	979610.35	7.91	-4.94	0.16	7.91	-4.78	ED16	ED89C	89
ED90C	33 51.21	82 4.12	359.0	979614.04	11.55	-0.85	0.16	11.54	-0.70	ED16	ED90C	90
ED91C	33 56.76	82 13.53	447.0	979626.56	24.61	9.17	0.19	24.60	9.36	ED16	ED91C	91
ED92C	33 56.69	82 14.29	440.0	979627.96	25.45	10.25	0.19	25.44	10.44	ED16	ED92C	92
ED93C	33 56.72	82 15.51	486.0	979624.03	25.80	9.02	0.21	25.80	9.22	ED16	ED93C	93
ED94C	33 57.75	82 16.16	450.0	979636.00	32.95	17.41	0.19	32.94	17.60	ED16	ED94C	94
ED95C	33 58.27	82 16.96	479.0	979634.72	33.67	17.13	0.21	33.67	17.33	ED16	ED95C	95
ED96C	33 59.04	82 17.64	535.0	979628.94	32.08	13.61	0.23	32.08	13.83	ED16	ED96C	96
ED97C	33 59.07	82 16.56	539.0	979628.20	31.68	13.06	0.23	31.67	13.29	ED16	ED97C	97
ED98C	33 58.90	82 15.08	543.0	979627.77	31.86	13.11	0.23	31.86	13.34	ED16	ED98C	98
ED99C	33 58.42	82 8.82	470.0	979632.10	29.99	13.76	0.20	29.99	13.96	ED16	ED99C	99
ED100C	33 59.45	82 13.26	484.0	979635.97	33.74	17.03	0.21	33.74	17.23	ED16	ED100C	100

TABLE C-1 (continued).

GRAVITY REDUCTIONS: GRAVITY MEASUREMENTS NEAR THE GRANITIC PLUTON LOCATED NEAR MCCORMICK, SC. DATE: 14/02/78

STATION	LATITUDE	LONGITUDE	ELEV	OBS GRAV	(USGS) FREE-AIR	(USGS) BOUGUER	CC	(NOAA) FREE-AIR	(NOAA) BOUGUER	REFERENCE STATION	STATION	COUNT
ED101C	33 58.06	82 14.65	546.0	979624.89	30.44	11.58	0.23	30.43	11.81	ED16	ED101C	101
ED102C	33 53.21	82 8.05	452.0	979601.19	4.66	-10.95	0.20	4.66	-10.76	ED16	ED102C	102
ED103C	33 52.08	82 9.25	416.0	979607.31	8.67	-5.70	0.18	8.66	-5.52	ED16	ED103C	103
ED104C	33 52.33	82 8.25	433.0	979604.54	7.45	-7.51	0.19	7.44	-7.32	ED16	ED104C	104
ED105C	33 51.64	82 9.14	416.0	979607.77	10.04	-4.33	0.18	10.04	-4.15	ED16	ED105C	105
ED106C	33 50.97	82 9.03	416.0	979608.03	11.23	-3.13	0.18	11.23	-2.96	ED16	ED106C	106
ED107C	33 49.46	82 9.37	371.0	979614.95	16.02	3.21	0.16	16.02	3.37	ED16	ED107C	107
ED108C	33 47.46	82 8.01	370.0	979611.02	14.79	2.01	0.16	14.78	2.16	ED1	ED108C	108
ED109C	33 45.94	82 6.10	473.0	979597.48	13.05	-3.29	0.20	13.05	-3.09	ED16	ED109C	109
ED110C	33 46.29	82 3.12	514.0	979594.17	13.11	-4.64	0.22	13.11	-4.43	ED16	ED110C	110
ED111C	33 47.34	82 0.86	504.0	979599.59	16.13	-1.28	0.22	16.12	-1.07	ED16	ED111C	111
ED112C	33 49.92	82 3.20	426.0	979610.89	16.50	1.78	0.18	16.49	1.96	ED16	ED112C	112
ED113C	33 47.61	82 3.06	462.0	979605.95	18.16	2.20	0.20	18.16	2.40	ED16	ED113C	113
ED114C	33 50.04	82 1.04	429.0	979613.60	19.32	4.51	0.19	19.32	4.69	ED16	ED114C	114
ED115C	33 49.38	82 4.98	410.0	979610.33	15.18	1.02	0.18	15.18	1.20	ED16	ED115C	115
ED116C	33 49.79	82 6.85	284.0	979617.78	10.21	0.40	0.12	10.21	0.52	ED16	ED116C	116
ED117C	33 51.45	82 10.58	414.0	979609.14	11.49	-2.81	0.18	11.48	-2.64	ED16	ED117C	117
ED118C	33 51.49	82 12.60	438.0	979610.67	15.22	0.09	0.19	15.22	0.28	ED16	ED118C	118
ED119C	33 49.85	82 10.90	413.0	979611.64	16.12	1.86	0.18	16.12	2.03	ED16	ED119C	119
ED120C	33 54.92	82 3.43	445.0	979611.14	11.57	-3.80	0.19	11.56	-3.62	ED16	ED120C	120
ED121C	33 53.90	82 3.89	414.0	979606.26	5.19	-9.11	0.18	5.19	-8.93	ED16	ED121C	121
ED122C	33 55.02	82 0.42	433.0	979618.46	17.62	2.66	0.19	17.61	2.85	ED16	ED122C	122
ED123C	33 53.91	82 0.67	404.0	979617.16	15.14	1.18	0.17	15.13	1.36	ED16	ED123C	123
ED124C	33 57.58	82 7.61	440.0	979612.49	8.73	-6.46	0.19	8.73	-6.28	ED16	ED124C	124
ED125C	33 59.48	82 7.92	536.0	979620.77	23.39	4.88	0.23	23.39	5.11	ED16	ED125C	125
ED126C	33 59.77	82 8.36	517.0	979623.56	23.99	6.13	0.22	23.99	6.35	ED16	ED126C	126
ED127C	34 0.0	82 8.64	510.0	979625.22	24.67	7.06	0.22	24.67	7.27	ED16	ED127C	127
ED128C	34 0.99	82 9.86	588.0	979625.97	31.37	11.07	0.25	31.37	11.32	ED16	ED129C	128
ED129C	34 2.05	82 9.04	590.0	979627.09	31.20	10.83	0.25	31.20	11.08	ED16	ED129C	129
ED130C	34 2.89	82 8.16	613.0	979627.47	32.57	11.40	0.26	32.57	11.66	ED16	ED130C	130
ED131C	34 1.36	82 7.66	513.0	979629.54	27.37	9.66	0.22	27.37	9.87	ED16	ED131C	131
ED132C	33 56.49	82 6.68	541.0	979595.33	2.60	-16.09	0.23	2.59	-15.86	ED16	ED132C	132
ED133C	33 56.43	82 8.05	498.0	979598.83	2.13	-15.06	0.21	2.13	-14.85	ED16	ED133C	133
ED134C	33 55.90	82 10.52	381.0	979617.50	10.54	-2.62	0.17	10.54	-2.46	ED16	ED134C	134
ED135C	33 56.53	82 10.27	446.0	979614.78	13.05	-2.35	0.19	13.05	-2.16	ED16	ED135C	135
ED136C	33 56.51	82 9.94	434.0	979613.83	11.00	-3.99	0.19	11.00	-3.80	ED16	ED136C	136
ED137C	33 56.91	82 9.38	429.0	979613.52	9.66	-5.15	0.19	9.66	-4.97	ED16	ED137C	137
ED138C	33 56.98	82 9.94	460.0	979615.99	14.95	-0.93	0.20	14.95	-0.74	ED16	ED138C	138
ED139C	33 57.17	82 10.38	477.0	979618.95	19.25	2.77	0.21	19.24	2.97	ED16	ED139C	139
ED140C	33 57.26	82 10.59	489.0	979618.90	20.20	3.31	0.21	20.20	3.52	ED16	ED140C	140
ED10	33 55.01	82 8.71	497.0	979596.20	1.39	-15.77	0.21	1.39	-15.56	EDBA	ED10	141
ED20	33 54.17	82 8.88	479.0	979599.68	4.35	-12.19	0.21	4.35	-11.99	EDBA	ED20	142
ED30	33 53.46	82 9.48	476.0	979602.05	7.43	-9.01	0.20	7.42	-8.81	EDBA	ED30	143
ED40	33 53.21	82 9.42	449.0	979603.78	6.97	-8.54	0.19	6.96	-8.35	EDBA	ED40	144
ED50	33 54.32	82 9.83	495.0	979604.15	10.12	-6.98	0.21	10.11	-6.77	EDBA	ED50	145
ED60	33 53.61	82 10.17	435.0	979607.40	8.71	-6.31	0.19	8.71	-6.13	EDBA	ED60	146
ED70	33 53.34	82 10.87	456.0	979608.51	12.17	-3.58	0.20	12.17	-3.38	EDBA	ED70	147
ED80	33 53.76	82 11.32	490.0	979610.13	16.41	-0.52	0.21	16.40	-0.31	EDBA	ED80	148
ED90	33 54.47	82 10.95	452.0	979613.03	14.74	-0.87	0.20	14.74	-0.68	EDBA	ED90	149
ED100	33 54.85	82 10.05	466.0	979607.17	9.67	-6.43	0.20	9.67	-6.23	EDBA	ED100	150

Trend analysis. In order to estimate the low-frequency portion of the Bouguer field, we used measurements lying within two regions containing the pluton. The technique used was to fit, by least-squares, orthogonal polynomials directly to the irregularly distributed measurements in a manner described by Whitten (1970), using a modified version of the program of Whitten (1971). The advantage of using orthogonal polynomials is that each orthogonal coefficient is independent of other such coefficients; thus the deletion of any particular orthogonal polynomial does not affect the coefficients of any other polynomial. Moreover, the use of such a technique allows the construction of a z^2-array (Grant, 1957; Oldham and Sutherland, 1955) by which those orthogonal coefficients that contribute significantly to the trend may be identified. As discussed by Grant (1957), even the use of the z^2-array rarely permits an unambiguous distinction between polynomials that are associated with the trend and those which are not. Nevertheless, use of the z^2-array technique to identify those polynomials associated with the trend nearly always leads to trend surfaces which differ but little, even accounting for the above-mentioned ambiguities.

Two regions were used for the trend analysis of the Edgefield area because we wished to investigate the dependence of the estimated trend upon the size of the region considered. In each case, there was a remarkable

separation between those polynomials associated with very large z^2-values. Each analysis indicated that the (0,1) and (1,0) orthogonal polynomials were those associated with the trend(*). In the immediate vicinity of the Edgefield granite, differences between the calculated trend surfaces were < 1 mgal. Somewhat arbitrarily, we chose the surface calculated from the smaller region: this surface predicts a background field of roughly +8 mgal over the pluton, thus yielding a total anomaly of -27.2 mgal. Contours of the trend surface used are shown in Figure C-4, along with the distribution of stations and the station codes of Table C-1. The standard error of the surface fit was 5.0 mgal; this provides an estimate of the uncertainty of the maximum amplitude of the anomaly. This is important because this error is a major source of uncertainty in the determination of the total depth of the pluton.

Density contrast. The average modal analysis of the Edgefield granite is as follows (S.W. Becker, pers. comm., 1977): 35% plagioclase [An(01)-Or(01)-Ab(98)], 28% K-feldspar [An(0)-Ab(02)-Or(98)], 33% quartz, 2% white mica, 2% other minerals. The mean density of the rock based upon this average analysis (using 2.78 gm/cc for the density of the white mica) is 2.62 gm/cc. The density of this rock may change systematically with depth, but will probably remain at values < 2.70 gm/cc.

(*) The notation of Whitten (1970) is used to identify the particular orthogonal polynomials used.

The densities of the rocks into which the pluton has intruded are much less well-known than the density of the pluton itself. These rocks have been studied but little, partly because they are less well-exposed than the granitic rocks. The few exposures examined by this writer appear to be slightly metamorphosed pelitic rocks. These rocks are not expected tc have densities greatly exceeding 2.75 gm/cc, thus indicating an estimated density contrast of 0.15 gm/cc. However, because the mineral assemblages comprising these rocks are unkncwn and because the rccks have not been well-studied, the bulk density of these rocks may be as high as 2.85 - 2.90 gm/cc, implying a density contrast of -0.25 gm/cc. Densities > 2.90 gm/cc are possible but very unlikely, because such high densities would lead to a large Bouguer high in a broad region about the Edgefield pluton, a high that is not observed.

In summary, the density contrast between the Edgefield granite and the surrounding rocks may easily be within the range -0.25 to -0.15 gm/cc, the range of uncertainty being chiefly the result of the large uncertainty in the density of the country rock. Although the density contrast may well vary systematically with depth, so little is known about the density distribution in the ccuntry rock that construction of gravity models incorporating such systematic changes is not warranted.

Gravity models. Gravity models of the Edgefield granite were constructed using Plouff's (1976) technique, in which a three-dimensional approximation to the body is constructed using vertically-sided polygonal prisms of finite thickness. Each prism is constrained to have a horizontal top and base. This method differs from the very popular method of Talwani and Ewing (1960), which approximates a three-dimensional body with a vertical stack of polygonal lamellae. Plouff's method uses exact equations for each polygonal prism; thus for many bodies fewer polygonal prisms are necessary when Plouff's technique is used instead of Talwani's method.

Initial models were constant-density models whose polygonal boundaries were designed to coincide with the exposed outline of the Edgefield granite. The depth of each of these models was sufficient to fit the maximum amplitude of the observed anomaly, -27.2 mgal. All such models gave poor fits to the gravity anomaly, and it was apparent that an areally more extensive body was required, at least near the surface. Subsequent modeling of the pluton yielded bodies such as the one shown in Figure C-6. This model is not considered a final model, but is sufficiently close that only small changes in the shape of the upper portion of the body will be sufficient to match the anomalies satisfactorily. The rms error of the model shown is 4 mgal; the mean absolute error is 3 mgal. The distribution and values of the residuals are shown in Figure C-6. The NW

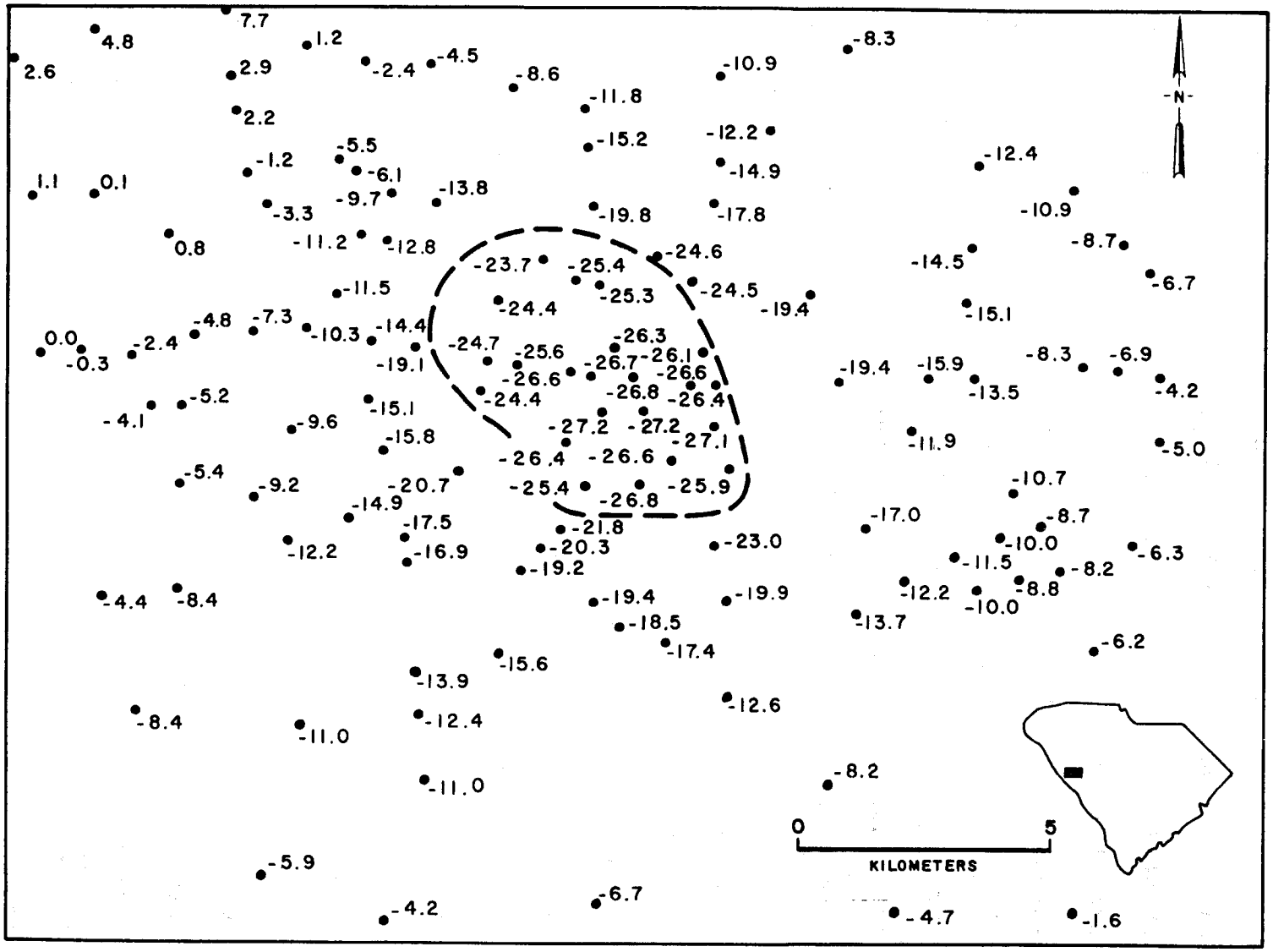

Figure C-5. Gravity anomalies near the Edgefield pluton. Bold outline is the exposed portion of the pluton.

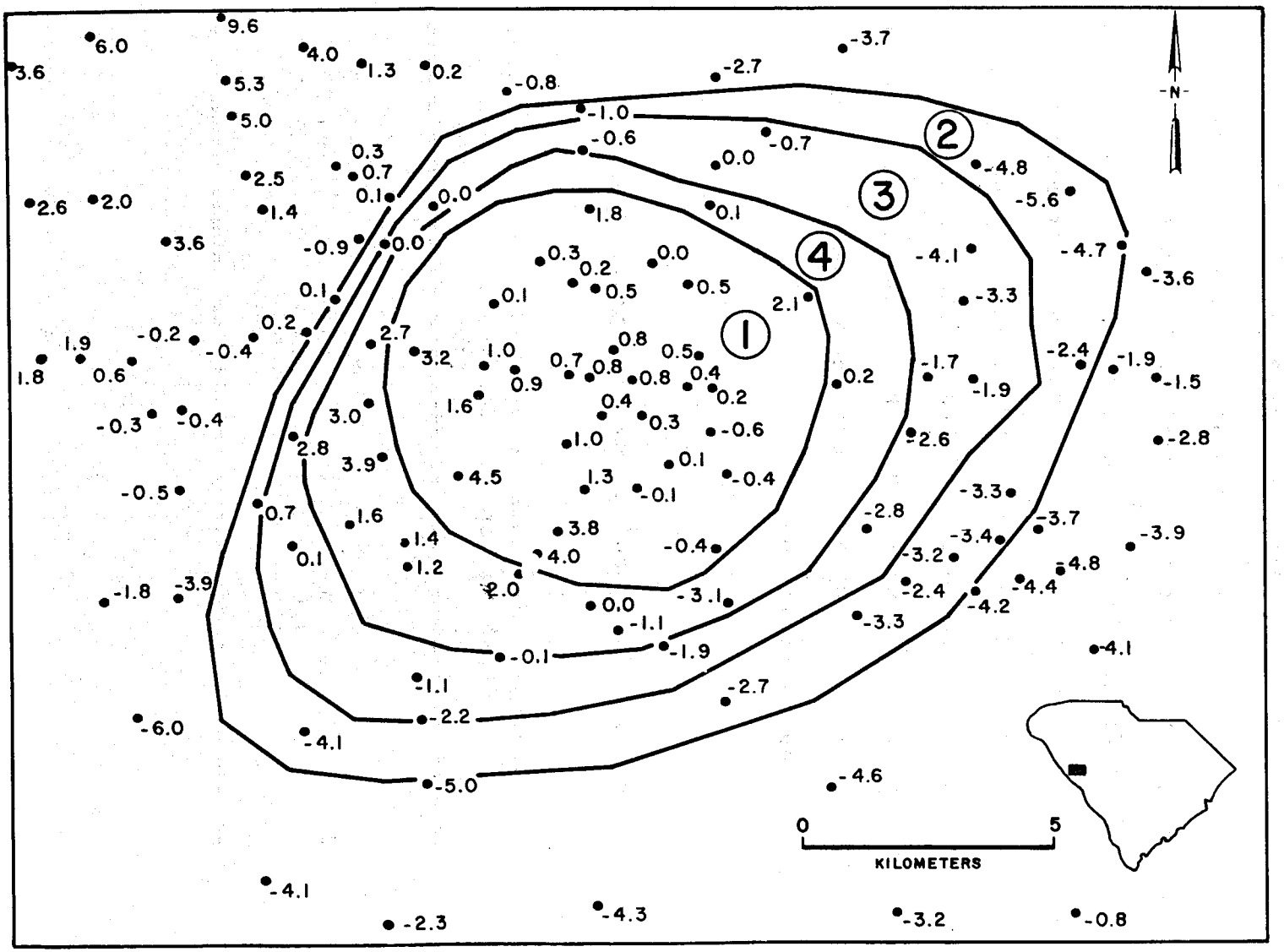

Figure C-6. Outlines of a polygonal body which models the granitic pluton: numbers shown are the residuals (observed ancmalies - calculated anomalies) from the model.

side of the model is fairly steep because of the fairly large gradient in the field in that area. However, there exists a positive source of unknown origin NW of the model (Figure C-5); hence, the high gradient in that vicinity is somewhat misleading. Until more is known about the source of the positive anomaly to the NW, nothing definite may be said about the steepness of NW side of the pluton. Generally, the inferred shape of the pluton is that of an elliptical funnel: the shape in plan of the model is shown in Figure C-6, and the vertical coordinates of the polygonal prisms are given in Table C-2.

Table C-2. Polygonal prisms of Figure C-6.

Prism No.	Depth to Top (km)	Thickness (km)	Density (gm/cm^3)
1	0.0	0.5	-0.20
2	0.5	0.5	-0.20
3	1.0	0.5	-0.20
4	1.5	4.7	-0.20

Because of the large uncertainty concerning the proper density contrast, Figure C-7 was prepared to display the possible models in a convenient manner. This figure shows, for several values of the density contrast, the total depth of prism #4 (Table C-2 and Figure C-6) required to fit the maximum amplitude of the gravity anomaly. For example, if we use 5.0 mgal as the uncertainty of the maximum amplitude of the anomaly, then for a density contrast of -0.20 gm/cc, the total depth of the pluton is 4.2 - 9.9 km, with a most probable value of 6.2 km. Depth limits for different density contrasts may be read from the figure. Interestingly, for density contrasts as small as -0.15 gm/cc, the required total depth of the pluton is 7.6 km to infinity, with a most probable value of 16 km. This seems an unreasonably large value for the depth of the pluton, and suggests that -0.15 is too small (in magnitude) a value for the density contrast.

Rolesville and Petersburg granitic rocks

We have used the data provided by NOAA to estimate the low-frequency components of the Bouguer field in the vicinity of the Rolesville batholith and the Petersburg granite. The techniques used thus far have been the same as those used to estimate the gravity trends in the vicinity of the Edgefield, SC, pluton.

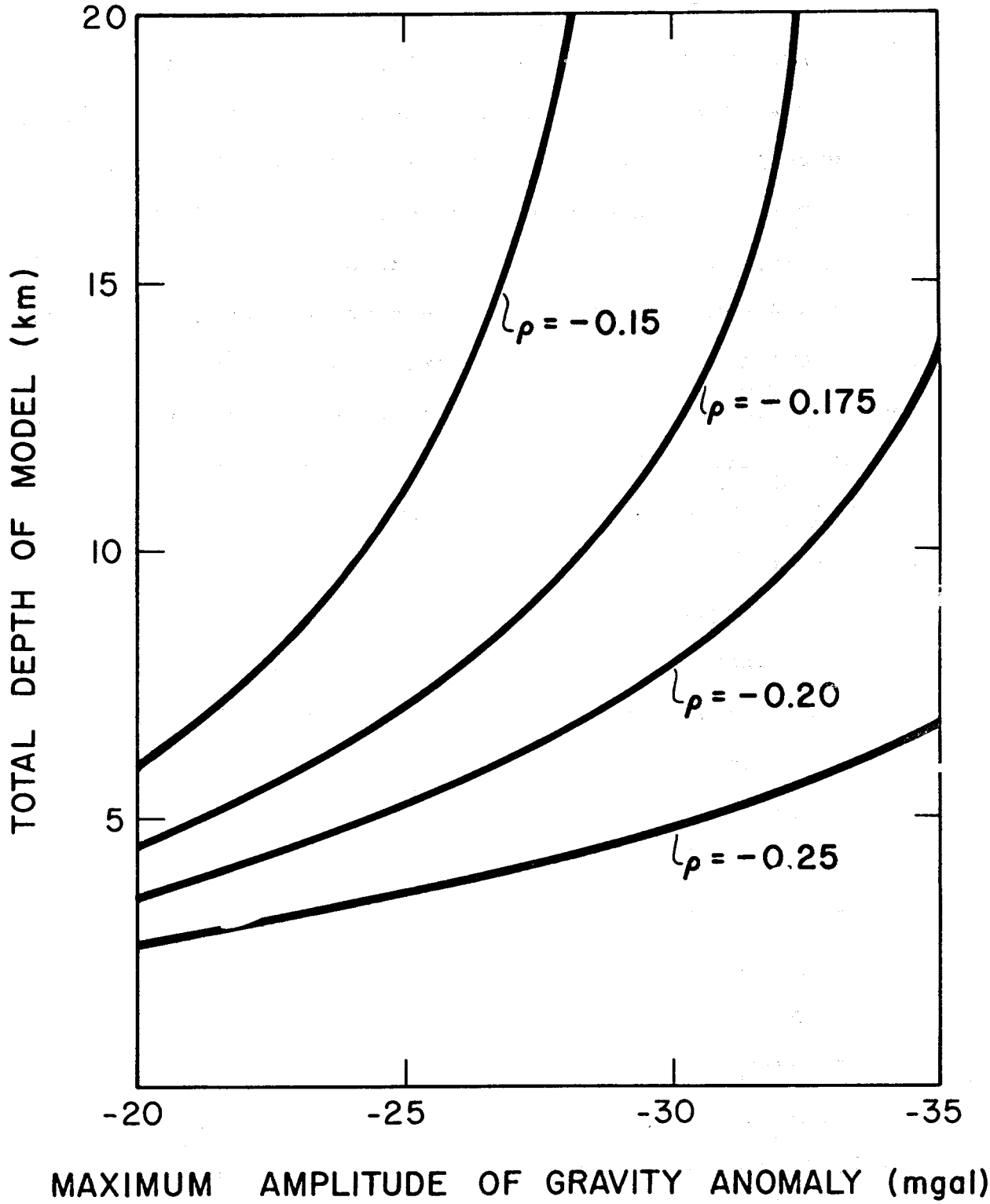

Figure C-7. Total depth of polygonal model of Figure C-6 shown as function of the maximum amplitude of the gravity anomaly for several assumed density contrasts.

Rolesville batholith. Sixth-degree, orthogonal polynomials were fit to about 2900 gravity measurements in the quadrangle 77°-80°W., 35°-37°N. The ordered z^2-array resulting associated with the orthogonal polynomials is shown in Figure C-8(a). Only those orthogonal polynomials indicated in that Figure were used to estimate the regional trend of the Bouguer field. The resulting trend surface is shown in Figure C-9, along with the outline of the Rolesville batholith. This trend surface predicts regional Bouguer values of up to +14 mgal, thus indicating a total anomaly of about -50 mgal over some portions of the batholith. The rms error associated with this trend surface is 15.9 mgal.

The NOAA catalog contains only 18 gravity measurements that are actually located upon the Rolesville batholith. Because of the small number of these measurements, we are presently acquiring more gravity measurements over this body. Further efforts will also be made to estimate the low-frequency gravity field over the batholith, as the estimated amplitude of the regional field will be critical to the estimation of the total depth of the batholith.

Petersburg granite. A similar analysis of the Bouguer field in the vicinity of the Petersburg granite in southeastern Virginia has begun. A Bouguer anomaly of -20 mgal occurs over this body (VPI&SU-5103-5, Figure C-5); the regional trend surface, calculated from the indicated

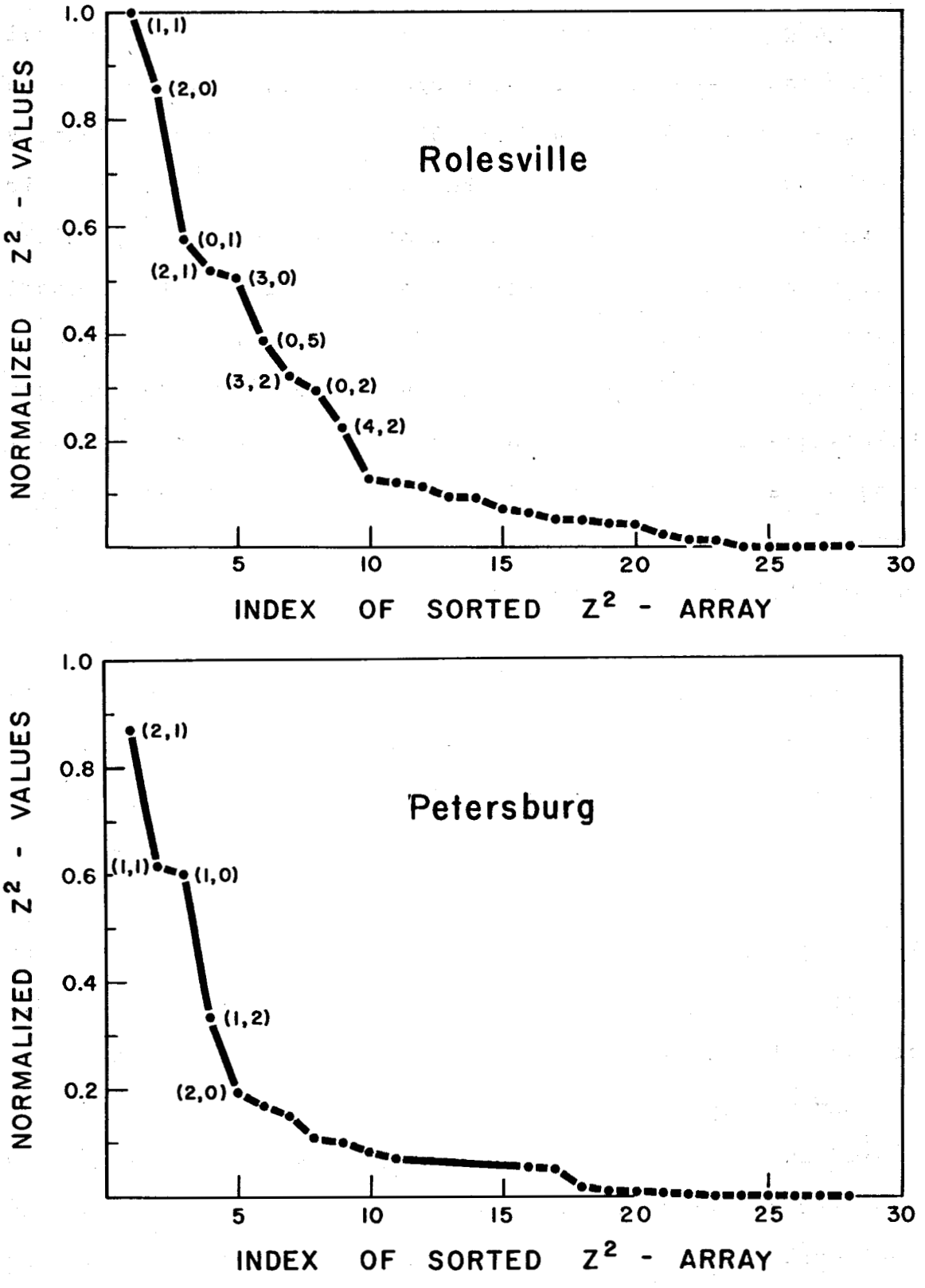

Figure C-8. Normalized z^2-array for (a) the Rolesville area trend surface and (b) Petersburg area trend surface. Numbers in parentheses refer to the orthogonal polynomials associated with each z^2 element.

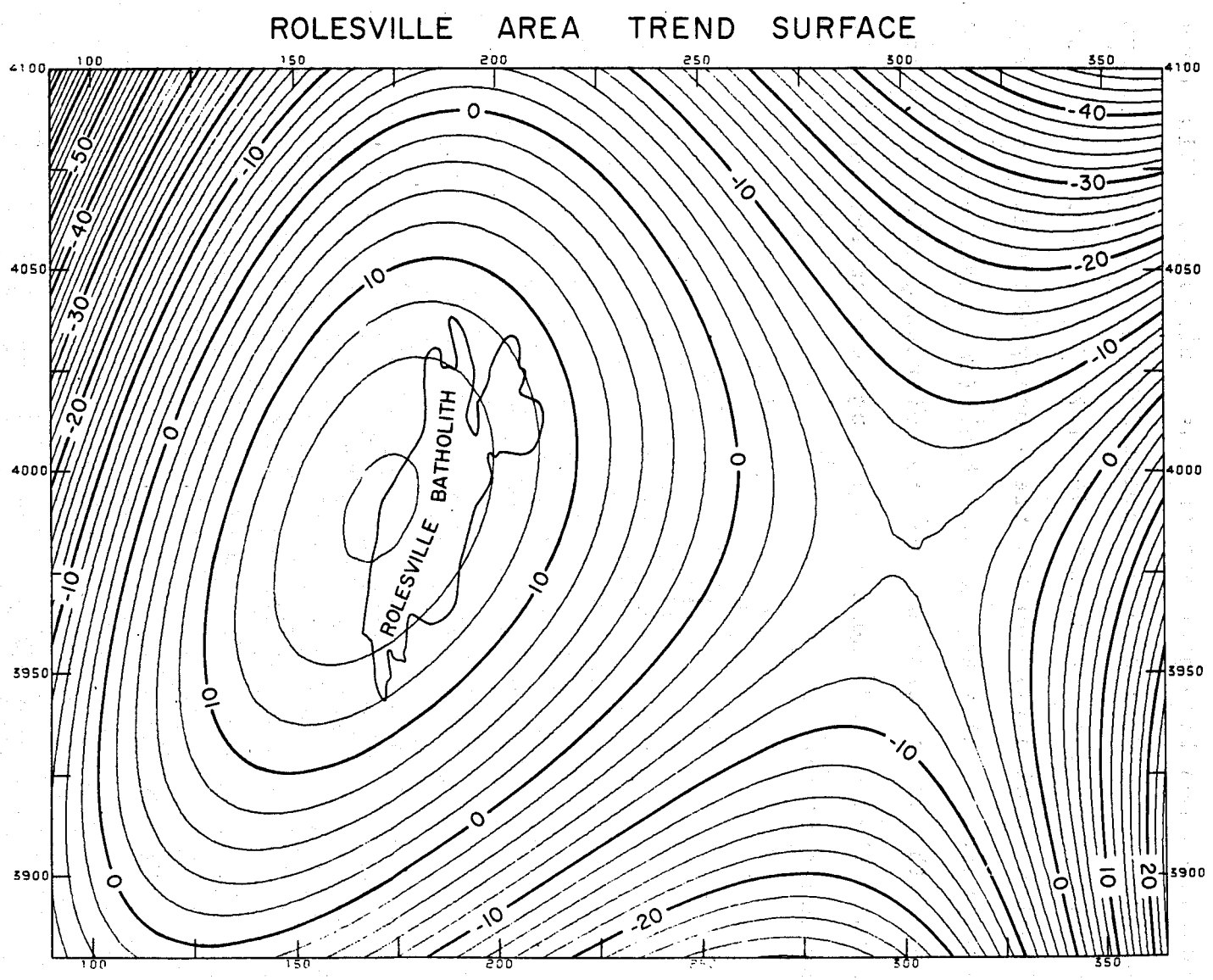

Figure C-9. Trend surface in the Rolesville area.

orthogcnal coefficients of Figure C-8(b), predicts Bouguer values of 0 to -13 mgal over this body (there is a pronounced negative gradient to the southeast). This trend surface was calculated from about 2800 gravity measurements occurring in the quadrangle 76 1/2°-78 1/2°W., 36°-38°N. Thus the tctal amplitude of the anomaly attributable to the Petersburg granite may be as high (in magnitude) as -30 mgal. The trend analysis in the Petersburg area is in its initial stages, and more work is ongoing to further define the regional field.

References

Grant, Fraser (1957), A problem in the analysis of geophysical data, Geophysics, 22, 309-344.

Oldham, C.H.G., and D.B. Sutherland (1955). Orthogonal polynomials: their use in estimating the regional effect, Geophysics, 20, 295-306.

Plouff, Donald (1976). Gravity and magnetic fields of polygonal prisms and application to magnetic terrain corrections. Geophysics, 41, 727-741.

Talwani, Manik and Maurice Ewing (1960). Rapid computation of gravitational attraction of three-dimensional bodies of arbitrary shape, Geophysics, 25, 203-225.

Whitten, E.H.T. (1970). Orthogonal polynomial trend surfaces for irregularly spaced data, Math. Geology, 2, 141-152.

Whitten, E.H.T. (1974). Orthogonal-polynomial contoured trend-surface maps for irregularly-spaced data, Tech. Report 2, U.S. Army Research Office, Durham, NC, Contract # DA-ARO-D-31-124-72-G74.

GEOTHERMAL GRADIENTS, HEAT FLOW, AND HEAT GENERATION

J. K. Costain, L. D. Perry and J. A. Dunbar

Figure C-10 shows locations of holes drilled to date by VPI&SU in the southeastern United States. Table C-3 summarizes geothermal gradients, thermal conductivity and heat flow determinations available to date for this contract. This table appears in each report, beginning with VPI&SU-5103-4, and is periodically updated as thermal conductivity and heat flow determinations are completed. Slight changes in the gradients that will appear in Table C-3 are the result of relogging these holes as they reach thermal equilibrium. Changes in gradient are not expected to be more than a few percent. Holes drilled in the Rolesville batholith are now being relogged.

The methods by which thermal conductivity and gradients are determined are described in previous reports (VPI&SU-5103-1,2,3,4). New thermal conductivity values are reported herein for RL1, RL2, and SB1 and are included in Tables C-4, C-5, and C-6. Additional thermal conductivity values for RL1 and SB1 resulted in changes of thermal conductivity of -1.2% and -2.2%, respectively. In both cases the standard deviation decreased.

Heat flow values are determined in two ways: (1) multiplication of the average thermal conductivity over an interval by the gradient corresponding to that interval; and

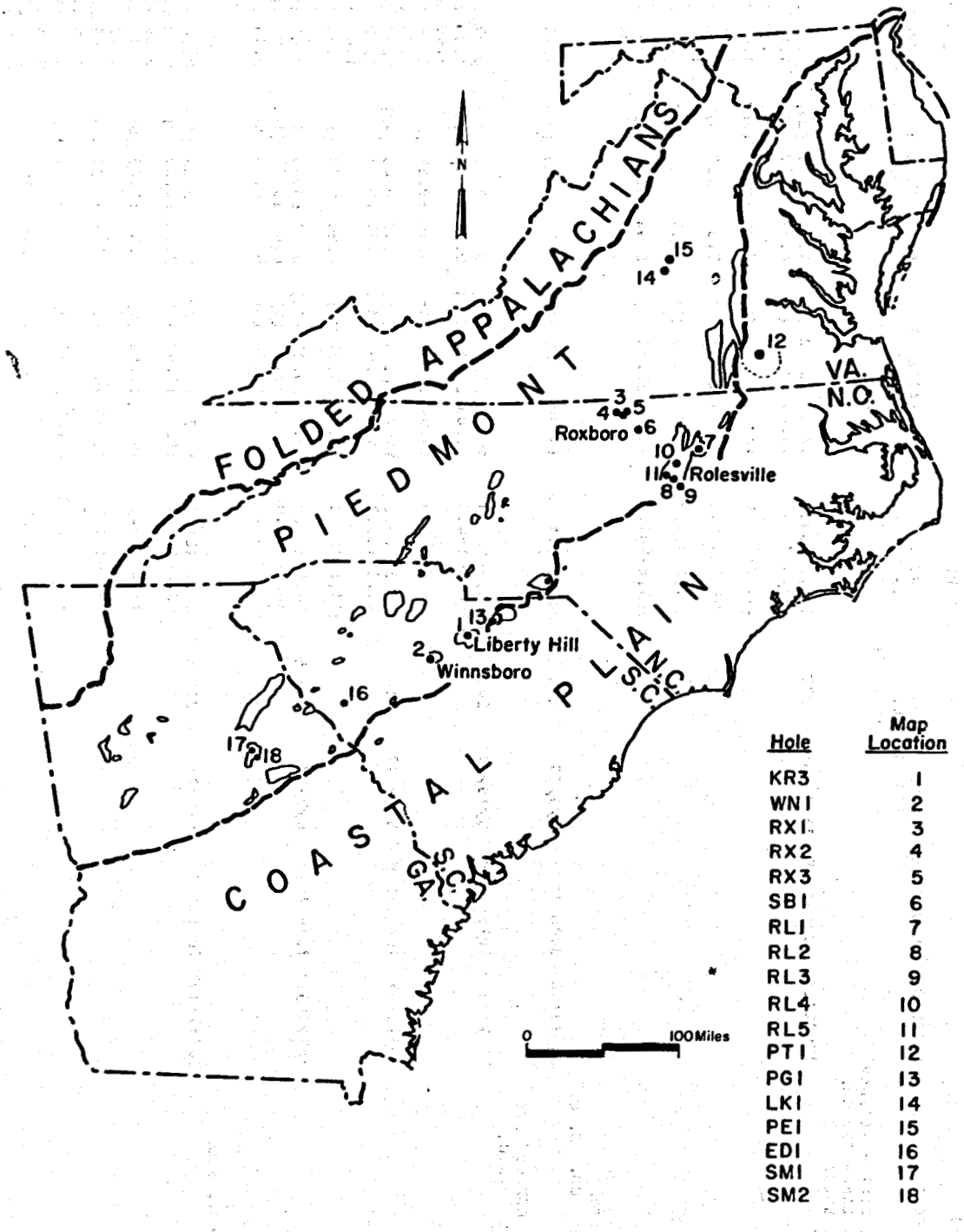

Figure C-10. Location of holes drilled to date by VPI&SU.

TABLE C-3 SUMMARY OF HEAT FLOW DATA FEBRUARY 17, 1978

LOCATION	LATITUDE	LONGITUDE	DATE LOGGED	HOLE DEPTH (METERS)	DEPTH INTERVAL (METERS)	GRADIENT[3] (°C/KM)	CONDUCTIVITY[3] (MCAL/CM-SEC-°C)	HEAT FLOW (CAL/CM²-SEC)
LIBERTY HILL - KERSHAW PLUTON, LANCASTER CO., SOUTH CAROLINA								
KR3	34°32'20"	80°44'51"	11/18/76	277	316.8-404.3	14.91 ±0.02 (36)	7.14 ±0.57 (24)*	1.07 ±0.09[1]
					334.3-341.8	14.68 ±0.07 (4)	6.94 ±0.47 (3)*	1.02 ±0.07[1]
								1.02 ±0.03[2]
					344.3-356.8	15.06 ±0.07 (6)	7.09 ±0.54 (5)*	1.07 ±0.09[1]
								1.05 ±0.02[2]
					359.3-369.3	14.88 ±0.07 (5)	7.33 ±0.20 (4)*	1.09 ±0.04[1]
								1.09 ±0.01[2]
					371.8-384.3	14.85 ±0.06 (6)	7.07 ±0.28 (5)*	1.05 ±0.05[1]
								1.05 ±0.01[2]
					386.8-401.8	15.00 ±0.13 (7)	6.94 ±0.69 (6)*	1.04 ±0.11[1]
								1.04 ±0.01[2]
RION PLUTON, FAIRFIELD CO., S. C.								
WN1	34°18'48"	81°08'42"	7/5/77	574.3	24.24-571.74	18.18 ±0.04 (220)	8.06 ±0.24 (26)	1.47 ±0.05[1]
ROXBORO METAGRANITE, PERSON CO., N.C.								
RX1	36°23'12"	78°58'00"	5/19/77	240	146.8-249.3	10.83 ±0.03 (42)	8.97 ±0.41 (32)	0.97 ±0.05[1]
					146.8-184.3	11.03 ±0.06 (16)	9.08 ±0.11 (15)	1.00 ±0.02[1]
								1.00 ±0.01[2]
					219.3-231.8	10.94 ±0.12 (16)	9.76 ±0.59 (5)	0.96 ±0.08[1]
								0.95 ±0.01[2]
RX2	36°25'31"	79°01'53"	5/19/77	214	149.3-209.3	11.20 ±0.04 (25)	8.77 ±0.45 (23)	0.98 ±0.05[1]
					149.3-189.3	11.30 ±0.07 (17)	8.87 ±0.21 (16)	1.00 ±0.03[1]
								1.00 ±0.03[2]
					191.8-209.3	11.05 ±0.04 (8)	8.54 ±0.73 (7)	0.94 ±0.08[1]
								0.95 ±0.01[2]
RX3	36°25'39"	78°53'42"	8/7/77	211.5	134.9-199.9	10.36 ±0.22 (14)	8.33 ±0.58 (14)	0.86 ±0.08[1]
					144.3-169.9	10.43 ±0.37 (6)	8.40 ±0.67 (10)	0.88 ±0.10[1]
					181.9-194.9	9.00 ±0.46 (3)	8.14 ±0.25 (4)	0.73 ±0.06[1]
SLATE BELT PERSON CO., N.C.								
SB1	36°19'40"	78°50'00"	6/5/77	211.5	81.7-181.7	11.70 ±0.09 (28)	8.21 ±0.86 (10)	0.96 ±0.11[1]
					99.2-136.7	11.08 ±0.50 (8)	8.28 ±0.69 (7)	0.92 ±0.12[1]
								0.89 ±0.05[2]
					139.2-151.7	14.47 ±0.53 (6)	7.87 ±1.03 (5)	1.14 ±0.20[1]
								1.12 ±0.03[2]
					166.7-171.7	12.80 ±0.23 (3)	8.23 ±0.23 (2)	1.05 ±0.05[1]
								1.05 ±0.01[2]
					174.24-179.24	13.80 ±0.12 (3)	7.01 ±0.64 (2)	0.97 ±0.10[1]
								0.96 ±0.04[2]
					181.7-204.2	10.95 ±0.33 (6)	8.18 ±0.24 (5)	0.90 ±0.05[1]
								0.89 ±0.03[2]

TABLE C-3 SUMMARY OF HEAT FLOW DATA FEBRUARY 17, 1978

ROLESVILLE BATHOLITH, FRANKLIN CO., N.C.							
RL1	36°04'15"	78°07'43"	8/16/77	210.6	142.5-210.0	19.05 ±0.11 (28)	7.52 ±0.39 (26)	1.43 ±0.08[1]
					145.0-210.0	19.06 ±0.12 (27)	7.52 ±0.39 (26)	1.43 ±0.08[1]
								1.44 ±0.01[2]
RL2	36°47'17"	78°25'04"	9/14/77	212.8	27.4-209.8	18.61 ±0.20 (74)	7.22 ±0.35 (13)	1.34 ±0.08[1]
					104.9-129.9	16.00 ±0.00 (7)	7.33 ±0.40 (6)	1.17 ±0.07[1]
							7.13 ±0.32 (6)	1.18 ±0.01[2]
					192.4-207.4	18.00 ±0.46 (7)	7.13 ±0.32 (6)	1.28 ±0.09[1]
								1.28 ±0.04[2]
RL3	35°57'05"	78°20'00"	10/19/77	121.9	42.5-132.5	13.79 ±0.11 (37)		
					42.5- 52.5	14.80 ±0.40 (5)		
					55.0- 65.0	10.80 ±0.40 (5)		
					67.5- 82.5	13.14 ±0.26 (7)		
					85.0- 95.0	18.80 ±0.40 (5)		
					97.5-132.5	13.17 ±0.14 (15)		
RL4	35°43'36"	78°19'45"	10/19/77	196.3	102.4-194.9	15.34 ±0.12 (38)		
					102.4-124.9	15.01 ±0.44 (10)		
					152.4-194.9	16.63 ±0.08 (18)		
RL5	35°51'17"	78°28'54"	10/20/77	211.5	72.5-210.0	16.23 ±0.03 (56)		
PETERSBURG GRANITE, SUSSEX CO., VA.								
PT1	36°49'45"	77°19'15"	10/21/77	253.0	14.9- 87.4	23.09 ±0.23 (30)[5]		
					92.4-154.9	17.73 ±0.04 (26)[6]		
					192.4-252.4	18.88 ±0.14 (25)[6]		
PAGELAND PLUTON, LANCASTER CO., S.C.								
PG1	34°34'25"	80°50'52"		213.4				
LAKESIDE CUMBERLAND CO., VA.								
LK1	37°41'25"	78°08'52"	9/16/77	205.0	59.3-204.3	13.46 ±0.07 (58)		
					59.3- 81.8	11.49 ±0.07 (10)		
					121.3-144.3	14.30 ±0.17 (10)		
					164.3-204.3	13.31 ±0.05 (17)		
PEGMATITE BELT, GOOCHLAND CO., VA.								
PE1	37°45'56"	78°05'37"	9/16/77	200.0	119.8-199.8	15.17 ±0.10 (33)		

TABLE C-3 SUMMARY OF HEAT FLOW DATA FEBRUARY 17, 1978

CUFFYTOWN (EDGEFIELD), S.C.			
ED1	33°55'11"	82°07'10"	294.0
SILOAM (GREENE CO.), GA.			
SM1	32°31'	83°6'	ON SITE
SM2	33°28'	83°3'	

1 - INDICATES HEAT FLOW VALUE IS THE PRODUCT OF A MEAN GRADIENT AND A MEAN THERMAL CONDUCTIVITY
2 - INDICATES HEAT FLOW VALUE IS FROM THE BULLARD APPROXIMATION
3 - VALUE IN PARENTHESES IS THE NUMBER OF TEMPERATURE POINTS OR THE NUMBER OF THERMAL CONDUCTIVITY VALUES
4 - THERMAL CONDUCTIVITY VALUES FROM 1.270 CM THICK SAMPLES
5 - GRADIENT FROM THE SEDIMENTARY COVER OF THE PLUTON
6 - GRADIENT FROM WITHIN THE PLUTON

TABLE C-4.

THERMAL CONDUCTIVITY VALUES FOR CORE FROM DRILL HOLE RL1 (CASTALIA PLUTON).

THERMAL CONDUCTIVITY VALUES FROM CORE OF DRILL HOLE RL1
(SAMPLES ARE 2.680 CM IN DIAMETER BY 1.270 CM THICK)

SAMPLE NAME	DEPTH (METERS)	THERMAL CONDUCTIVITY MCAL/CM-SEC-°C
RL1-163	49.7	7.70
RL1-476	145.1	6.40
RL1-484	147.5	7.81
RL1-492	150.0	7.51
RL1-500	152.4	7.06
RL1-508	154.8	7.58
RL1-516	157.3	7.87
RL1-525	160.0	7.59
RL1-533	162.5	7.62
RL1-541	164.9	7.36
RL1-549	167.3	7.15
RL1-558	170.1	7.57
RL1-565	172.2	7.49
RL1-574	175.0	7.69
RL1-582	177.4	7.63
RL1-590	179.8	7.31
RL1-598	182.3	7.94
RL1-607	185.0	7.86
RL1-615	187.5	7.02
RL1-623	189.9	7.87
RL1-631	192.3	8.22

TABLE C-4 (CONTINUED).

THERMAL CONDUCTIVITY VALUES FROM CORE OF DRILL HOLE RL1
(SAMPLES ARE 2.680 CM IN DIAMETER BY 1.270 CM THICK)

SAMPLE NAME	DEPTH (METERS)	THERMAL CONDUCTIVITY MCAL/CM-SEC-°C
RL1-639	194.8	7.36
RL1-647	197.2	7.93
RL1-656	199.9	7.54
RL1-664	202.4	6.90
RL1-672	204.8	7.53
RL1-680	207.3	7.88
AVERAGE		7.53
STANDARD DEVIATION		0.38

TABLE C-5.

THERMAL CONDUCTIVITY VALUES FOR CORE FROM DRILL HOLE RL2 (ROLESVILLE BATHOLITH).

THERMAL CONDUCTIVITY VALUES FROM CORE OF DRILL HOLE RL2
(SAMPLES ARE 2.680 CM IN DIAMETER BY 1.270 CM THICK)

SAMPLE NAME	DEPTH (METERS)	THERMAL CONDUCTIVITY MCAL/CM-SEC-°C
RL2-348	106.1	7.19
RL2-356	108.5	7.25
RL2-364	111.0	6.95
RL2-374	114.0	8.11
RL2-380	115.8	7.37
RL2-388	118.3	7.14
RL2-405	123.4	7.07
RL2-635	193.5	6.84
RL2-643	196.0	7.58
RL2-651	198.4	6.77
RL2-660	201.2	6.95
RL2-668	203.6	7.32
RL2-684	208.5	7.30
AVERAGE		7.22
STANDARD DEVIATION		0.35

TABLE C-6.

THERMAL CONDUCTIVITY VALUES FOR CORE FROM DRILL HOLE SB1 (SLATE BELT).

THERMAL CONDUCTIVITY VALUES FROM CORE OF DRILL HOLE SB1
(SAMPLES ARE 2.680 CM IN DIAMETER BY 1.270 CM THICK)

SAMPLE NAME	DEPTH (METERS)	THERMAL CONDUCTIVITY MCAL/CM-SEC-°C
SB1-178	54.3	7.89
SB1-218	66.5	8.03
SB1-284	86.6	8.17
SB1-333	101.5	8.02
SB1-407	124.0	6.83
SB1-415	126.5	8.62
SB1-424	129.2	8.56
SB1-432	131.7	8.84
SB1-440	134.1	8.45
SB1-448	136.6	8.65
SB1-457	139.3	7.70
SB1-465	141.7	9.18
SB1-473	144.2	6.65
SB1-481	146.6	8.62
SB1-497	151.5	7.21
SB1-555	169.2	8.40
SB1-563	171.6	8.07
SB1-572	174.4	7.46
SB1-580	176.8	6.56
SB1-612	186.5	8.05
SB1-621	189.3	8.48

TABLE C-6 (CONTINUED).

THERMAL CONDUCTIVITY VALUES FROM CORE OF DRILL HOLE SB1
(SAMPLES ARE 2.680 CM IN DIAMETER BY 1.270 CM THICK)

SAMPLE NAME	DEPTH (METERS)	THERMAL CONDUCTIVITY MCAL/CM-SEC-°C
SB1-629	191.7	8.29
SB1-645	196.6	7.86
SB1-662	201.8	8.23
AVERAGE		8.03
STANDARD DEVIATION		0.68

(2) the Bullard approximation (Bullard, 1939). The results are the same within experimental error.

Heat flow values determined to date for this contract are shown in Figure C-11.

Some ground water disturbance and effects of thermal disequilibrium are evident on the temperature profile and gradient in RL2 (VPI&SU-5103-5, Figure C-2, p. C-4), especially at a depth of about 150 m. Table C-3 lists three heat flow determinations from three different intervals. The heat flow value with the smallest standard deviation is 1.18 ± 0.01 HFU from a 15-meter interval at a depth of 105 m. Until the hole is relogged, the value from this interval will be taken as representative of the heat flow at RL2.

Additional values of heat generation are now available from core (RL1) from the Castalia pluton and are given in Table C-7. New values from the Rolesville batholith (RL2, RL4, RL5) are given in Tables C-8, C-9, and C-10. Additional values from our reconnaissance survey are listed in Table C-11. Heat generation values from core from the Petersburg granite are given in Table C-12. New values of heat generation for surface samples of the Petersburg are given in Table C-13. All of the values from RX2 in the Roxboro metagranite are now complete and are given in Table C-14.

A hole drilled almost to basement by private industry in Wayne County, Georgia (31°32'N Lat., 81°43'W Long.) in

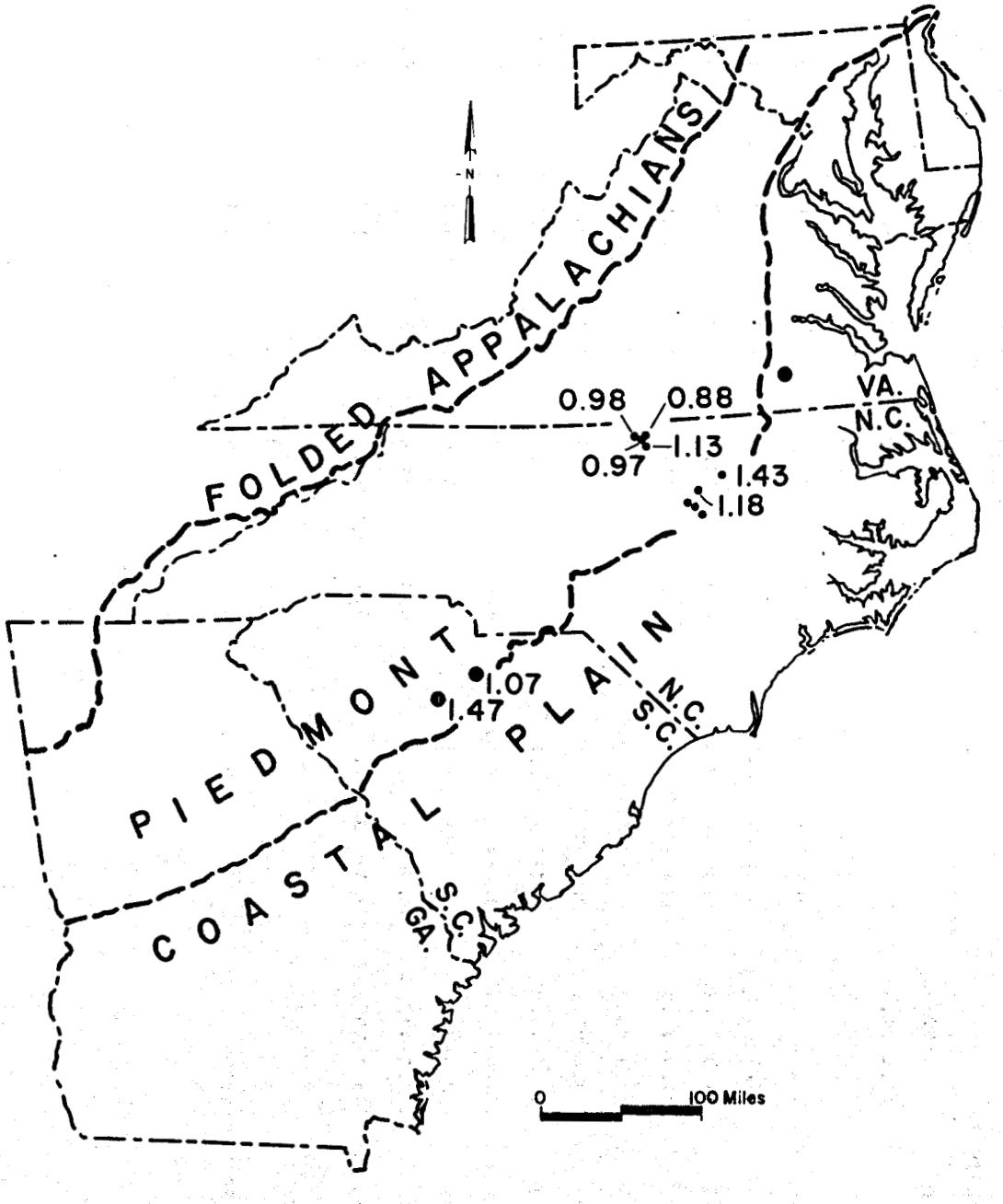

Figure C-11. Heat flow values determined to date for this contract.

TABLE C-7 HEAT GENERATION DATA FROM CORE OF DRILL HOLE RL1

DEPTH INTERVALS (FEET)	DEPTH INTERVALS (METERS)	SAMPLE NO.	DENSITY, GM/CM³	URANIUM (U), PPM	THORIUM (TH), PPM	POTASSIUM (K), %	K2O, %	HEAT GENERATION, A X 10^{-13} CAL/CM³-SEC
90-96	27.4-29.3	RL1-090	2.63	5.8	12.2	2.9	3.4	6.1
180-186	54.9-56.7	RL1-180	2.66	5.2	11.4	2.9	3.5	5.6
203-210	61.9-64.0	RL1-203	2.66	4.6	11.9	2.9	3.5	5.4
220-226	67.1-68.9	RL1-220	2.66	4.8	11.8	2.7	3.2	5.4
234-240	71.3-73.2	RL1-234	2.65	4.5	12.0	2.9	3.4	5.3
253-259	77.1-78.9	RL1-253	2.65	4.7	11.6	3.0	3.5	5.4
273-279	83.2-85.0	RL1-273	2.65	5.0	11.7	2.8	3.3	5.5
294-300	89.6-91.4	RL1-294	2.63	4.9	11.8	2.8	3.3	5.4
312-318	95.1-96.9	RL1-312	2.66	4.9	11.6	2.8	3.4	5.5
408-414	124.4-126.2	RL1-408	2.65	4.6	11.0	2.8	3.4	5.2
584-590	178.0-179.8	RL1-584	2.64	5.5	12.0	2.8	3.3	5.8
624-630	190.2-192.0	RL1-624	2.59	6.0	11.8	2.7	3.2	6.0
673-680	205.1-207.3	RL1-673	2.64	5.4	13.0	2.8	3.3	5.9
AVERAGE			2.64	5.1	11.8	2.8	3.4	5.6
STANDARD DEVIATION			0.02	0.5	0.5	0.1	0.1	0.3

TABLE C-8 HEAT GENERATION DATA FROM CORE OF DRILL HOLE RL2 C-8-1

DEPTH INTERVALS (FEET)	DEPTH INTERVALS (METERS)	SAMPLE NO.	DENSITY, GM/CM³	URANIUM (U), PPM	THORIUM (TH), PPM	POTASSIUM (K), %	K2O, %	HEAT GENERATION, A X 10^{-13} CAL/CM³-SEC
67-71	24.4-21.6	RL2-066	2.65	4.4	14.9	3.4	4.1	5.8
135-140	41.1-42.7	RL2-135	2.64	4.0	13.5	2.5	3.0	5.1
204-209	62.2-63.7	RL2-204	2.67)	6.9	14.5	2.0	2.4	7.0
296-301	90.2-91.7	RL2-296	2.64	5.4	11.5	2.7	3.2	5.7
483-488	147.2-148.7	RL2-483	2.64	5.0	11.2	3.3	3.9	5.5
573-578	174.7-176.2	RL2-573	2.66	4.0	18.6	3.2	3.8	6.2
654-659	199.3-200.9	RL2-654	2.62	5.7	14.9	3.7	4.4	6.6
293-698	211.2-212.8	RL2-693	2.66	5.9	13.6	2.4	2.8	6.3
AVERAGE			2.65	5.2	14.1	2.9	3.5	6.0
STANDARD DEVIATION			0.02	1.0	2.3	0.6	0.7	0.6

(2.67) . . ASSUMED DENSITY

TABLE C-9 HEAT GENERATION DATA FROM CORE OF DRILL HOLE RL4

DEPTH INTERVALS (FEET)	DEPTH INTERVALS (METERS)	SAMPLE NO.	DENSITY, GM/CM³	URANIUM (U), PPM	THORIUM (TH), PPM	POTASSIUM (K), %	K2O, %	HEAT GENERATION, A X 10⁻¹³ CAL/CM³-SEC
10-15	3.0-4.6	RL4-003	2.64	5.3	19.6	3.5	4.2	7.2
69-74	21.0-22.6	RL4-021	2.64	5.4	18.6	3.4	4.1	7.0
145-150	44.2-45.7	RL4-044	2.67	8.8	14.1	2.8	3.3	8.2
212-216	64.6-65.8	RL4-065	2.65	4.7	16.1	3.4	4.0	6.2
221-224	67.4-68.3	RL4-067	2.63	5.1	16.7	3.1	3.8	6.4
262-267	79.9-81.4	RL4-080	2.67	6.7	17.8	3.2	3.9	7.7
298-303	90.8-92.4	RL4-091	2.64	5.3	18.7	3.1	3.7	6.9
377-382	114.9-116.4	RL4-115	2.66	3.5	13.2	3.3	4.0	5.0
385-391	117.3-119.2	RL4-117	2.64	7.6	17.1	3.5	4.2	8.1
432-436	131.7-132.9	RL4-132	2.67	4.3	18.8	3.2	3.8	6.4
442-446	134.7-135.9	RL4-135	2.67	8.4	13.9	3.9	4.7	8.2
490-495	149.4-150.9	RL4-149	2.66	4.8	17.4	3.4	4.1	6.5
528-531	160.9-161.8	RL4-161	2.67	3.1	9.7	4.6	5.6	4.5
550-555	167.6-169.2	RL4-168	2.69	3.0	13.5	2.7	3.3	4.6
564-569	171.9-173.4	RL4-172	2.62	3.1	13.7	4.0	4.8	4.9
597-602	182.0-183.5	RL4-182	2.66	5.3	16.8	3.4	4.1	6.7
619-625	188.7-190.5	RL4-189	2.67	8.1	19.0	3.8	4.6	8.9
625-630	190.5-192.0	RL4-191	2.66	5.0	18.0	3.4	4.1	6.7

TABLE C-9 HEAT GENERATION DATA FROM CORE OF DRILL HOLE RL4

DEPTH INTERVALS (FEET)	DEPTH INTERVALS (METERS)	SAMPLE NO.	DENSITY, GM/CM³	URANIUM (U), PPM	THORIUM (TH), PPM	POTASSIUM (K), %	K2O, %	HEAT GENERATION, A X 10^{-13} CAL/CM³-SEC
639-643	194.8-196.0	RL4-195	2.64	5.7	19.0	3.5	4.2	7.3
AVERAGE			2.66	5.4	16.4	3.4	4.1	6.7
STANDARD DEVIATION			0.02	1.8	2.7	0.4	0.5	1.3

TABLE C-10 HEAT GENERATION DATA FROM CORE OF DRILL HOLE RL5 C-10-1

DEPTH INTERVALS (FEET)	DEPTH INTERVALS (METERS)	SAMPLE NO.	DENSITY, GM/CM³	URANIUM (U), PPM	THORIUM (TH), PPM	POTASSIUM (K), %	K2O, %	HEAT GENERATION, A X 10^{-13} CAL/CM³-SEC
54-60	16.5-18.3	RL5-016	2.62	3.1	19.8	3.6	4.3	5.8
94-100	28.7-30.5	RL5-029	2.64	6.0	20.3	3.5	4.2	7.7
234-240	71.3-73.2	RL5-071	2.64	2.8	22.6	3.6	4.3	6.1
334-340	101.8-103.6	RL5-102	2.64	2.5	17.8	3.3	3.9	5.1
472-478	143.9-145.7	RL5-144	2.65	6.5	13.8	3.1	3.7	6.9
569-575	173.4-175.3	RL5-173	2.65	4.2	17.6	3.4	4.1	6.1
AVERAGE			2.64	4.2	18.7	3.4	4.1	6.3
STANDARD DEVIATION			0.01	1.7	3.0	0.2	0.2	0.9

TABLE C-11 HEAT GENERATION DATA FROM RECONNAISSANCE SURVEY IN S. E. UNITED STATES C-11-1

LOCATION		SAMPLE NO.	DENSITY, GM/CM^3	URANIUM (U), PPM	THORIUM (TH), PPM	POTASSIUM (K), %	K2O, %	HEAT GENERATION, A X 10^{-13} CAL/CM^3-SEC
ELBERTON	GA	F7-40	(2.67)	1.4	41.8	4.0	0.0	8.8
CHURCHLAND	NC	F7-16	(2.67)	2.5	5.5	3.2	3.9	3.2
GASTONIA	NC	F7-27	(2.67)	2.2	18.1	3.2	3.9	5.2
MT MOURNE	NC	F7-24	(2.67)	3.0	18.1	4.1	4.9	5.9
GREAT FALLS	SC	Z7-3	2.63	3.0	10.1	3.2	3.9	4.1
MT CARMEL	SC	F7-42	(2.67)	0.4	0.6	5.0	6.0	1.5
NEWBERRY	SC	CB7-23	2.63	7.4	28.6	4.1	4.9	10.2
NEWBERRY	SC	CB7-24	2.64	4.5	20.6	3.5	4.2	7.0
FINE CREEK MILLS	VA	FCMGR	(2.67)	4.9	14.5	3.6	4.4	6.3

(2.67). . .ASSUMED DENSITY.

TABLE C-12 HEAT GENERATION DATA FROM CORE OF DRILL HOLE PT1 C-12-1

DEPTH INTERVALS (FEET)	DEPTH INTERVALS (METERS)	SAMPLE NO.	DENSITY, GM/CM³	URANIUM (U), PPM	THORIUM (TH), PPM	POTASSIUM (K), %	K2O, %	HEAT GENERATION, A X 10^{-13} CAL/CM³-SEC
1083-1106	330-337	PT1-110*	2.65	7.6	51.5	0.7	0.8	13.1
1345-1368	410-417	PT1-140	2.67	4.4	19.0	3.4	4.1	6.5
1772-1794	540-547	PT1-180	2.65	4.0	15.4	3.4	4.1	5.7
2083-2106	635-642	PT1-207	2.65	5.4	14.7	6.4	7.7	7.1
2234-2257	681-688	PT1-224	2.66	5.4	13.0	3.2	3.8	6.1
2411-2434	735-742	PT1-247	2.67	4.7	12.5	3.4	4.1	5.6
AVERAGE			2.66	4.8	14.9	4.0	4.8	6.1
STANDARD DEVIATION			0.01	0.6	2.6	1.4	1.7	0.6

*...SAMPLE NOT INCLUDED IN COMPUTATION OF MEAN AND STANDARD DEVIATION

TABLE C-13 HEAT GENERATION DATA FROM SURFACE SAMPLES OF THE PETERSBURG GRANITE

LOCATION		SAMPLE NO.	DENSITY, GM/CM^3	URANIUM (U), PPM	THORIUM (TH), PPM	POTASSIUM (K), %	K2O, %	HEAT GENERATION, A X 10^{-13} CAL/CM^3-SEC
PETERSBURG	VA	AB7-11C	(2.67)	14.2	4.9	5.1	6.2	10.8
PETERSBURG	VA	AB7-118	2.65	7.5	22.3	3.8	4.5	9.0
PETERSBURG	VA	AB7-17	2.62	8.1	20.1	3.4	4.1	8.8
PETERSBURG	VA	AB7-21	2.61	6.5	16.3	3.7	4.4	7.3
PETERSBURG	VA	AB7-23	2.64	7.(	21.8	3.5	4.2	8.5
PETERSBURG	VA	AB7-26A	2.71	8.7	21.1	3.4	4.1	9.6
PETERSBURG	VA	AB7-26B	2.64	5.0	19.9	3.9	4.7	7.1
PETERSBURG	VA	AB7-3A	(2.67)	2.8	11.4	3.4	4.1	4.4
PETERSBURG	VA	AB7-38	2.74	2.6	13.9	3.2	3.9	4.7
PETERSBURG	VA	AB7-41	2.69	2.5	7.5	2.5	3.0	3.3
PETERSBURG	VA	AB7-46	2.63	8.1	33.4	4.6	5.5	11.2
PETERSBURG	VA	AB7-53	2.64	4.2	15.5	3.4	4.1	5.8
PETERSBURG	VA	AB7-6A	(2.67)	0.8	2.0	0.7	0.8	1.0
PETERSBURG	VA	AB7-6B	(2.67)	2.9	0.5	5.5	6.6	3.2
PETERSBURG	VA	AB7-61A	2.60	10.7	17.9	4.4	5.3	10.1
PETERSBURG	VA	AB7-61B	(2.67)	6.1	17.4	2.8	3.3	7.2
PETERSBURG	VA	AB7-62	2.70	3.8	10.4	2.4	2.9	4.6
PETERSBURG	VA	AB7-65	2.58	6.8	30.2	3.9	4.7	9.6

TABLE C-13 HEAT GENERATION DATA FROM SURFACE SAMPLES OF THE PETERSBURG GRANITE

LOCATION		SAMPLE NO.	DENSITY, GM/CM³	URANIUM (U), PPM	THORIUM (TH), PPM	POTASSIUM (K), %	K2O, %	HEAT GENERATION, A X 10^{-13} CAL/CM³-SEC
PETERSBURG	VA	AB7-73	2.61	7.3	28.8	3.7	4.4	9.7
PETERSBURG	VA	AB7-75	2.63	11.1	13.6	3.4	4.0	9.6
PETERSBURG	VA	AB7-76A	(2.67)	0.9	2.3	0.6	0.7	1.1
PETERSBURG	VA	AB7-76B	(2.67)	3.3	0.7	5.5	6.6	3.4
PETERSBURG	VA	AB7-8	(2.67)	8.5	9.6	3.7	4.5	7.6
PETERSBURG	VA	AB7-9A	(2.67)	2.2	14.1	4.2	5.0	4.6
PETERSBURG	VA	AB7-9B	(2.67)	11.9	34.4	3.6	4.3	13.7
PETERSBURG	VA	AB7-96B	2.60	11.1	18.6	4.2	5.1	10.4
PETERSBURG	VA	F7-3	(2.67)	8.4	13.0	3.6	4.4	8.2
PETERSBURG	VA	F7-7	(2.67)	5.4	20.3	3.5	4.2	7.6
PETERSBURG	VA	F7-8	(2.67)	6.9	20.2	4.3	5.1	8.6
PETERSBURG-RICHMOND	VA	F7-5	(2.67)	9.2	29.5	3.7	4.5	11.6
AVERAGE			2.64	6.5	16.4	3.6	4.3	7.4
STANDARD DEVIATION			0.04	3.4	9.4	1.1	1.2	3.2

(2.67). . .ASSUMED DENSITY.

TABLE C-14 HEAT GENERATION DATA FROM CORE OF DRILL HOLE RX2

LOCATION		SAMPLE NO.	DENSITY, GM/CM^3	URANIUM (U), PPM	THORIUM (TH), PPM	POTASSIUM (K), %	K2O, %	HEAT GENERATION, A X 10^{-13} CAL/CM^3-SEC
74-84	22.6-25.6	RX2-23	(2.67)	2.4	11.0	2.7	3.2	3.9
99-104	30.2-31.7	RX2-30	(2.67)	3.0	10.0	2.9	3.5	4.1
240.3-245.3	73.2-74.8	RX2-73	(2.67)	2.8	10.5	2.8	3.4	4.0
299.6-304	91.3-92.7	RX2-91	(2.67)	2.4	9.6	2.8	3.3	3.6
333-338	101.5-103.0	RX2-102	(2.67)	2.4	9.8	2.8	3.3	3.7
544-549	165.8-167.3	RX2-166	(2.67)	3.3	11.6	2.7	3.3	4.5
685.1-690	208.8-210.3	RX2-209	(2.67)	2.9	11.1	3.0	3.6	4.2
AVERAGE				2.7	10.5	2.8	3.4	4.0
STANDARD DEVIATION				0.4	0.8	0.1	0.1	0.3

(2.67). . .ASSUMED DENSITY.

sediments of the Atlantic Coastal Plain was deepened to 1332 m to obtain a basement core sample using DOE funds. The hole was logged by VPI&SU on January 12, 1978. Temperature profiles are shown in Figures C-12 and C-13. The bottom-hole temperature at a depth of 1331 m was 60°C. The least-squares gradient over the interval 47-1328 m was 29.3 ± 0.14 °C/km. Analysis of the basement core for thermal conductivity, heat generation, petrography, chemistry, and geochronology is in progress.

Justification for obtaining a bottom-hole core sample from this well was the apparently favorable location of the well with respect to a thermal anomaly shown on the AAPG Geothermal Gradient map for North America (1976). The gradient measured was about 10% less than anticipated, but the hole has not yet reached thermal equilibrium. It will be relogged by VPI&SU again in the near future. Disturbance from ground-water convection is apparent at several depths in the hole, particularly near the top of basement at a depth of about 1311 m. The Upper Cretaceous aquifer above basement is several hundred feet in thickness and apparently has a permeability and porosity favorable for ground-water production. The location of the hole seemed to be optimum with respect to published geothermal gradient data. It was less favorably situated with respect to available gravity coverage. Additional gravity data northeast of the Wayne County well are now being obtained by VPI&SU in an attempt

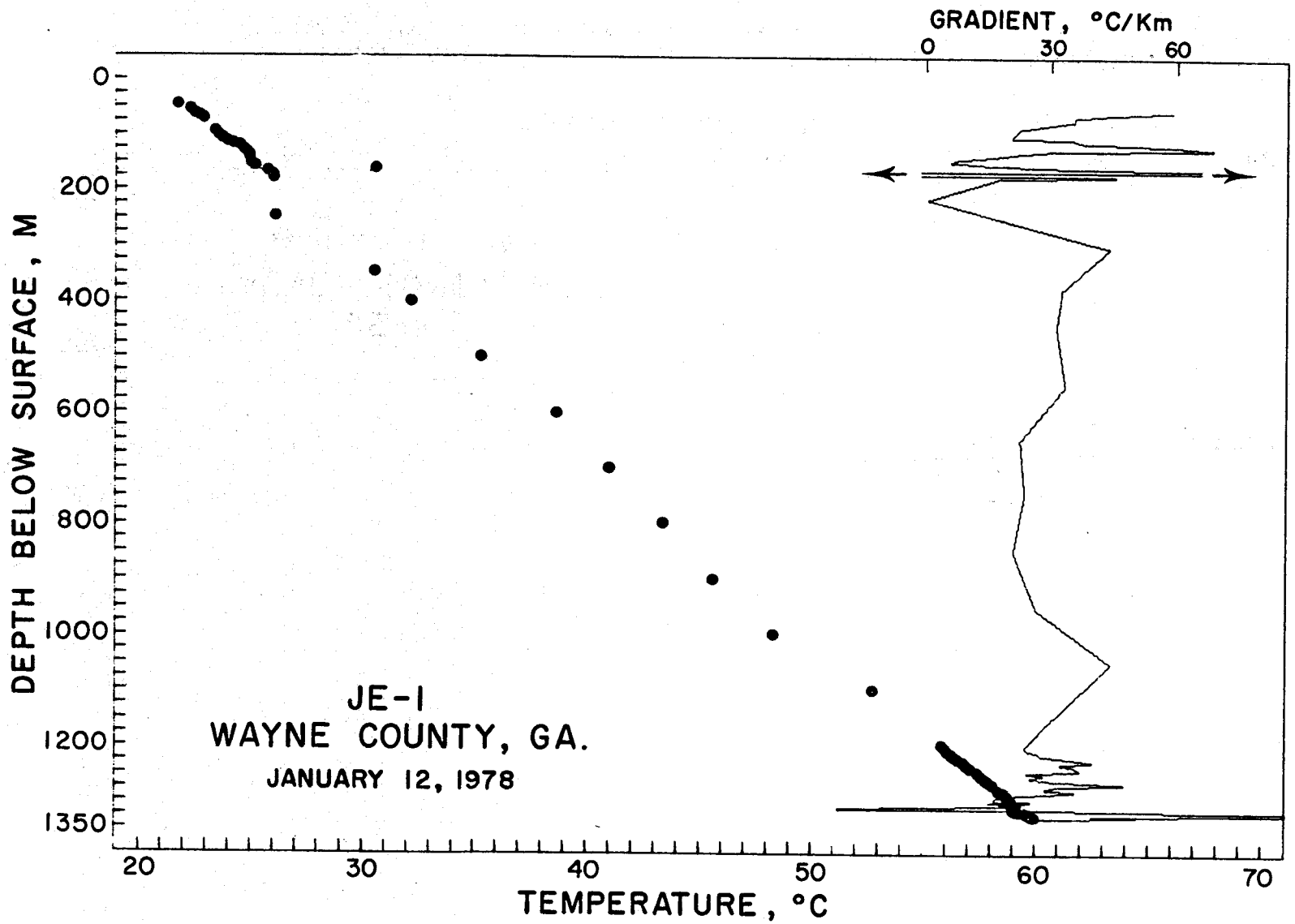

Figure C-12. Temperature profile in JE-1 in Wayne County, Georgia. Depth range 47 to 1331 m.

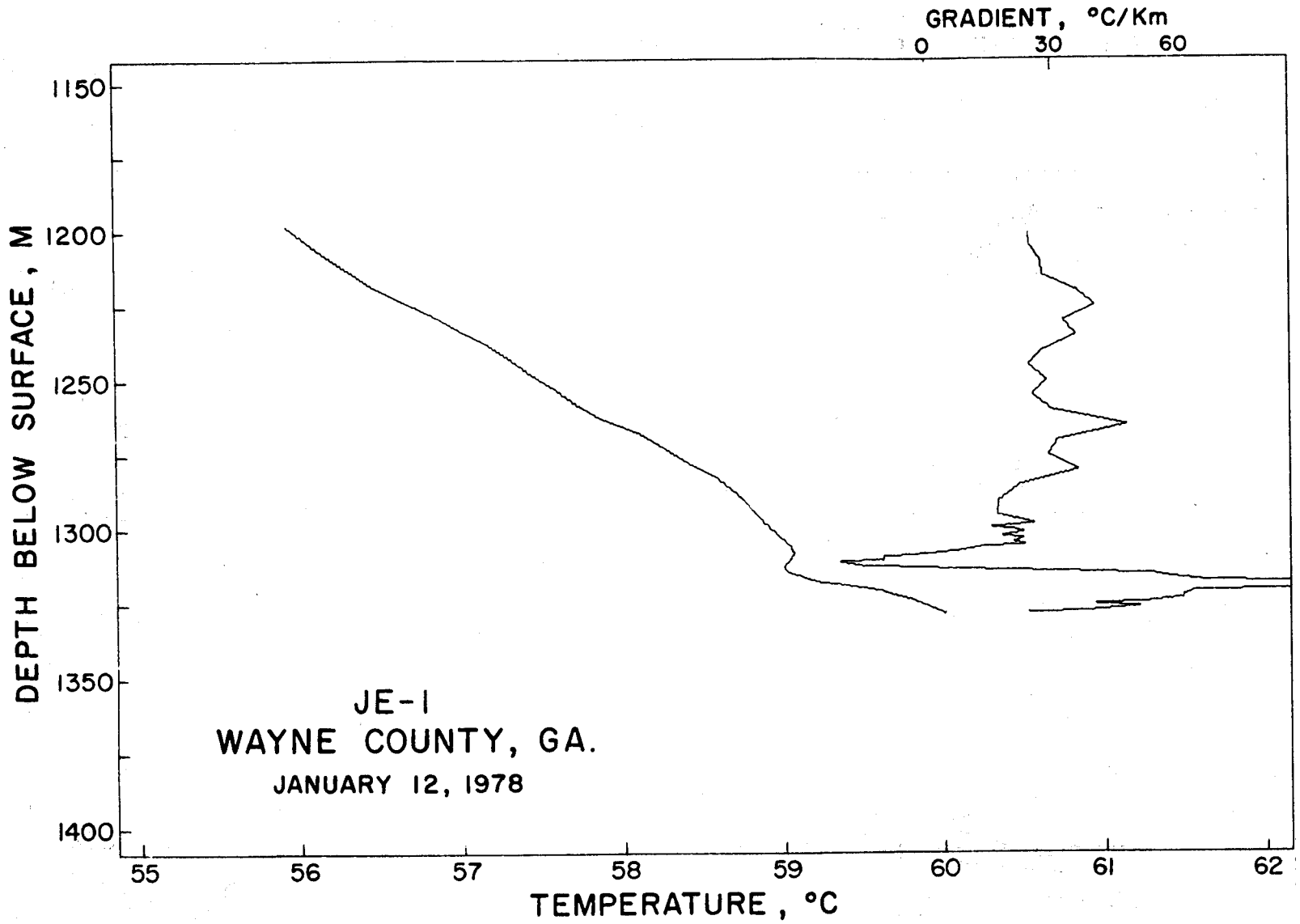

Figure C-13. Temperature profile in JE-1 in Wayne Co., Georgia. Depth range 1200 to 1322 m.

to define the magnitude and extent of the negative gravity anomaly shown on the Simple Bouguer Gravity map of Georgia (1972).

RELATIONSHIP BETWEEN SURFACE HEAT GENERATION AND SURFACE HEAT FLOW

J. K. Costain and L. D. Perry

Two new values have been added to Figure C-14 which shows the linear relationship discussed in VPI&SU-5103-4, and -5: RL1 (1.43 HFU; 5.6 HGU) from the Castalia pluton and RL2 (1.18 HFU; 6.0 HGU) from the Rolesville batholith. Neither falls on the regression line. The heat flow in the Castalia is about 0.35 HFU toc high, and in the Rolesville (RL2) about 0.08 HFU too high. The value in the Castalia (RL1) is too high to be attributed to experimental error. The first value in the Rolesville batholith (RL2) does fall near the regression line. A uniform distribution of 5.6 HGU to a depth of about 13 km would be required to produce the observed heat flow in the Castalia pluton.

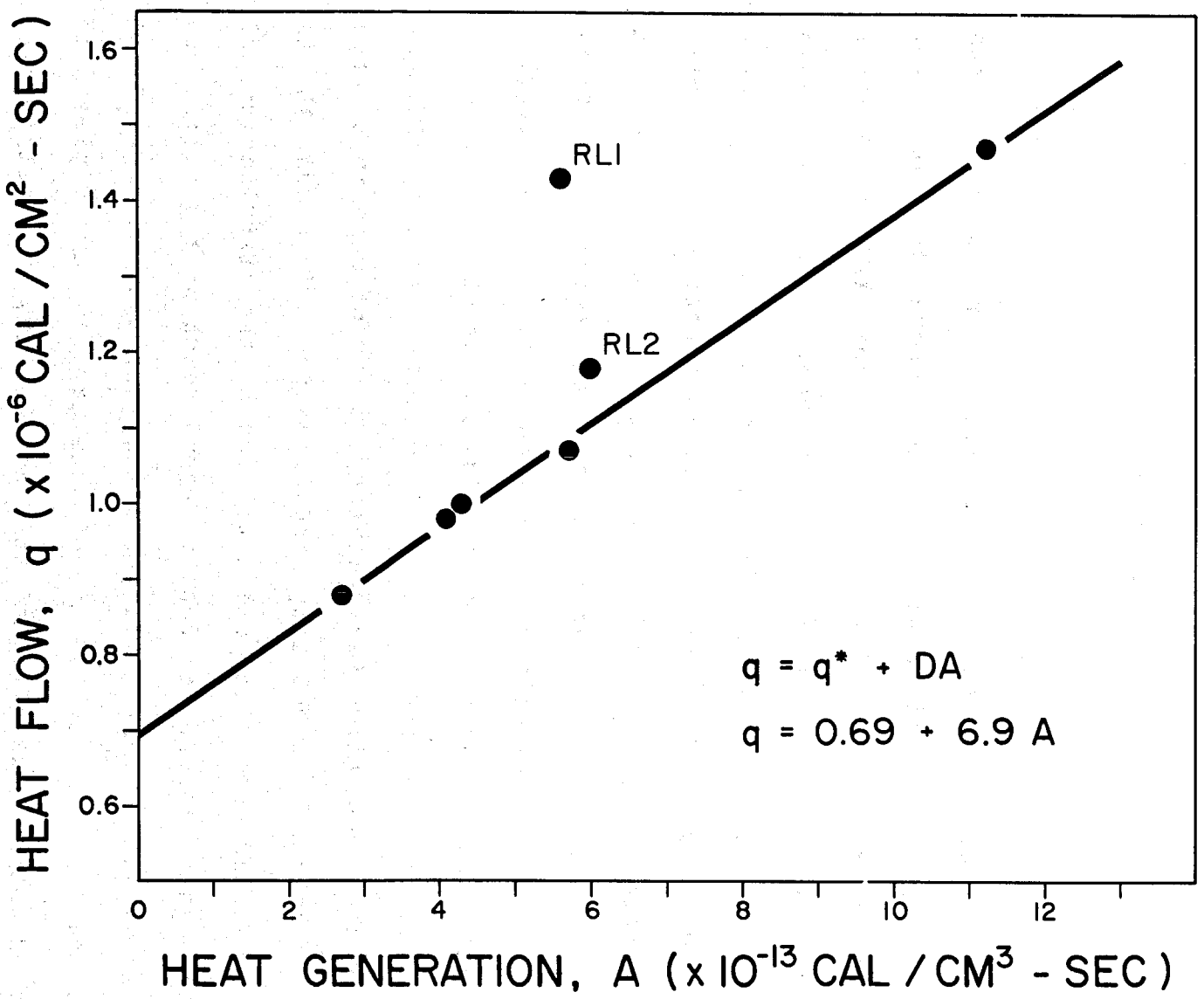

Figure C-14. Heat flow vs. heat generation for holes completed to date in granitic plutons in southeastern United States.

A NEW MODEL FOR THE LINEAR RELATIONSHIP BETWEEN HEAT FLOW AND HEAT GENERATION

J.K. Costain

New heat flow - heat generation values in the southeastern United States in widely-separated (450 km) granitic plutons and with a large age span (275 m.y.) again confirm the linear relationship between surface heat flow and surface heat generation in crystalline rocks (DOE Progress Report VPI&SU-5103-5). It is surprising to observe the relationship in widely-separated plutons with such a large age span, and in both pre- and post-metamorphic rocks. The empirical relationship implies some kind of regular distribution of uranium and thorium in the crust. Since the occurrence of U and Th in granitic rocks has a significant effect on subsurface temperatures, it is of some importance to consider the mobility and location of U and Th in crystalline rocks in order to model the distribution of radiogenic elements at depths beyond reach of the drill. In this discussion, it is proposed that the zone of microcracks in the upper 7 to 10 km of the earth's crust plays an important role with regard to the mobility and distribution of U and Th in the upper crust.

The presence of microcracks is known to dominate the physical properties of rocks at pressures below a few kilobars. Following the classification of Simmons and Richter (1976), microcracks include the following:

a) cracks starting at grain boundaries, or occurring between grains, caused by differences in the tensor properties of adjacent mineral grains (dP/dT cracks). Such cracks can exist in one mineral grain and be absent in the adjacent grain;

b) stress-induced cracks caused by non-hydrostatic stress and independent of relative crystallographic orientations. Cracks may cross several grains;

c) radial or concentric cracks about completely enclosed grains caused by differences in the coefficient of volume expansion between a host grain and a totally enclosed grain;

d) tube cracks, apparently abundant in igneous rocks, caused by simple solution by late-stage magmatic fluids, or possibly by meteoric ground water;

e) thermal cycling cracks. These are cracks coincident with grain boundaries. Grains are separated from adjacent grains by wide grain-boundary cracks;

f) thermal gradient cracks caused by stress differentials associated with high thermal gradients;

g) cracks produced by shock waves. The crack porosity is related to the peak shock pressure;

h) cleavage cracks parallel to cleavage planes in minerals;

i) cracks of unknown origin. Simmons and Richter (1976) give several examples.

It is speculated herein that the zone of microcrack porosity and the depth of emplacement of igneous rocks with respect to this zone play an important role in the observed linearity between heat flow and heat generation because of the greater mobility of uranium and thorium in this zone. The closure of microcracks in crystalline rocks is believed to be complete at pressures of about 2 to 3 kilobars. Darcy's law is known to hold in igneous rocks at pressures as great as 4 kb and for permeabilities as low as 4 nanodarcies (Brace et al., 1968). Migration of uranium and thorium from initial sites on grain boundaries and microcrack surfaces via a network of microcracks with subsequent redeposition on grain boundaries and other microcrack surfaces should take place throughout the domain of microcracks. Continuous redistribution of uranium and thorium over a depth range of D = 7 to 10 km might take

place by zone refining. If redistribution takes place by zone refining, then an exponential distribution might result. Restricting an exponential distribution to the depth, D, we have

$$\int_0^D Ao\, e^{-z/D^1}\, dz = A^1 D$$

where

Ao = surface heat generation

A^1 = average heat generation over the depth D

D^1 = logarithmic decrement of exponential distribution over the depth D

Thus

$$Ao = \frac{A^1 D}{D^1[1 - e^{-D/D^1}]}$$

or

$$Ao = \frac{A^1 R}{[1 - e^{-R}]}$$

where $R = D/D^1$.

Tabulating values of D^1, R, and Ao/A^1 for D = 7 km, we have

D^1	R	Ao/A^1
∞	0.0	1.00
60	0.12	1.06
40	0.18	1.09
20	0.35	1.19
10	0.70	1.39
7	1.0	1.58

The implication intended for the proposed model is that migration of uranium and thorium is facilitated within the domain of microcracks not only during periods of metamorphism, but also after thermal equilibrium has been reached and while continuous erosion and unroofing develop new microcracks and maintain a zone of microcrack porosity of approximately constant thickness. The proposed model would thus be defined by a layer of essentially constant thickness, but the linear relationship would survive differential erosion. The nature of the distribution within the zone of microcracks is unknown; if redistribution takes place by zone refining, then an exponential distribution might result within the zone. Consequences of the proposed model are:

a) a linear relationship between heat flow and heat generation should be observed in country rock as well as in adjacent intrusive rocks;

b) attenuation of edge effects caused by contrasts in heat generation between intrusive rocks and host rocks into which they were intruded;

c) observation of uranium and thorium on grain boundaries and other microcracks in igneous rocks and adjacent country rocks.

Fission-track analysis of selected core samples from WN1 and KR3 is now underway in cooperation with the U.S. Geological Survey to investigate the occurrence of U and Th on microcrack surfaces.

If the zone of microcrack porosity does facilitate the migration of uranium and thorium, recognition of this will contribute to an understanding of the mobility and depositional sites of uranium in igneous rocks. At the present time, this writer favors an essentially constant distribution of radiogenic elements from the surface to a depth, D, corresponding to the effective depth of penetration of microcracks.

Analysis of gravity data over the Edgefield pluton in South Carolina is discussed elsewhere in this report by A.H. Cogbill. Coincidentally, one of the most plausible interpretations of the gravity data assumes a density contrast of of about -0.0175 gm/cm^3 which places the base of the Edgefield pluton at a depth of about 7 km. This density contrast is appropriate elsewhere in the southeast. Unpublished density values of L. Glover support a similar density contrast for the Roxboro metagranite in North Carolina.

The heat flow values in the Rolesville batholith and Castalia pluton discussed elsewhere in this report are higher than surface heat generation values would predict. Additional gravity data over the Rolesville batholith and

Castalia pluton should indicate whether or not portions of this batholith extend to greater depths to account for the higher heat flow.

MODELING OF TEMPERATURE DISTRIBUTIONS ASSOCIATED WITH RADIOGENIC SOURCES BENEATH SEDIMENTARY INSULATORS

J.A. Dunbar

Introduction

The search for low-temperature geothermal resources has, in part, been directed toward locating igneous intrusive rocks which have relatively high heat generation and which are insulated by overlying sediments with low thermal conductivities. In the following section a steady-state conduction model is proposed which considers the effects of three-dimensional bodies overlain by strata of contrasting conductivity.

The temperature field will be viewed as a composite of a normal field produced primarily by heat flow from the lower crust and upper mantle and an anomalous field produced by a radiogenic body. The heat flow from the lower crust and upper mantle will not be allowed to vary over the model region. Lateral variations in temperature will then result only from the radiogenic bodies. Two main assumptions must be made in order to apply such a model to terrestrial environments: (1) the amount of heat transported by ground water is negligible; and (2) the heat producing elements, thermal conductivities, and surface

conditions have existed, unchanged, long enough to allow the temperature field to reach equilibrium. Although these assumptions may not be viable in some instances, it is felt that the model will be applicable to a number of situations of interest.

The Modeling Approach

Steady-state sources in infinite media

The expression for the steady-state temperature field, v, produced by a continuous point source in an infinite medium is given by Carslaw and Jaeger (1959, p. 422) and is

$$v = \frac{Q}{4\pi K r'} \qquad (1)$$

where

Q = the (constant) rate of heat production of the source,

K = the thermal conductivity of the medium,

r' = the distance between the point of observation and the source.

The temperature field produced by a volume source is then given by

$$v = \frac{A}{4\pi K} \iiint_V \frac{dV}{r'} \qquad (2)$$

where

A = the rate of heat production per unit volume of the source.

Solutions of equation (2) are known or can be easily found for sources of a number of shapes useful for modeling geologic bodies. Vertical circular cylinders, rectangular prisms and polygonal prisms are particularly useful shapes because they are compatible with existing gravity and magnetic modeling techniques. Cylindrical sources are commonly used to approximate gravity and magnetic anomalies over three-dimensional bodies. The automatic method for interpreting gravity anomalies, given by Cordell and Henderson (1968), utilizes rectangular prismatic source elements. Talwani's method (1960 and 1965) and later Plouff's method (1976) for computing the gravity and magnetic anomalies produced by irregularly shaped three-dimensional bodies are based on polygonal prism source elements. Vertical cylinders, rectangular prisms, and polygonal prisms can therefore be used to approximate geological shapes.

Along the axis of a vertical cylinder,

$$v = \frac{A}{4\pi K} \int_{Z_1}^{Z_2} \int_{0}^{2\pi} \int_{0}^{R} \frac{4 dr d\theta dz}{[r^2+z^2]^{1/2}}$$

$$v = \frac{A}{4K} \left[Z_2\sqrt{R^2+Z_2^2} - Z_1\sqrt{R^2+Z_1^2} + R^2 \ln \left(\frac{Z_2+\sqrt{R^2+Z_2^2}}{Z_1+\sqrt{R^2+Z_1^2}} \right) - Z_2^2 + Z_1^2 \right] , \quad (3)$$

where

R = the radius of the cylinder,

Z_1 = the distance from the point of observation to the top of the cylinder,

Z_2 = the distance from the point of observation to the bottom of the cylinder.

The solution of equation (2) for a vertical rectangular prism is given by Haaz (1953) and is

$$v = \frac{A}{4\pi K}\left[xy\ln(z+R) + xz\ln(y+R) + yz\ln(x+R) - \frac{1}{2}\left(x^2\tan^{-1}\frac{yz}{xR} + y^2\tan^{-1}\frac{xz}{yR} + z^2\tan^{-1}\frac{xy}{zR}\right)\right]\Bigg|_{X_1}^{X_2}\Bigg|_{Y_1}^{Y_2}\Bigg|_{X_1}^{Z_2} \quad (4)$$

where

$$R = \sqrt{x^2+y^2+z^2}\ , \quad \text{and}$$

X_1, X_2, Y_1, Y_2, Z_1, Z_2 are the extremities of the prism.

The solution of equation (2) for a polygonal prism can be found by first noting that the potential of a volume source [equation (2)] is homogeneous of degree 2.

That is,

$$v(\lambda x,\lambda y,\lambda z) = \frac{A}{4\pi K}\iiint_V \frac{\lambda dx\lambda dy\lambda dz}{[(\lambda x)^2+(\lambda y)^2+(\lambda z)^2]^{1/2}}$$

$$= \frac{\lambda^2 A}{4\pi K}\iiint_V \frac{dxdydz}{[x^2+y^2+z^2]^{1/2}}$$

Euler's theorem of homogeneous functions holds that if f is a homogeneous function of x, y, and z of degree n, then

$$nf = x\frac{\partial f}{\partial x} + y\frac{\partial f}{\partial y} + z\frac{\partial f}{\partial z} \qquad (5)$$

Then the potential of a polygonal prism is related to its first derivatives by the expression

$$v = \frac{1}{2}\left[xv_x + yv_y + zv_z\right] \qquad (6)$$

Differentiating with respect to x we find that

$$2v_x = xv_{xx} + u_x = yv_{xy} + zv_{xz} ,$$

$$u_x = xv_{xx} + yv_{xy} + zv_{xz} .$$

Similarly,

$$v_y = Xv_{yx} + yv_{yy} + zv_{yz} ,$$

and

$$v_z = xv_{zx} + yv_{zy} + zv_{zz} .$$

The potential of a polygonal prism can then be written in terms of its second derivatives as,

$$v = \frac{1}{2}\left[x^2v_{xx} + 2xyv_{xy} + y^2v_{yy} + 2xzv_{xz} + 2yzv_{yz} + z^2v_{zz}\right] . \qquad (7)$$

The second derivatives in equation (7) are given by Plouff (1976, p. 732). Substituting Plouff's

expressions for the second derivatives in equation (7), the temperature effect of a polygonal prism becomes,

$$v = \frac{A}{8\Pi K} \{ \sum_{i=1}^{m} (\Delta X)^2 (SCF - C^2W) + 2 \sum_{i=1}^{m} (\Delta X)(\Delta Y)(SCW + C^2F)$$

$$- \sum_{i=1}^{m} (\Delta Y)^2 (SCF_2 + S^2Wi) + 2 \sum_{i=1}^{m+1} (\Delta X)(\Delta Z)\, CQ$$

$$- 2 \sum_{i=1}^{m} (\Delta Y)(\Delta Z) SQ + \sum_{i=1}^{m+1} (\Delta Z)^2\, W \} .$$

where

$C = \Delta Y/\Delta S$

$S = \Delta X/\Delta S$

$$F = \ln \left[\frac{R_{i+1,i+1} + Z_2}{R_{i,i+1} + Z_2} \; \frac{R_{i,i} + Z_1}{R_{i+1,i} + Z_1} \right]$$

$$Q = \ln \left[\frac{R_{i+1,i+1} + d_{i+1}}{R_{i,i+1} + d_i} \; \frac{R_{i,i} + d_i}{R_{i+1,i} + d_{i+1}} \right]$$

$$W = \tan^{-1} \frac{Z_2 d_{i+1}}{PR_{i+1,i+1}} - \tan^{-1} \frac{Z_2 d_i}{PR_{i,i+1}}$$

$$- \tan^{-1} \frac{Z_1 d_{i+1}}{Pr_{i+1,i}} + \tan^{-1} \frac{Z_1 d_i}{PR_{i,i}} \qquad (8)$$

m = the number of sides of the prism.

$\Delta S = \sqrt{(\Delta X)^2 + (\Delta Y)^2}$

$\Delta X = X_{i+1} - X_i$; $\Delta Y = Y_{i+1} = Y_i$

$R_{jk}^2 = r_j^2 + Z_k^2$

Z_1 = the vertical distance to the top of the prism.

Z_2 = the vertical distance to the bottom of the prism.

$d_i = X_i S + Y_i C$

(X_1,Y_1), (X_2,Y_2), (X_3,Y_3) ... (X_i,Y_i) ... X_m,Y_m

are the corner points of the prism.

Boundary conditions

Equations (3), (4), and (8) apply only to sources in infinite media of constant conductivity. These equations may, however, be used in conjunction with the method of images, used in electrostatics, to develop expressions which are useful in satisfying boundary conditions.

The first case to be considered is the situation in which the source is in a semi-infinite medium $z > 0$ of conductivity K. It is required that solutions to this problem satisfy Laplace's equation $D^2v = 0$ for all $z > 0$ and that at $z = 0$ the thermal effect of the source be zero. This situation is considered by Carslaw and Jaeger (1959, p. 276). It is found that an expression satisfying the above conditions can be obtained by adding the effect of a source in an infinite medium with the effect of a sink of equal intensity, which is the mirror image of the source across the $z = 0$ plane. For a point source at $z^1 > 0$,

$$v = \frac{Q}{4\pi K}\left[\frac{1}{R} - \frac{1}{R^1}\right]$$

where

$R = (x - x^1)^2 + (y - y^1)^2 + (z - z^1)^2$,

$R^1 = (x - x^1)^2 + (y - y^1)^2 + (z + z^1)^2$,

(x,y,z) = the coordinates of the point of observation,

(x^1,y^1,z^1) = the source point.

For volume sources in a semi-infinite medium

$$v = \frac{A}{4\pi K}\left[\iiint_V \frac{dV}{R} - \iiint_V \frac{dV^1}{R}\right] \qquad (9)$$

where V' is a mirror image of the source volume V, across the z = 0 plane.

The second case that will be considered is one in which the source is in a semi-infinite medium z > 0 of conductivity K_2, which is overlain by a stratum 0 < z ≤ D of conductivity K_1. The solution to this problem is required to satisfy the following conditions:

1) It must satisfy Laplace's equation for all z > 0.

2) It must be zero at z = 0.

3) It must be continuous for all z > 0.

4) The heat flow from medium 1 must equal the heat flow into medium 2 for all points on the z = D plane.

If the example of the first case is followed and an image sink is placed at a location symmetric to the source, across the z = 0 plane it is found that although condition 2 is satisfied, condition 4 is not. If an additional image is placed at a location symmetric to the first, across the z = D plane, condition 4 is satisfied but condition 2 is not. Further inspection reveals that in order to satisfy all 4 conditions simultaneously it is necessary to add an infinite series of images.

For a point source at $z' > D$,

$v = 0 < z \leq D$

$$v = \frac{Q}{4\Pi}\left\{\frac{1}{K_2[x^2+y^2+(z-z')^2]^{1/2}} + \frac{K_2 - K_1}{K_2(K_1+K_2)}\frac{1}{[x^2+y^2+(2A-z-z')^2]^{1/2}} + \sum_{i=0}^{\infty}\frac{4(K_1-K_2)^i}{(K_1+K_2)^{i+2}}\frac{(-1)^{i+1}}{[x^2+y^2+(-2iA-z-z')^2]^{1/2}}\right\} . \quad (10)$$

$$v = z > D$$

$$v = \frac{Q}{4\Pi}\left\{\frac{2}{K_1+K_2}\,\frac{1}{[x^2+y^2+(z-z')^2]^{1/2}}\right.$$

$$+\sum_{i=0}^{\infty}\left[\frac{2(K_1-K_2)^i}{(K_1+K_2)^{i+1}}\,\frac{(-1)^{i+1}}{[x^2+y^2+(-2iA-z-z')^2]^{1/2}}\right.$$

$$\left.\left.+\frac{2(K_1-K_2)^{i+1}}{(K_1+K_2)^{i+2}}\,\frac{(-1)^{i+1}}{[x^2+y^2+(2(i+1)D-z+z')^2]^{1/2}}\right]\right\}. \qquad (11)$$

The expressions for volume sources follow directly from equations (10) and (11), and are comprised of series of volume images at symmetric locations across the planes z = D and z = 0.

The Normal Temperature Field

The model temperature, v, field is given by

$$v = v(\text{body}) = v(\text{normal}) \qquad (12)$$

where

v(body) = the temperature effect of the body computed with a heat production of A = A(b) - A(c),

A_b = the heat production of the body,

A_c = the heat production of the country rock,

v(normal) = the temperature that would be observed in the absence of the body.

v(normal) is defined by the one-dimensional heat flow equation

$$K \frac{\partial v}{\partial z} = q_c - A_c z \qquad (13)$$

where q_o = the heat flow at the surface and z is positive down.

For case 1, the solution to equation (13) is

$$v_n = \frac{1}{K} [q_o z - \frac{1}{2} A z^2] + v_o$$

where

v_o = the mean annual surface temperature.

For case 2 the solution to equation (13) is

$$v_n = \frac{1}{K} q_o z + v_o \quad 0 < z \leq A$$

$$v_n = \frac{1}{K} q_o [A + z - D) - \frac{1}{2} A_c (z - A)^2] + v_o \quad z > A$$

Application to Terrestrial Environments

To apply the model outlined above to a particular region both the normal and anomalous fields must be adequately described. The normal field is described by the heat flow at the surface measured away from the anomalous body, the mean annual surface temperature, and the rate of heat generation in the country rock. The anomolous field is described by the geometry of the body, taken, for example, from gravity and magnetic models, and the rate of heat generation in the body.

At the present time the parameters listed above are not well known for any areas in the southeastern U.S. As more information becomes available, the model will be tested against a known temperature field, and then, if there is adequate agreement, it will be used as a predictive tool to direct further work.

References

Carslaw, H.S., and Jaeger, J.C., 1959. Conduction of heat in solids, 2nd edition. Clarendon Press, Oxford.

Cordell, L., and Henderson, R.G., 1968. Interactive three-dimensional solution of gravity anomaly data using a digital computer. Geophysics, V. 33, p. 596-601.

Haaz, I.B., 1953. Relations between the potential of the attraction of the mass contained in a finite rectangular prism and its first and second derivations: _____, p. 57-66.

Plouff, D., 1976. Gravity and magnetic fields of polygonal prisms and applications to magnetic terrain corrections. Geophysics, V. 41, p. 727-741.

Talwani, M., 1965. Computation with help of a digital ccmputer of magnetic anomalies caused by bodies of arbitrary shape. Geophysics, V. 30, p. 797-817.

Talwani, M., and Ewing, M., 1960. Rapid computation of gravitational attraction of three-dimensional bodies of arbitrary shape. Geophysics, V. 25, p. 203-225.

SUMMARY

The acquisition and interpretation of gravity data on the Atlantic Coastal Plain to constrain the locations and geometry of concealed radiogenic sources has now begun in a systematic manner. Preliminary interpretation of selected gravity anomalies in the Piedmont supports a density contrast associated with granitic intrusive rocks of between -0.150 and -0.250 gm/cc. Additional gravity coverage is being obtained on the Atlantic Coastal Plain by VPI & SU personnel in anticipation of the 60-hole intermediate drilling program to be initiated during the Spring.

Structural studies of the Rolesville batholith are continuing in North Carolina to provide a geologic base for the geophysical interpretation of Piedmont stratigraphy beneath the Coastal Plain. The southern Raleigh belt and adjacent Carolina slate belt have undergone a minimum of three deformational events prior to late brittle faulting.

Low heat generation values measured for the Concord syenite and Mt. Carmel syenite (part of an older magma series approximately 400 m.y.o.) indicate that differentiation alone is insufficient to explain high heat generation. The composition of the parent magma is a critical factor.

The least-squares geothermal gradient over the interval 47-1328 m in a hole drilled by private industry in Wayne County, Ga., is 29.3 ± 0.14°C/Km. Using D.O.E. funds, a bottom-hole core sample was obtained from basement rocks. Determinations of thermal conductivity, heat generation, petrography, and geochronology of the basement core are in progress.

☆U.S. GOVERNMENT PRINTING OFFICE: 1978-740-094/1432